J. M. HOOVER

AUGUST 1970

Final Report
ISU-ERI-AMES-81400

GRANULAR BASE MATERIALS FOR FLEXIBLE PAVEMENTS

IOWA HIGHWAY RESEARCH BOARD PROJECT HR-131
FOR IOWA STATE HIGHWAY COMMISSION
IN COOPERATION WITH FEDERAL HIGHWAY
ADMINISTRATION, BUREAU OF PUBLIC ROADS

ERI Project 704-S

ENGINEERING RESEARCH INSTITUTE
IOWA STATE UNIVERSITY
AMES, IOWA 50010 USA

ENGINEERING RESEARCH

ENGINEERING RESEARCH
ENGINEERING RESEARCH
ENGINEERING RESEARCH
ENGINEERING RESEARCH

FINAL REPORT

GRANULAR BASE MATERIALS FOR FLEXIBLE PAVEMENTS

J. M. Hoover
Project Director

August 1970

Submitted to Iowa Highway Commission and Federal Highway Administration, Bureau of Public Roads

The opinions, findings and conclusions expressed in this publication are those of the authors and not necessarily those of the Iowa State Highway Commission nor the Bureau of Public Roads.

Iowa Highway Research Board Project HR-131

Contribution No. 70-4 of the Soil Research Laboratory

ISU-ERI-AMES-81400
ERI Project 704-S

ENGINEERING RESEARCH INSTITUTE
IOWA STATE UNIVERSITY AMES

1. Report No.	2. Government Accession No.	3. Recipient's Catalog No.
ISU-ERI-AMES-81400		

4. Title and Subtitle	5. Report Date
GRANULAR BASE MATERIALS FOR FLEXIBLE PAVEMENTS	August 1970
	6. Performing Organization Code

7. Author(s)	8. Performing Organization Report No.
J. M. Hoover, Project Director	ISU-ERI-AMES-81400

9. Performing Organization Name and Address	10. Work Unit No.
Soil Research Laboratory Engineering Research Institute Iowa State University Ames, Iowa 50010	11. Contract or Grant No. Project HR-131
	13. Type of Report and Period Covered Final Report
12. Sponsoring Agency Name and Address Iowa State Highway Commission Ames, Iowa 50010 In cooperation with Federal Highway Administration, Bureau of Public Roads	14. Sponsoring Agency Code

15. Supplementary Notes

16. Abstract

The first phase of this project relates untreated and asphalt-treated Iowa materials to those used in the AASHO Road Test. Material coefficients of relative strength are established for use with the AASHO interim design procedure for flexible pavements. The analyses utilized rely on volumetric strain-axial strain data from a triaxial test, at a point of failure defined as minimum volume during shear.

The second phase of the project is basically two-fold and centers around (a) the response of asphalt-treated granular base materials to triaxial compression under repetitive axial loads and (b) the effect of fines content of untreated granular base materials under repetitive axial load triaxial tests.

17. Key Words	18. Distribution Statement
	Unlimited

19. Security Classif. (of this report)	20. Security Classif. (of this page)	21. No. of Pages	22. Price
Unclassified	Unclassified		

CONTENTS

FIGURES

TABLES

1. INTRODUCTION AND OBJECTIVES

Performance of a flexible pavement structure is related to the physical properties and supporting capacity of the various structural components. The AASHO Interim Guide for the Design of Flexible Pavement Structures, based on the pavement performance-serviceability concept developed from the AASHO Road Test, utilizes the physical properties and supporting capacity of granular base materials through an evaluation of the materials coefficient of relative strength. The term coefficient of relative strength implies that materials vary in their physical properties, thus affecting the supporting capacity of the pavement structure. The coefficients developed from the AASHO road test are indicative of a materials variance.

The first phase of this research project related Iowa materials to those used in the AASHO Road Test, establishing material coefficients of relative strength for use with the AASHO interim design procedure for flexible pavements. The test method and analyses utilized relied heavily on those factors influencing the stability of granular base course mixes developed under Iowa Highway Research Board project HR-99[1].

The second phase of this project centered predominantly around the response of asphalt-treated granular base materials to repetitive loads. The equations developed from this study provide a more rational basis for further studies of factors affecting deformation of granular materials under stress conditions similar to those of a pavement subjected to transient traffic loads.

2. PHASE I: COEFFICIENTS OF RELATIVE STRENGTH

K. L. Bergeson, J. M. Hoover, D. E. Fox*

On the basis of laboratory tests only, coefficients of relative strength (hereinafter referred to as CORS) for various bituminous treated and untreated Iowa base course materials were determined. The CORS established for the bituminous treated and untreated AASHO Road Test base materials were utilized as the comparative control values.

2.1. MATERIALS

Twenty-one materials of varying aggregate types and sources were studied. All untreated aggregates and bituminous treated field mixes were furnished through cooperation of the office of the Research Engineer, Iowa State Highway Commission (ISHC).

Bituminous-treated field mixed samples were obtained by ISHC personnel from construction batch plants immediately following mixing with asphalt. Aggregates used for all laboratory mixes were obtained by sampling prior to batching or from stockpiled materials. Asphalt cement for the laboratory mixes, penetration grade 120-150, was also furnished by the ISHC.**

Samples of AASHO Road Test base material were provided in a limited quantity as obtained from the Road Test site. The base material included

---

*Respectively, graduate research assistant, associate professor and graduate research assistant, Civil Engineering Department and Engineering Research Institute, Iowa State University.

**Results of ASTM Standard D2171, asphalt viscosity-temperature tests were as follows: 77°F, 6.25×10^5 poises; 100°F, 4.41×10^4 poises; 140°F, 9.50×10^2 poises; and 212°F, 20.1 poises.

a hard dolomitic limestone, recommended by the ISHC for use in an untreated condition, and a coarse graded gravel, recommended for use in a bituminous treated condition.

Appendix A summarizes all materials tested, test results and testing conditions as obtained from the study presented herein plus portions of data supplied for each aggregate by the ISHC.

2.2. SPECIMEN PREPARATION

2.2.1. Compaction

All 4-in. diameter by 8-in. high cylindrical test specimens were prepared by a vibratory compaction procedure utilizing a Syntron model V-60 electromagnetic vibrator operating at a constant frequency of 3600 cycles/min and amplitude of 0.368 mm, a surcharge weight of 35 lb, and a vibration duration of 2 min. This procedure, previously reported by Hoover[1], minimizes aggregate degradation and segregation while producing uniform densities comparable to other methods. Figure 1 summarizes the specimen preparation procedure.

All densities given in this report are on the basis of weight per unit volume and were obtained by unimmersed height, diameter, and weight measurement of each specimen. As a means of comparison, a number of specimens of several bituminous treated field mixes were immersed in distilled water for volumetric measurement. The densities thus calculated compared favorably with the Marshall compaction densities supplied by the ISHC for each field mixed material.

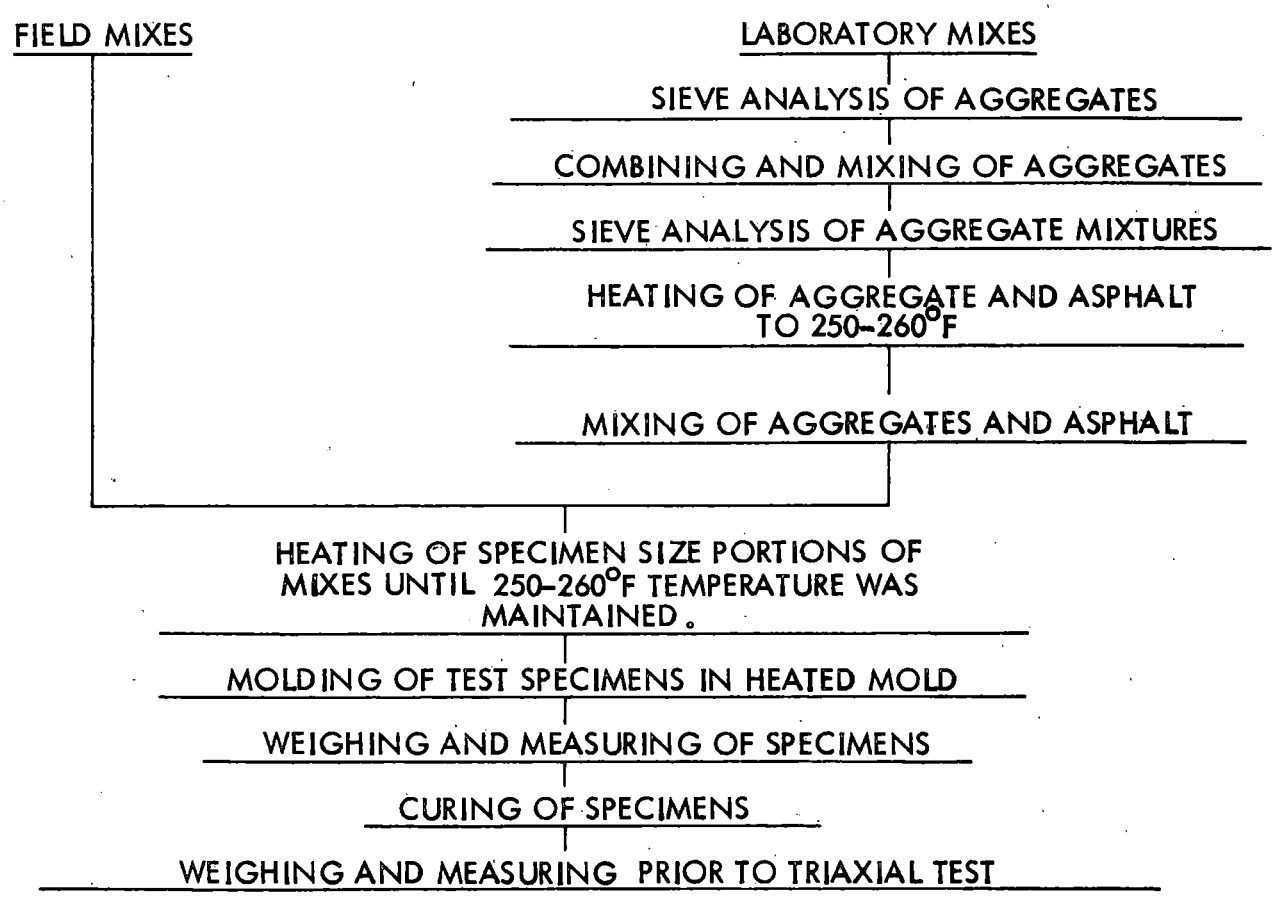

Fig. 1. Specimen preparation flow chart.

2.2.2. Bituminous-Treated Materials

Laboratory and field mixed materials were molded and tested in a similar manner. The major difference was in the initial preparation and combining with asphalt of the laboratory mixes, of known gradation, and then molding as a one step operation. The field mixed samples, by contrast, had to be reheated from a previously mixed condition and relatively unknown gradation and asphalt content.

Field Mixes. Field mixed materials were separated into specimen-sized portions and heated to 250-260°F. The mixture was placed in the heated vibratory mold in three equal layers, each layer being rodded

25 times with a 3/4-in. diameter rounded tip rod. The surcharge weight was set in place and the specimen compacted. Following compaction the height of the specimen was measured while the sample was in the mold. The specimen was extruded, weighed and allowed to cool before being transferred to the curing room. Curing was maintained for a minimum of seven days at about 75°F. Prior to testing all samples were re-measured and reweighed.

Laboratory Mixes. Aggregates for the lab-mixed bituminous-treated materials were blended in accordance with ISHC recommended proportions. Sieve analyses were performed on the blended material and results compared with the recommended gradation. The blend was adjusted, if needed, to meet recommended gradation within ±2% of each individual sieve fraction.

Specimen-sized portions of blended material and asphalt were heated in controlled temperature ovens until a temperature of 250-260°F was maintained. Two specimen-sized samples were combined and mixed in a mechanical mixer whose bowl and mixing head were heated before the addition of aggregate and asphalt. The mixing head consisted of a rotating paddle and scraper attachment to minimize loss of fine material by adherence to bowl sides.

After mixing, the material was separated into specimen-sized portions and returned to the oven until a temperature of 250-260°F was maintained throughout. Specimens were then molded, extruded, weighed and cured in the same manner as the field-mixed specimens.

AASHO Control Mix. AASHO coarse graded gravel material, to be used in a bituminous treated condition, was separated into individual sieve

fractions and blended in accordance with HRB Special Report 61B, Table 37, page 74. A sieve analysis was performed on the blend which was then adjusted to within one standard deviation from the AASHO mean gradation for bituminous-treated base material. Test specimens were molded at 5% asphalt content. Mixing, molding and curing conditions were the same as for laboratory-mixed bituminous-treated specimens.

2.2.3. Untreated Materials

Laboratory Mixes. Seven materials were selected for use in an untreated condition, as representative of the various aggregate types. Each was blended and adjusted in the same manner as the laboratory-mixed bituminous-treated materials. Upon completion of the blending process a portion of each sample was quartered and a moisture-density curve established for that material utilizing the vibratory compactor. Table 1 summarizes optimum moistures and dry densities determined for the untreated materials.

The remainder of each material sample was quartered into specimen-sized portions and weighed to a predetermined figure that would yield a 4-in. diameter by 8-in. high specimen, plus about 200 g for moisture content determination. An appropriate amount of distilled water, as determined from the moisture-density curve, was added to the sample and thoroughly mixed. The sample was introduced into a humid atmosphere and remained undisturbed for at least five minutes. It was then remixed, covered and allowed to stand an additional five minutes or more. The sample was introduced into the compaction mold and compacted in a manner similar to the bituminous-treated specimens, the only difference being

Table 1. Optimum Moisture-Density Relationships for the Untreated Materials, by Vibratory Compaction.

Material	Optimum moisture, %	Dry density, pcf
429	7.3	137.3
479	9.4	132.9
1485	7.3	131.4
1676	8.0	135.4
1846	7.0	140.0
1855	6.7	143.0
1904	5.3	144.0

that moisture samples were taken before the second and third layers were introduced into the mold.

Upon completion of compaction the height of the specimen was measured while in the mold. The specimen was extruded, weighed, wrapped in two layers of saran wrap and sealed with a taped layer of aluminum foil. Specimens were transferred to a curing room maintained at about 75°F and 100% relative humidity until testing. Prior to testing all samples were remeasured and reweighed.

AASHO Control Mix. The untreated AASHO crushed limestone material was separated into individual sieve fractions and then blended in accordance with HRB Special Report 61B, Table 31, page 68. The blend was subjected to successive sieve analyses and adjustments until it was within one standard deviation from the AASHO mean gradation for untreated crushed limestone base material. Specimens were molded at 6% moisture content.

Mixing, molding and curing methods were the same as for laboratory mixed untreated materials.

2.3. TESTING PROCEDURE

This investigation utilized the consolidated-undrained triaxial shear test for all specimens. All testing was performed in the twin-bay triaxial compression machine shown in Figs. 2 and 3. The unit was

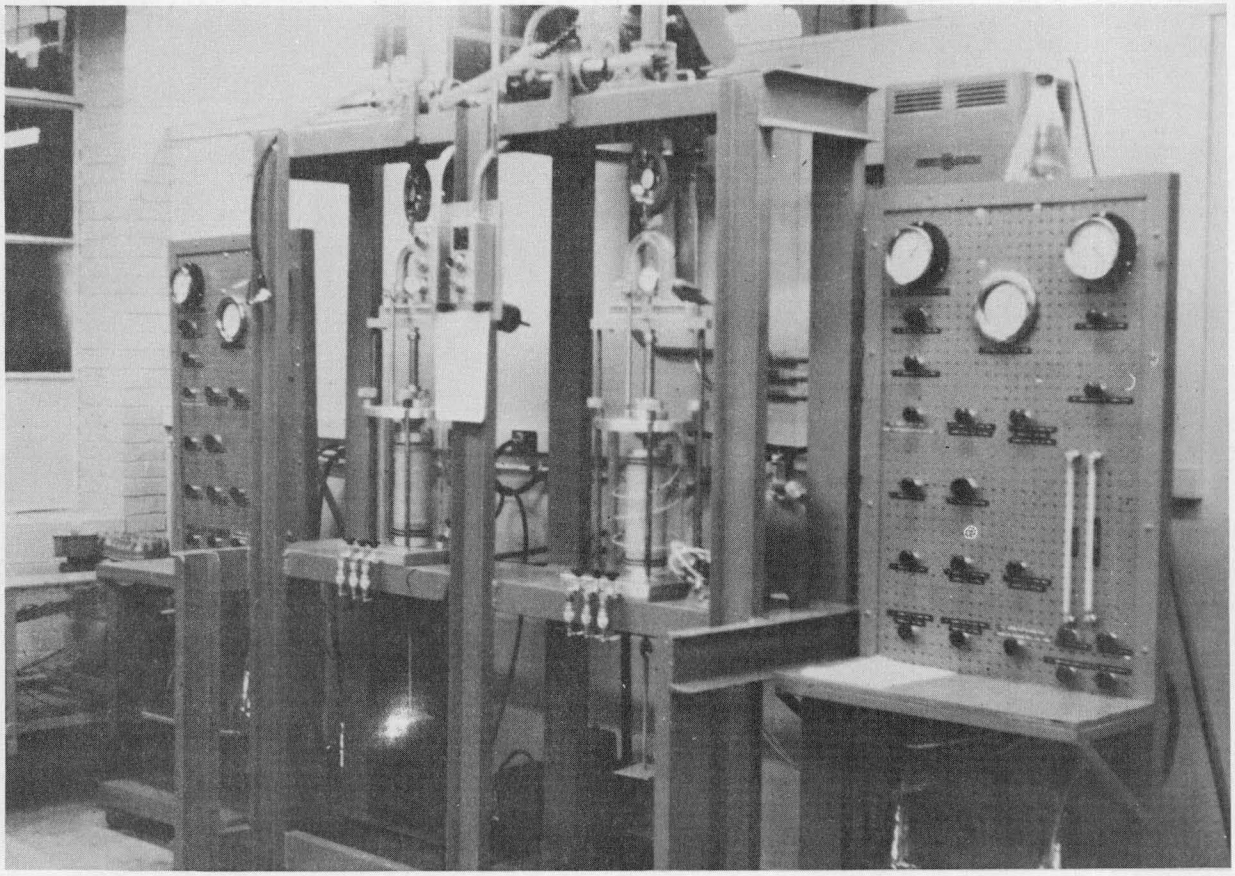

Fig. 2. Double-bay triaxial compression testing machine.

designed by the Engineering Research Institute (ERI) Soil Research Laboratory and constructed by ERI Fabrication Shop. Two specimens may be tested simultaneously under different lateral pressures but at the

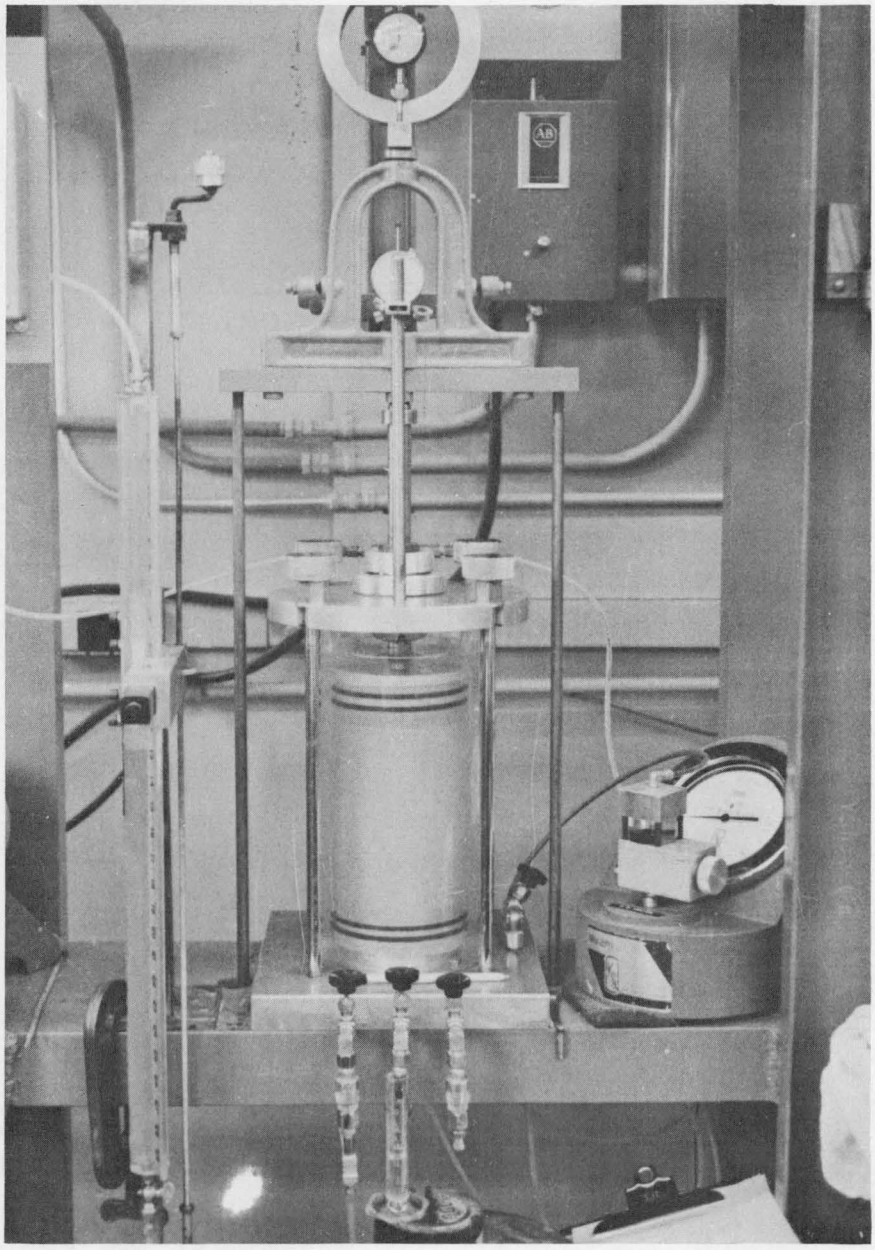

Fig. 3. Triaxial test cell, pore pressure unit, volume change device.

same deformation rate. Each cell has an axial load capacity of 11,000 lb delivered to the specimen through calibrated proving rings. Deformation rates may be varied from 0.0001 to 0.1 in./min. Pore pressures are measured by a Karol-Warner Model 53-PP pore pressure device measuring

both positive and negative pore pressures. Specimen volume changes can be measured to a precision of 0.01 in.^{3}

All testing in this study was conducted at a deformation rate of 0.01 in./min. A minimum of four tests were performed within each material type (Field mix, 4% Lab mix, 5% Lab mix, and selected untreated mixes) at 10, 20, 30, and 40 psi lateral pressure. Once a series had been started in a cell for a particular material type, remaining tests were also performed in that cell to minimize cell variations.

2.3.1. Bituminous-Treated Materials

Immediately prior to testing, each specimen was removed from the curing room, reweighed, and the height and diameter remeasured. The specimen was placed in a vacuum jar filled with distilled water and subjected to a vacuum of about 29 in. Hg for a minimum of 45 min. Upon completion of saturation the sample was transferred to a preheated water bath and maintained at 100°F until testing. The specimen was then placed in the cell with saturated 1/2-in. corrundum stones on the top and bottom and enclosed by a 0.025-in. thick seamless rubber membrane. The cell was filled with de-aired distilled water and a circular coil cell heater, located at the base of the cell, was turned on. The heater was manually controlled by a powerstat voltage regulator. Thermocouple wires, inserted through the top of the cell and connected to a potentiometer, provided temperature monitoring. The temperature was maintained at $100 \pm 1^{\circ}F$ for a minimum of 30 min after which the specimen was consolidated, drainage being permitted, under σ_3 lateral pressure for

a minimum of 36 min prior to shearing. Volume change, and deflection data were recorded during consolidation. The specimen was then sheared, drainage not being permitted, under constant lateral pressure and temperature. The pore pressures, volume change and axial load were recorded at vertical deflection intervals of 0.01 to 0.20 in., every 0.025 to 0.400 in., every 0.05 to 0.60 in. deflection. The test was normally terminated at or less than 0.6 in. deflection, which is great enough to create more than maximum σ_1 for each confining pressure with all mixes.

Figure 4 summarizes the bituminous-treated materials specimen test procedure.

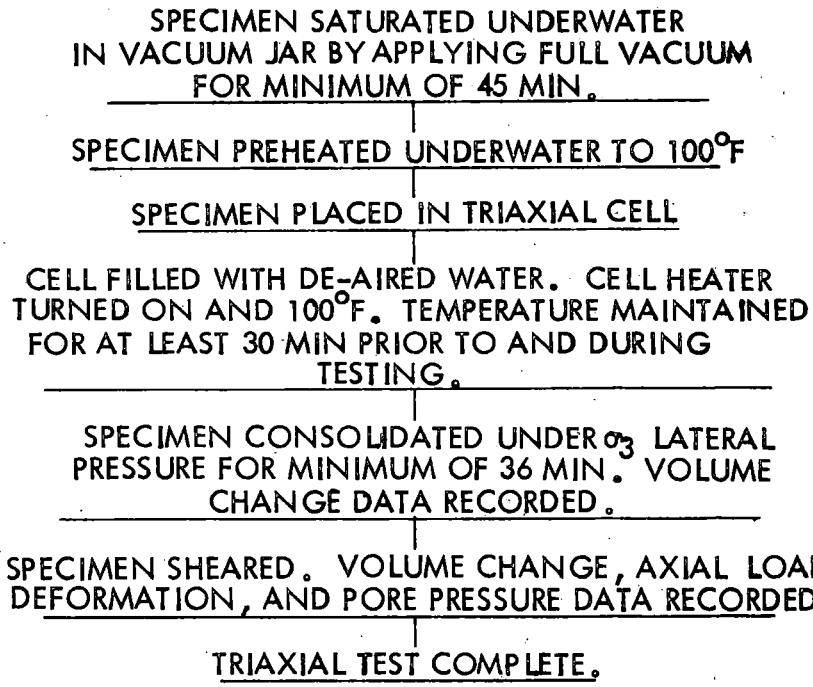

Fig. 4. Bituminous-treated materials specimen test procedure flow chart.

2.3.2. Untreated Materials

The test procedure was similar to that for asphalt-treated materials except that (a) the specimens could not be saturated, and (b) were not heated, but maintained at room temperature.

2.4. METHODS OF ANALYSIS

2.4.1. Failure Criterion

Results of this investigation were analyzed on the basis of two criteria of failure:

(a) Minimum volume (MV), defined as that point of loading at which the specimen has consolidated to its smallest volume during triaxial shear. As the specimen is loaded, volume decreases to some minimum value and pore pressure in the undrained specimen increases to its maximum positive value. It is believed that at this point failure has begun and may be considered a "proportional limit" when viewed in conjunction with a stress/strain curve. On further axial loading volume increases, and interparticle sliding and/or crushing will begin. Pore pressure will also decrease. Further illustrations of this concept are presented by Fish and Hoover[2] and Ferguson and Hoover[3].

(b) Maximum effective stress ratio (MESR), defined as that point in a triaxial shear test at which the effective stress ratio $\frac{\bar{\sigma}_1 - \bar{\sigma}_3}{\bar{\sigma}_3}$ is at a maximum. Effective stresses are intergranular stresses corrected for pore pressures. At MESR the specimen volume has increased substantially and negative pore pressures normally exist. Further illustrations of this concept are presented by Fish and Hoover[2] and Best and Hoover[4].

2.4.2. Calculations

A Fortran IV program, developed for the IBM 360/65 computer, was used to determine stress, strain, volume change, and pore pressure conditions at each data point in the shear portion of the triaxial test.* This program was also capable of producing plots of effective stress ratio, percent volume change and pore pressure versus percent axial strain, utilizing a Calcomp Digital Incremental Plotter. The program was designed so that initial calculated results were stored in the computer memory and could be further manipulated by using subroutines. In this manner values of cohesion, friction angle, modulus of deformation[2], and Poisson's ratio were determined from each series of tests and output, at the appropriate failure criterion being investigated. The printed output and graphical data were used in the analyses of test results. A summary of test results is presented in Appendix A.

2.4.3. Statistical Analysis

In the initial phases of this study it was recognized that some means must be sought to adequately analyze the tremendous volume of results being generated. One means investigated was the statistical method of factorial analysis[5]. This method has recently been used by hydrologists and agronomists to analyze a large number of observations of a particular set of variables describing a specific system. The

*Copies of the computer program will be supplied to sponsors of the project upon request. Due to size of the program, it was not included in this report.

purpose of factorial analysis is to statistically manipulate data and extract that combination of variables that is contributing the most common variance to the system. The mechanics of this process becomes highly complex and the interpretation of results therefrom have been questioned[6]. As an initial step in factorial analysis, however, the variables involved are put into what is termed a correlation matrix. This is simply a matrix of correlation coefficients between all possible pairs of variables involved. For example consider Fig. 5.

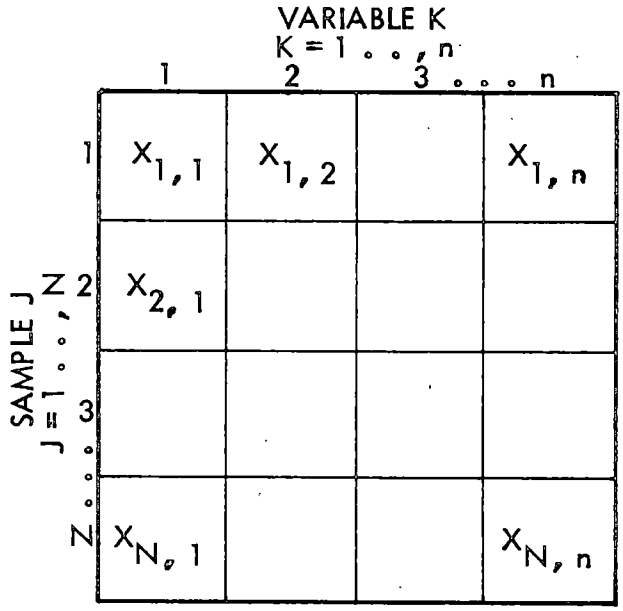

Fig. 5. Representation of data.

The mean value of any variable K with N observations of that variable is

$$\bar{X}_k = \frac{\sum X_{j,k} (j = 1 \; .. \; N)}{N} \; .$$

If we define

$$x_{j,k} = X_{j,k} - \bar{X}_k \; ,$$

then for any two variables K_x and K_y the coefficient of correlation as given by Spiegel[6] is:

$$r = \frac{\sum x_{j,k(K_x)} x_{j,k(K_y)}}{\left[\left(\sum x^2_{j,k(K_x)}\right)\left(\sum x^2_{j,k(K_y)}\right)\right]^{1/2}} .$$

The correlation coefficients determined for all the variables are put into matrix form as indicated in Fig. 6.

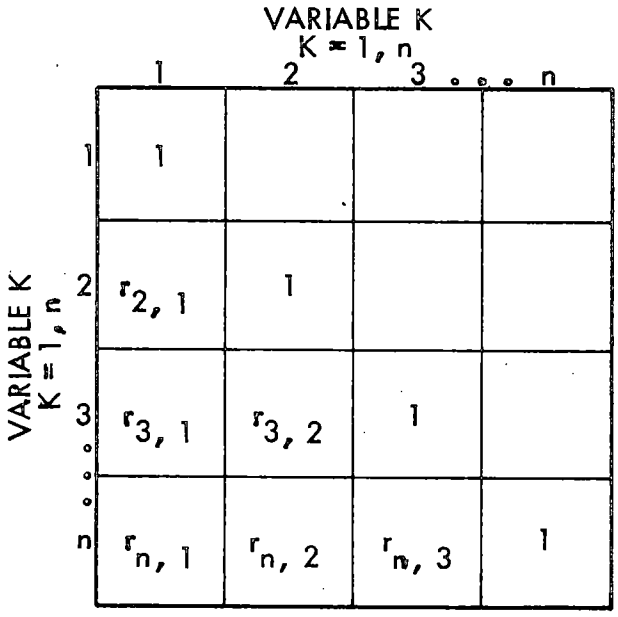

Fig. 6. Correlation matrix.

Thus this initial step in factorial analysis is in itself an appropriate tool for determining if significant linear relationships exist among large numbers of variables. The coefficient of correlation is a very good measure of linear correlation between two variables because it remains the same regardless of whether K_x or K_y is considered the independent variable. The IBM 360/65 program utilized for computing the correlation matrices was obtained from the Statistical Laboratory at ISU. It should be emphasized that the correlation coefficients developed are indicative of linear trends only. A low correlation

coefficient as used in this report means only that no significant linear trend exists and consequently a nonlinear relationship may possibly exist. The coefficient may vary from + 1 to - 1. A positive value indicates positive linear correlation, a negative value indicates negative linear correlation. A value of zero indicates no correlation at all.

A flow chart indicating the variables used for the correlation matrix at minimum volume failure criteria is as indicated in Fig. 7.

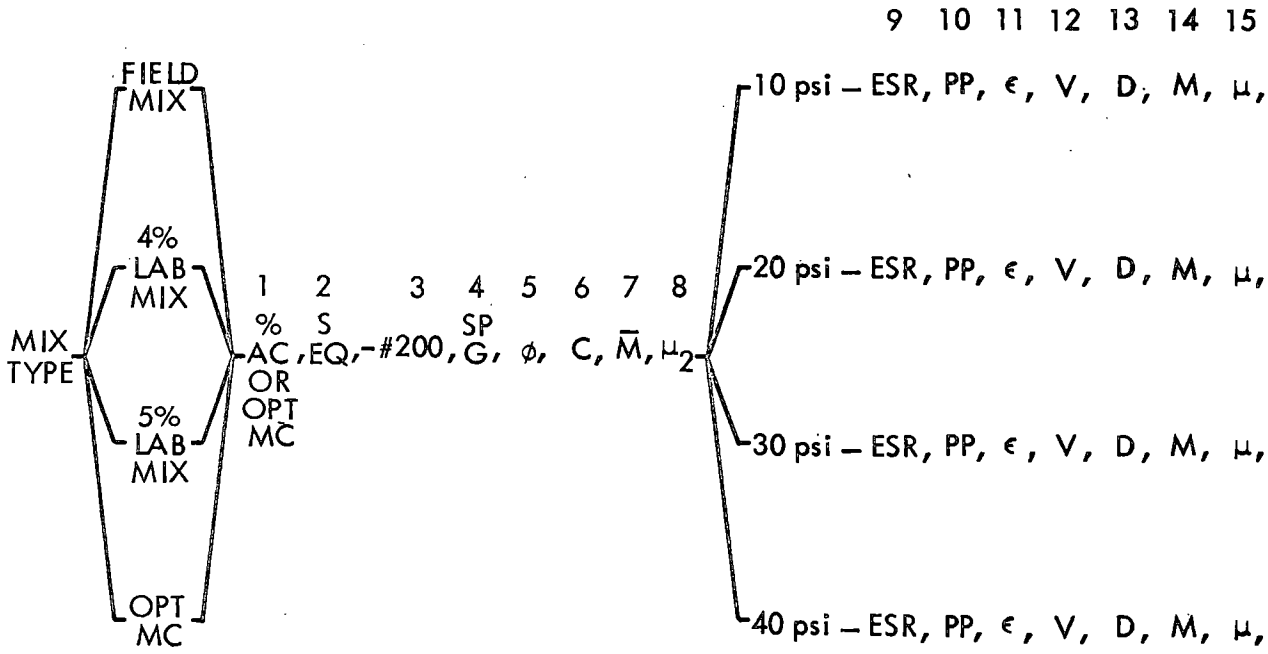

Fig. 7. Flow chart indicating variables used at minimum volume conditions for correlation determinations.

Correlation matrices were produced separately for the field mixes, 4% laboratory mixes, 5% laboratory mixes, and the untreated mixes, at 10, 20, 30, and 40 psi lateral pressures. Appendix B presents one illustration of the correlation matrices used in this study. Figure 8

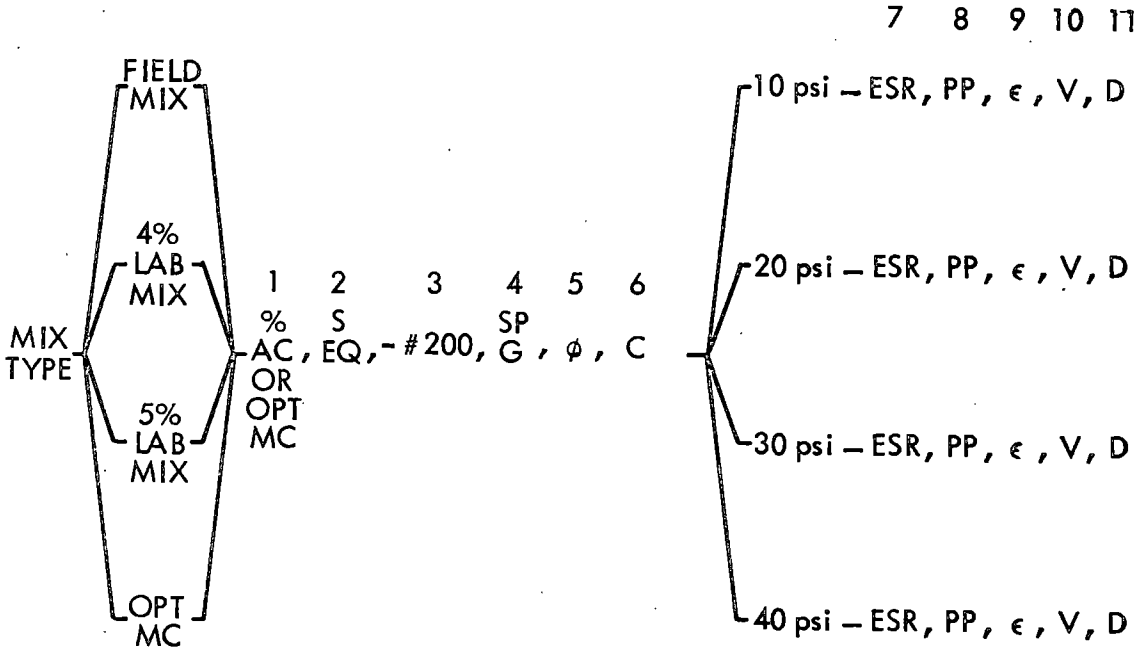

Fig. 8. Flow chart indicating variables used at maximum effective stress ratio conditions for correlation determinations.

is a flow chart indicating the variables used for the correlation matrices at maximum effective stress ratio failure criteria.

In addition to the variables gathered from the triaxial tests, several material properties, as determined by the ISHC, were included as variables for the correlation matrices. These variables are presented in Table 2.

The AASHO materials were not included as a part of any of the correlation matrices since they were considered strictly as control samples. Later in this report it will be noted on the various figures that the AASHO materials fit into the correlations at minimum volume criteria but not at maximum effective stress ratio criteria.

Table 2. Material Properties and Related Variables.

Material number	Specific[a] gravity	Sand[a] equivalent	Minus #200 lab mixes, %	Minus #200[a] field mixes, %
429	2.660	32	10.2	7.1
479	2.695	36	10.7	9.1
728	2.694	47[b]	6.4	8.0
1241	2.690[c]	47[b]	6.7	8.0
1269	2.690[c]	47[b]	8.4	8.0
1485	2.680[c]	69	6.1	4.6
1676	2.652	36	10.7	10.0
1677	2.680	50	9.0	8.6
1743	2.650	36	3.6	6.5
1746	2.642	32	11.6	10.0
1750	2.684	25	9.6	8.9
1751	2.684	25	9.6	9.9
1788	2.743	42	7.3	8.1
1822	2.762	67	11.8	7.8
1846	2.666	43	7.0	5.4
1855	2.753	56	9.4	11.0
1903	2.720	60	7.9	8.1

[a]Values for these variables are ISHC determinations obtained from the material identification sheets.

[b]Values for these materials were obtained by using the average sand equivalent of all materials.

[c]These are corrected values supplied by the ISHC. Incorrect values were used in the initial correlation determinations.

Table 2. Continued.

Material number	Specific[a] gravity	Sand[a] equivalent	Minus #200 lab mixes, %	Minus #200 field mixes, %
1904	2.720	60	7.9	8.3
2318	2.679	72	8.8	8.9
2514	2.669	50	7.6	6.8
2515	2.669	50	7.6	6.8

The primary purpose of this phase of analysis was to determine which pair, or pairs, of variables exhibited a significant degree of correlation and was consistent between the various materials. The value of these variables could then be compared to the value of the same variables of the AASHO control mixes and ranked accordingly, in order to obtain the coefficient of relative strength (CORS).

2.5. RESULTS

2.5.1. Minimum Volume Criteria

Investigation of correlation matrices developed for the various mix types (field mix, 4% laboratory mix, 5% laboratory mix and untreated mixes) at minimum volume failure conditions, indicated the highest degree of correlation was obtained between volumetric strain* and axial

*Volumetric strain is defined as percentage ratio of unit volume change to original volume at start of shear phase of triaxial test. Volumetric strain thus referred to herein is the volumetric strain at the point of minimum volume failure criteria.

strain*. Such correlations were consistent for all lateral pressures within each mix type and between mix types.

Least squares linear regressions were performed on values of volumetric strain-axial strain within the mix types at each lateral pressure. Results are presented in Table 3 and Figs. 9, 10 and 11. Slope of the volumetric strain-axial strain lines, as determined by regression, remained relatively consistent among treated mixes within a given lateral pressure though there appeared to be a decrease in slope with increase in lateral pressure for the treated mixes.

Slopes of volumetric strain-axial strain lines for untreated mixes were considerably greater than for treated mixes and appeared to increase with lateral pressure. Slopes for the untreated mixes, however, were determined by only seven data points at each lateral pressure. A linear regression was run on all values of volumetric strain-axial strain for all lateral pressures, yielding a slope of 0.3795 and a correlation coefficient of 0.965, indicating that the increase of slope due to lateral pressure for untreated materials was not too significant.

The volumetric strain-axial strain regression lines for the 10, 20 and 30 psi lateral pressures for untreated and treated mixes are approximated in Fig. 12 and were used for qualitative observations. It can be shown that when Poisson's ratio is zero, volumetric strain is equal to axial strain and lateral strain is zero. It can also be

---

*Axial strain is defined as percentage ratio of axial deformation to original axial length at start of shear phase of triaxial test. Axial strain thus referred to herein is the axial strain at the point of minimum volume failure criteria.

Table 3. Regression Results[a].

Material type	Lateral pressure	Intercept	Slope	Correlation coefficient
Field mix	10	- 0.016	- 0.243	0.855
	20	- 0.012	- 0.234	0.841
	30	- 0.030	- 0.190	0.948
	40	- 0.022	- 0.228	0.931
4% lab mix	10	- 0.017	- 0.243	0.816
	20	- 0.026	- 0.203	0.943
	30	- 0.050	- 0.179	0.973
	40	- 0.048	- 0.186	0.986
5% lab mix	10	- 0.006	- 0.267	0.722
	20	- 0.010	- 0.241	0.860
	30	- 0.049	- 0.167	0.881
	40	- 0.060	- 0.191	0.945
Optimum moisture content	10	- 0.094	- 0.118	0.400
	20	- 0.028	- 0.321	0.903
	30	- 0.023	- 0.353	0.899
	40	- 0.012	- 0.377	0.966

[a]AASHO values were not included in the regressions.

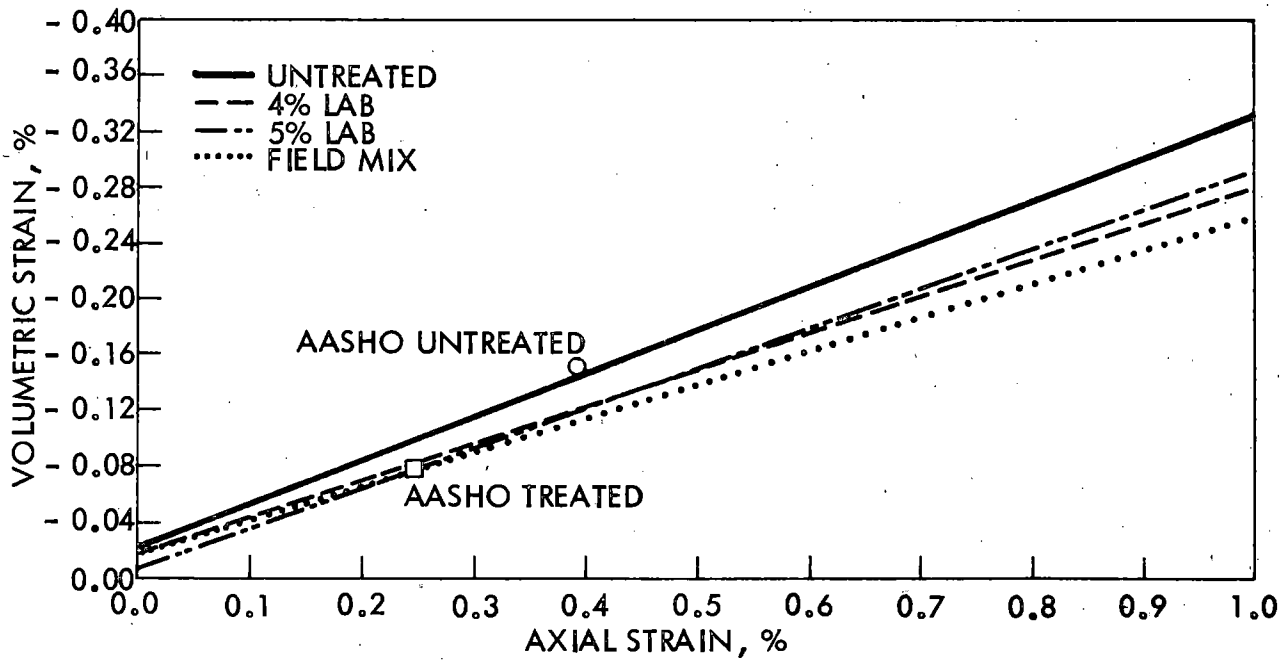

Fig. 9. Regression lines of 10 psi tests, all materials minimum volume criteria.

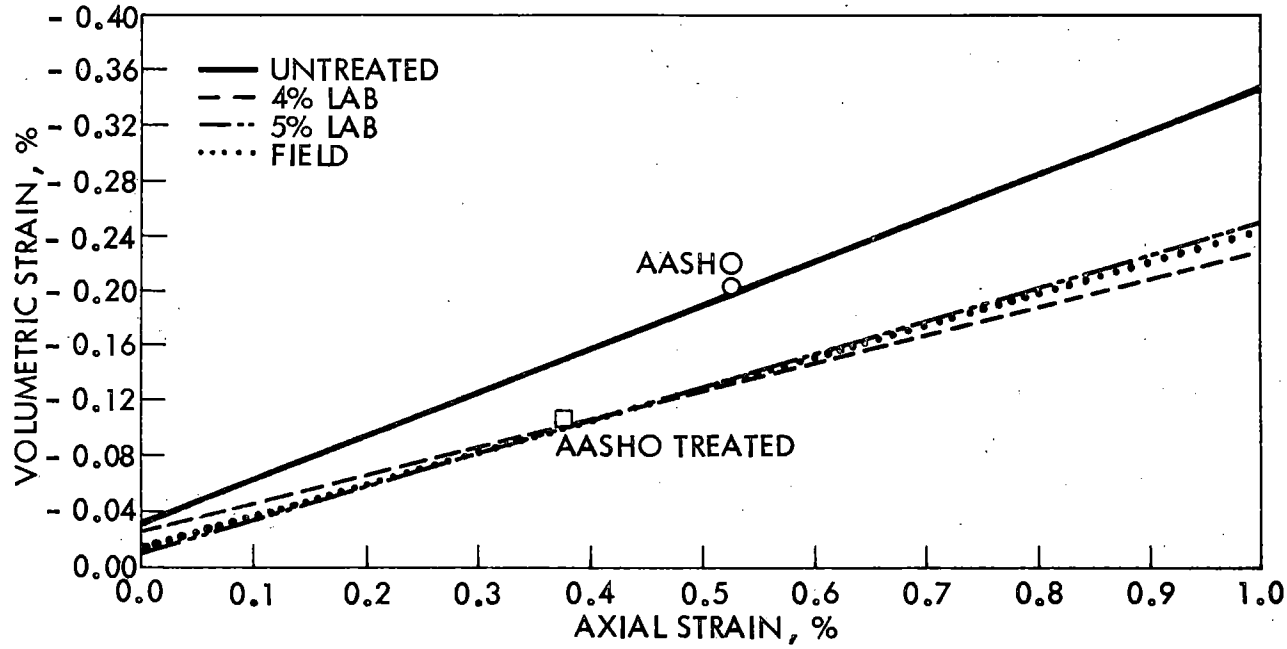

Fig. 10. Regression lines of 20 psi tests, all materials minimum volume criteria.

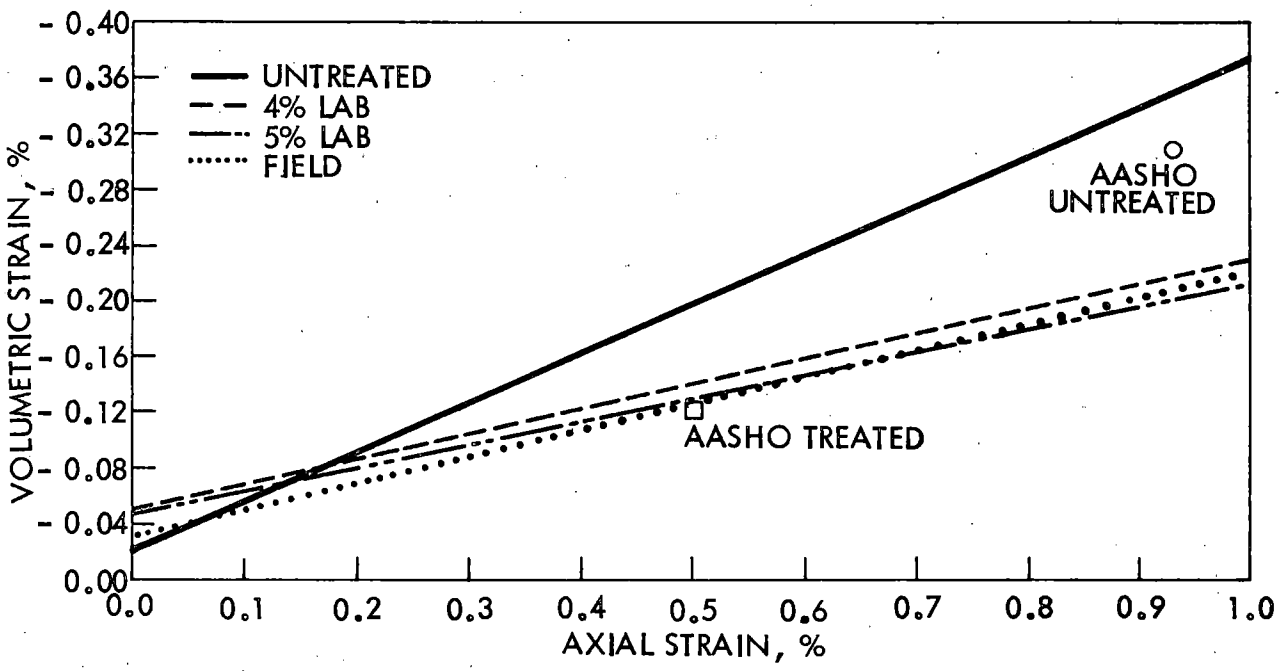

Fig. 11. Regression lines of 30 psi tests, all materials minimum volume criteria.

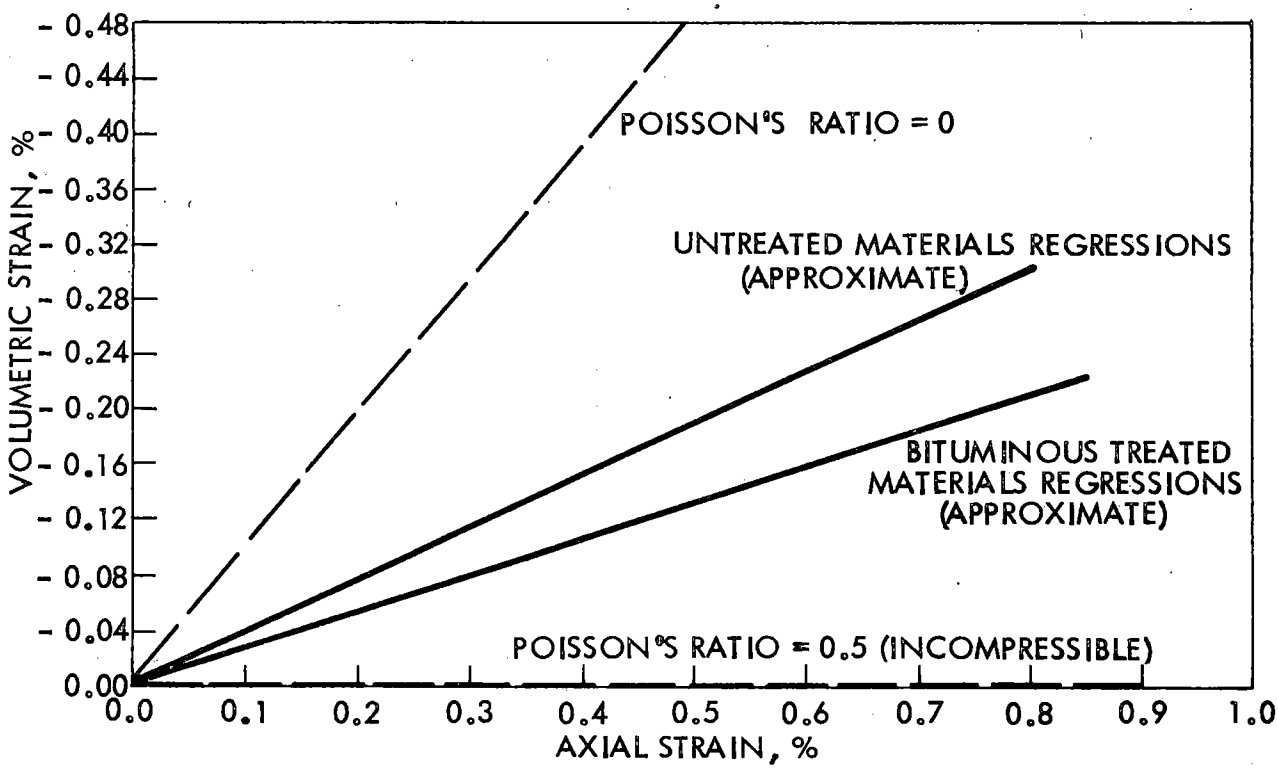

Fig. 12. Comparison of volumetric strain-axial strain characteristics, minimum volume criteria.

shown that when Poisson's ratio equals 0.5, volumetric strain is zero (incompressible) and axial strain equals twice the lateral strain. These conditions are shown on Fig. 12.

Untreated materials exhibited greater slopes than treated materials indicating that at a given value of axial strain the amount of volume decrease is greater for the untreated materials. It also indicates that both materials exhibited a limited amount of lateral strain although volume was decreasing. Treated materials underwent more lateral strain, at a given axial strain, than untreated materials.

The variation in slopes between the untreated and treated materials can be attributed to (a) test temperature (the treated materials were tested at 100°F), (b) the density difference from untreated to treated condition, (c) degree of saturation, or (d) the asphalt content. If it is assumed that the temperature difference at testing was the cause of the deviation, such should allow the asphalt treated specimens to undergo volume decrease without lateral strain easier than if tested at room temperature. This, however, would only tend to lessen the deviation since if temperature is contributing, it is tending to equalize and not cause the variance.

Dry densities of the untreated specimens were generally higher than those of treated specimens of the same material as indicated in Table 4. This is probably due to the asphalt increasing specimen volume by separation of soil particles with a film of asphalt and fines, thereby decreasing the specimen weight. Also, the cohesive property of asphalt does not allow as much freedom for particle reorientation during compaction as water in the untreated specimens.

Table 4. Average Dry Densities, pcf[a].

Material	Field	4% lab	5% lab	Untreated
429	129.3	129.4	130.3	136.5
479	124.8	125.1	126.2	131.2
1485	128.8	127.3	130.4	127.6
1676	127.6	124.8	128.4	132.1
1846	133.3	132.8	134.7	135.5
1855	129.3	134.0	133.5	138.0
1904	138.0	133.4	–	138.6

[a]Dry density of A.C. treated mixes computed on the basis of average A.C. content.

If density is thus assumed to cause the deviation in volumetric strain at a given vertical strain, it can be reasoned that the less dense specimen of a given material would normally have a greater void ratio and consequently should be able to undergo a volume decrease without lateral strain easier than more dense specimens. This again would tend to equalize the deviation and not contribute to it.

All field and lab mix bituminous-treated materials were vacuum saturated. As previously indicated, the untreated material specimens could not be saturated. The latter was due to complete disintegration of the specimens under vacuum saturation and severe flotation removal of fines when capillary saturated.

Calculated degree of saturation of the untreated materials ranged from a low of less than 60% to near 95% saturation. Theoretically, materials at a low percentage of saturation should undergo a greater

volumetric strain than materials at a higher percentage saturation. No correlation was found between calculated degree of saturation and volumetric strain. Instead, untreated materials of high saturation exhibited both high and low volumetric strain. Similar data were noted for the low degree of saturation untreated materials.

Thus, by the process of elimination it can only be concluded that the primary cause of deviation in regression slopes of the treated materials to the untreated materials is the asphalt itself. It should not be concluded, however, that density and temperature have no effect whatsoever. Instead, the effect of these variables would appear to decrease the deviation. This behavior can possibly be explained by the fact that the cohesive properties of the asphalt tend to lock the individual particles together in a matrix of asphalt and fine material. During the initial shear portion of a test, when the specimen is being further consolidated, the particles are not as able to reorient themselves into a more compact state without a greater amount of lateral strain than the untreated specimens, even though the latter are less dense initially.

Referring again to Fig. 12, more solid materials such as concrete mixtures will have slopes of volumetric strain-axial strain approaching the line representing Poisson's ratio equal to zero. Such materials exhibit very little lateral strain upon loading while stability is primarily dependent on individual material properties. The other extreme is fluids and fluid mixtures which are nearly incompressible and will have slopes of volumetric strain-axial strain approaching Poisson's

ratio of 0.5. Fluids are entirely dependent upon lateral restraint to support loads.

In Fig. 12 one can imagine a succession of lines beginning at Poisson's ratio equal to zero and representing materials that derive stability from individual material properties, to the line representing Poisson's ratio equal to 0.5 and representing materials deriving their stability primarily from lateral restraint. As the slope of this line decreases, stability becomes more dependent on some form of lateral restraint. Asphaltic concrete is a fluid-solid mixture and (from Fig. 12) is more dependent on lateral restraint for stability than on individual material properties.

Ferguson and Hoover[3] in a study of cement treated granular base materials advanced the hypothesis that the stability of untreated granular bases may be a function of lateral restraint existing prior to loading and its ability to increase the restraint through resistance to lateral expansion. The results of this study appear to confirm this hypothesis, extending it to include bituminous-treated base materials.

A study of the shear strength parameters of cohesion and friction angle at minimum volume for the seven materials used in the treated and untreated condition (Table 5) revealed that the addition of asphalt generally reduced the angle of friction and slightly increased cohesion but did not substantially alter overall shear strength characteristics. This indicates that strength alone does not account for the differences in stabilities of bituminous-treated and untreated base materials.

Table 5. Shear Strength Parameters at Minimum Volume.

Material	4% lab		5% lab		Untreated	
	C, psi	ϕ, degrees	C, psi	ϕ, degrees	C, psi	ϕ, degrees
429	2.10	39.86	- 0.06[a]	42.69	- 4.51	45.18
479	- 1.15	42.05	1.39	40.13	0.38	42.52
1485	- 0.16	33.54	1.84	32.01	1.15	38.93
1676	5.60	40.38	6.71	35.71	3.00	41.79
1846	1.04	37.60	2.38	36.31	- 1.83	44.33
1855	1.65	43.63	- 1.35	44.15	- 3.16	46.55
1904	—	—	- 4.79	42.97	0.67	42.02

[a]Negative values of cohesion are invalid and due in part to regression.

A mechanism which may account, in part, for the stability differences and may not be as nearly dependent on strength is suggested. Under similar field conditions bituminous-treated materials will exhibit more lateral strain per given amount of vertical strain than untreated materials. This would give rise to greater lateral support from adjacent material for the bituminous-treated materials, and hence greater stability by virtue of being able to undergo lateral strain.

A study by Csanyi and Fung[7] concluded that there was no direct relationship between performance of an asphaltic mix and its stability regardless of the method used to determine stability. This indicates that while asphaltic mixes may meet stability requirements and may not fail in terms of shear, they may fail in performance from rutting and channeling. It therefore seems that some measure of rutting

potential is needed that would also be a measure of strength. The volumetric strain-axial strain characteristics of a particular material would seem to satisfy these requirements. A material which has a high value of volumetric strain-axial strain at minimum volume must undergo more densification and decrease in volume before reaching the condition where lateral strain will provide additional support. This material will have begun to fail in performance as a result of densification, which is the beginning of rutting. A material having a low value of volumetric strain-axial strain will need to densify very little before reaching the condition of additional lateral support.

The above discussion also indicates that compaction and sufficient lateral support are variables that affect the stability of bituminous-treated base materials to a large degree. Nichols[8] concluded in a flexible pavement research project in Virginia that deflections and performance seemed more closely allied with compaction than with pavement design characteristics. Arena, et al.[9] concluded in a compaction study that sections of pavement rolled under pressures of 85 psi had rutted far less after three years of exposure to heavy traffic than those rolled at 55 to 75 psi. This indicates that compaction of an asphaltic-treated material is a critical factor contributing to the stability of that material and substantiates the use of minimum volume criteria and volumetric strain-axial strain characteristics as a means of evaluating stability and performance.

Coefficients of Relative Strength (CORS): Volumetric Strain-Axial Strain Basis. CORS were determined at 10, 20 and 30 psi lateral pressures. AASHO bituminous-treated gravel and untreated crushed stone

were assigned CORS of 0.34 and 0.14 respectively in accordance with the AASHO Interim Guide for the Design of Flexible Pavement Structures. Each material was ranked according to its value of volumetric strain-axial strain (V-E), at minimum volume, on the triangular charts shown in Figs. 13, 14 and 15 — respectively the V-E minimum volume vs CORS plots of 10, 20 and 30 psi lateral pressures. It is readily noted that the final development of these charts relied on a straight-line relationship between only two points of control; i.e., the two AASHO samples recommended and supplied to the project. The charts are used as follows:

a. Volumetric strain and axial strain, as computed from the consolidated undrained triaxial shear test data at the point of minimum volume during shear, are respectively entered from the left and right sides of the chart.

b. At the intersection of the above values, a line is projected down and to the left, to the CORS scale.

Tables 6, 7, and 8 summarize the CORS determined for each material and mix type from Figs. 13, 14, and 15.* The validity of the CORS thus determined, can only be fully ascertained after extensive analysis of the pavement field performance where each material and mix type have been used.

However, it is obvious from Tables 6, 7 and 8 that definite physical property and supporting capacity differences exist among the various materials and mix types. The CORS from untreated to either 4 or 5% lab mix show that an optimum asphalt content could be significantly less

*Several CORS were determined as slightly negative values from Figs. 13, 14, and 15 but are shown in Tables 5, 6, and 7 as zero.

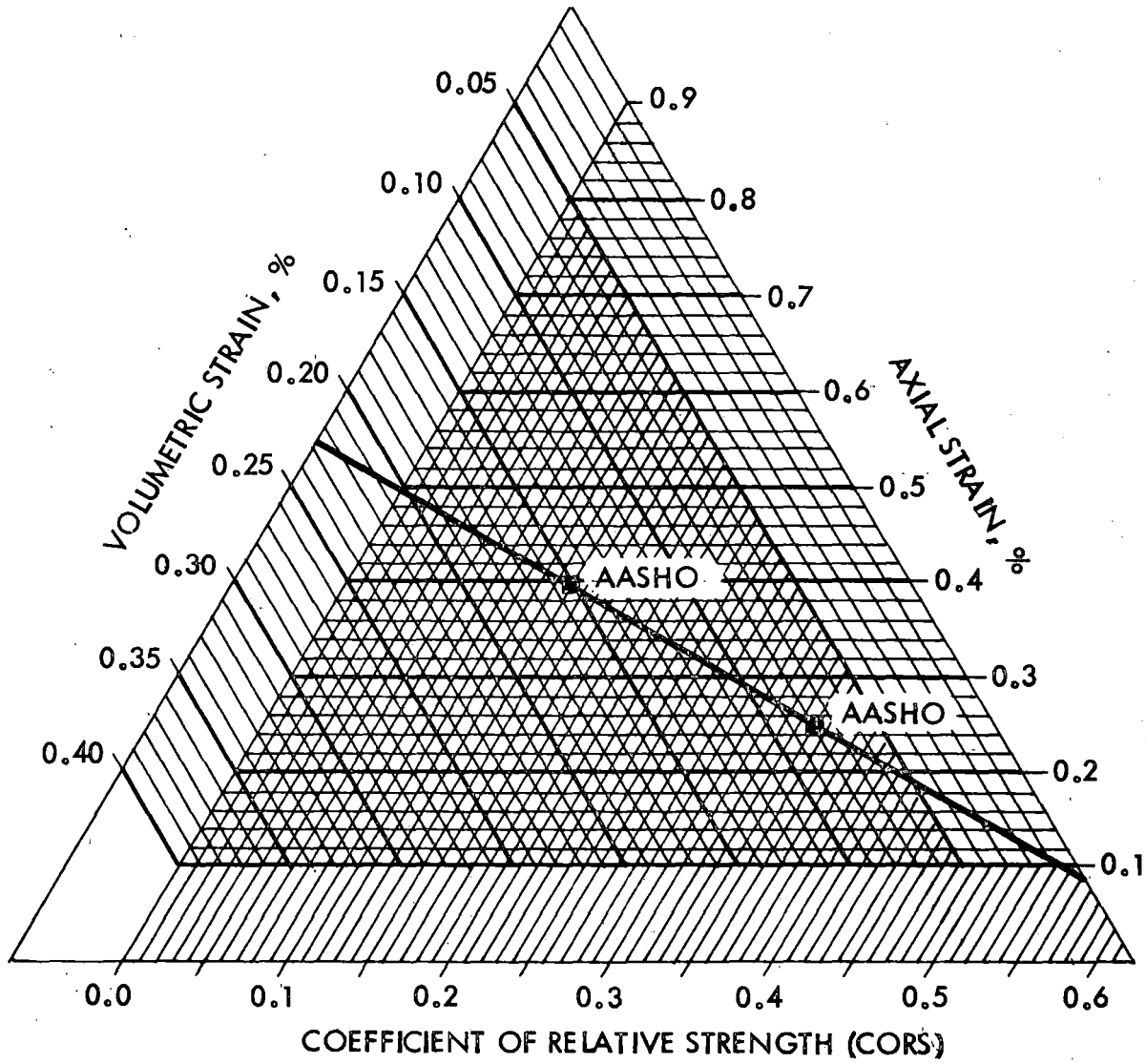

Fig. 13. Triangular chart for determining CORS at 10 psi lateral pressure.

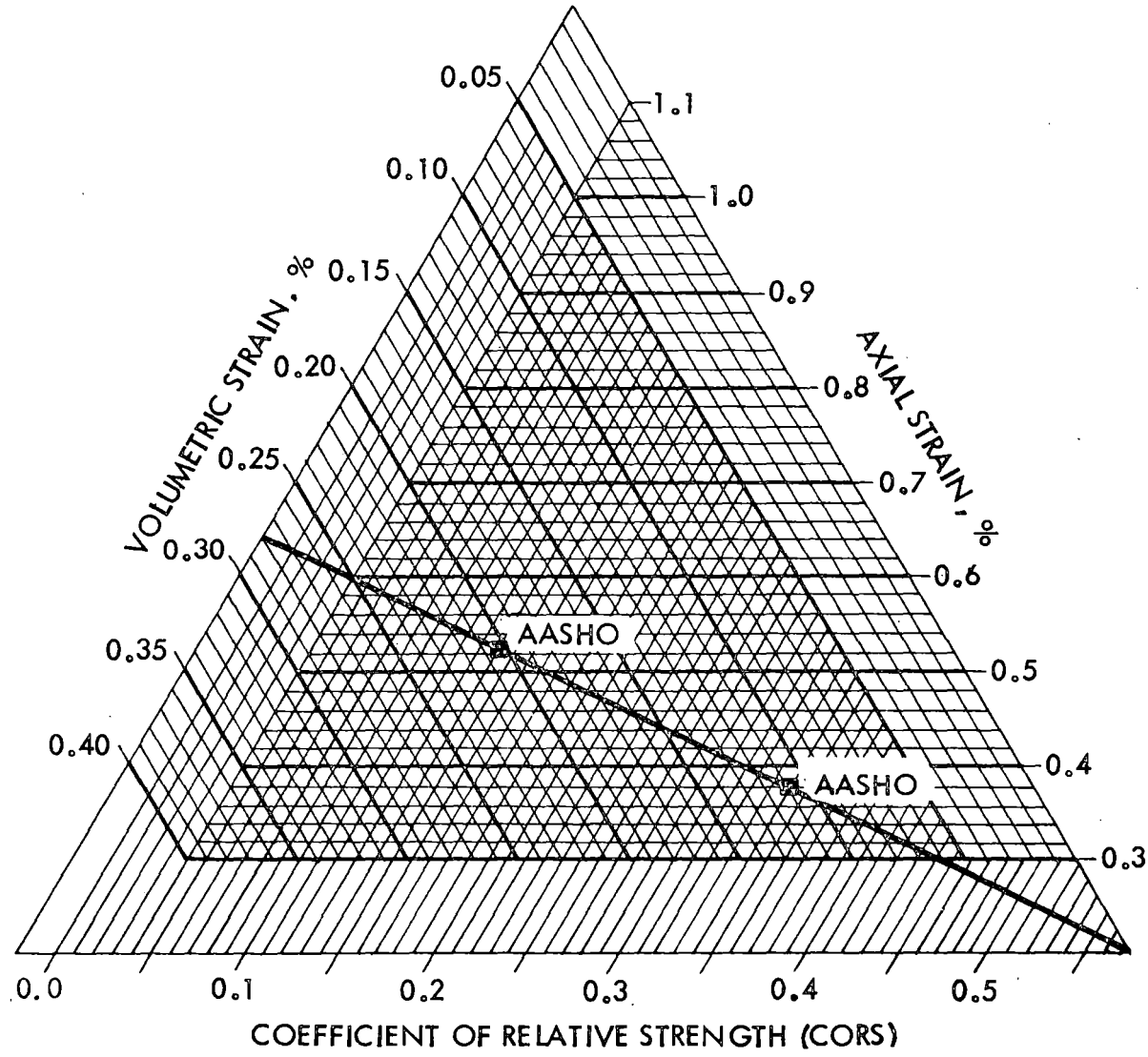

Fig. 14. Triangular chart for determining CORS at 20 psi lateral pressure.

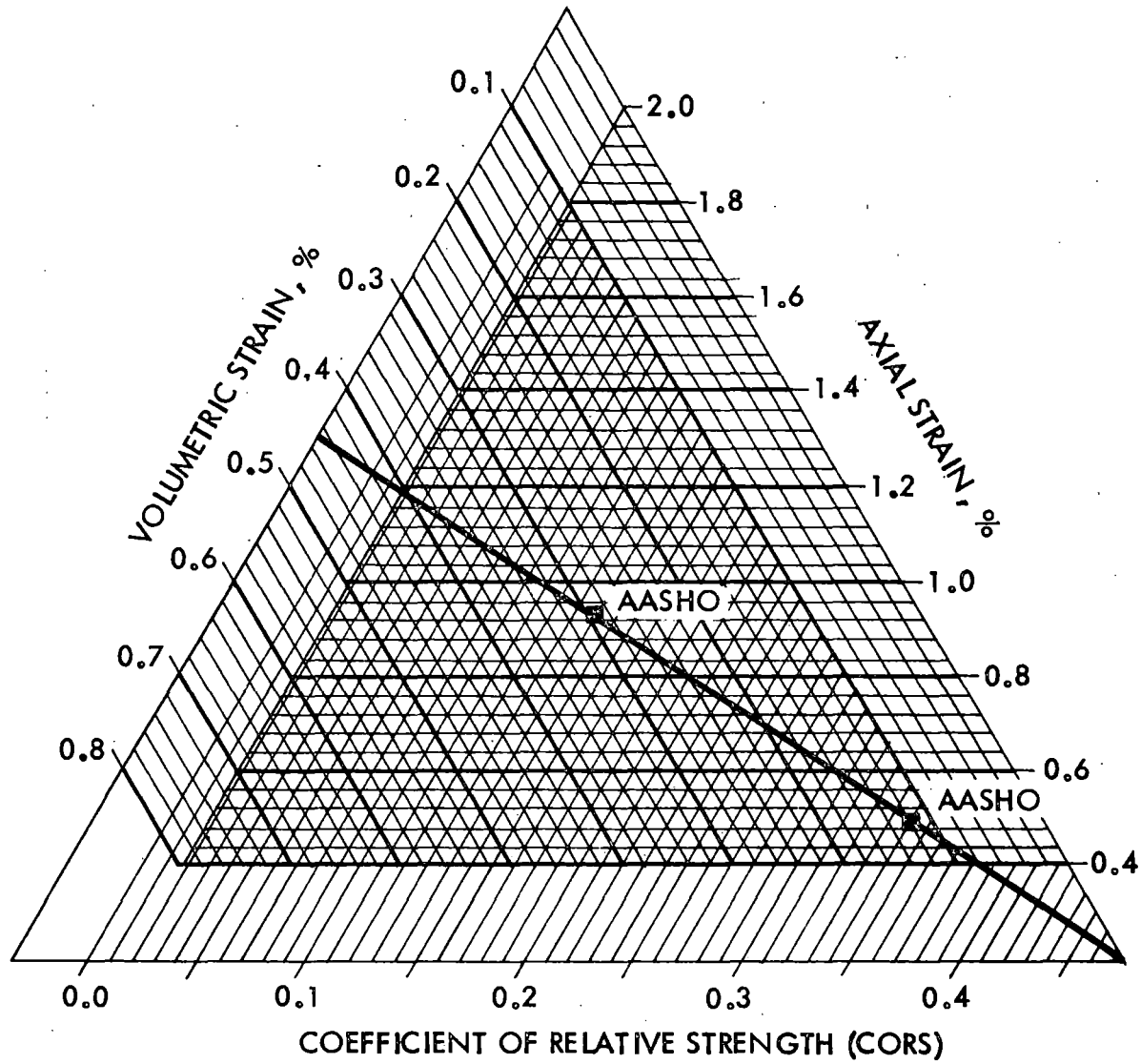

Fig. 15. Triangular chart for determining CORS at 30 psi lateral pressure.

Table 6. CORS Determined on the Basis of Volumetric Strain-Axial Strain Relationships at Minimum Volume and 10 psi Lateral Pressure.

Material	Field mix	4% Lab mix	5% Lab mix	Untreated
429	0	0.22	0.20	0.19
479	0.26	0.33	0.25	0.06
728	0.35	0.39	0.21	ND[b]
1241	0	0.34	–[a]	ND
1269	0	0.05	–[a]	ND
1485	0.21	0.34	0.38	0.16
1676	0.32	0.25	0.27	0.16
1677	0.07	0.21	0.54	ND
1743	0.10	0.33	0.23	ND
1746	0.19	0.17	0.31	ND
1750	0.09	0.09	–[a]	ND
1751	0	–[a]	0.19	ND
1788	0.45	0.45	0.36	ND
1822	0.34	0.17	0.45	ND
1846	0.26	0.38	0.37	0.25
1855	0.48	0.25	0.35	0.19
1903	0.38	–[a]	0.28	ND
1904	0.15	0.35	–[a]	0.27
2318	0.22	0.47	0.34	ND
2514	0.07	–[a]	0.24	ND
2515	0.20	0.22	–[a]	ND

[a]This percentage lab mix not recommended for testing by ISHC.

[b]Not determined.

Table 7. CORS Determined on the Basis of Volumetric Strain-Axial Strain Relationships at Minimum Volume and 20 psi Lateral Pressure.

Material	Field mix	4% Lab mix	5% Lab mix	Untreated
429	0.04	0	0.32	0.14
479	0.24	0.35	0.34	0
728	0.47	0.25	0.35	ND[b]
1241	0.09	0.32	–[a]	ND
1269	0	0	–[a]	ND
1485	0.46	0.36	0.21	0.18
1676	0.24	0.35	0.38	0
1677	0.25	0.13	0.10	ND
1743	0.22	0.34	0.21	ND
1746	0.33	0.16	0.14	ND
1750	0.23	0.12	–[a]	ND
1751	0.08	–[a]	0.23	ND
1788	0.45	0.43	0.27	ND
1822	0.17	0.18	0.35	ND
1846	0.27	0.28	0.31	0
1855	0.37	0.35	0.40	0.16
1903	0.20	–[a]	0.45	ND
1904	0.37	0.35	–[a]	0.21
2318	0.45	0.45	0.26	ND
2514	0.28	–[a]	0.34	ND
2515	0.16	0.24	–[a]	ND

[a]This percentage lab mix not recommended for testing by ISHC.

[b]Not determined.

Table 8. CORS Determined on the Basis of Volumetric Strain-Axial Strain Relationships at Minimum Volume and 30 psi Lateral Pressure.

Material	Field mix	4% Lab mix	5% Lab mix	Untreated
429	0.15	0.22	0.28	0.15
479	0.34	0.29	0.37	0.12
728	0.31	0.34	0.47	ND[b]
1241	0.30	0.29	–[a]	ND
1269	0	0	–[a]	ND
1485	0.36	0.33	0.36	0.28
1676	0.26	0.31	0.37	0.12
1677	0.18	0.06	ND	ND
1743	0.29	0.32	0.07	ND
1746	0.28	0.26	0.29	ND
1750	0.22	0	–[a]	ND
1751	0.22	–[a]	0.06	ND
1788	0.25	0.34	0.31	ND
1822	0.32	0.25	0.31	ND
1846	0.29	0.37	0.32	0.22
1855	0.36	0.37	0.37	0.31
1903	0.25	–[a]	0.29	ND
1904	0.33	0.33	–[a]	0.30
2318	0.35	0.33	0.34	ND
2514	0.29	–[a]	0.29	ND
2515	0.25	0.28	–[a]	ND

[a]This percentage lab mix not recommended for testing by ISHC.

[b]Not determined.

than 4% for some mixes, or higher than 5% for other mixes. Comparison of untreated with treated CORS generally show the benefit of addition of asphalt. Relation of CORS untreated, to those of the treated mixes, could be ascertained on an equivalency basis, though not attempted in this project.

Three pairs of field and laboratory mixes each used the same aggregate source, i.e., mixes 1750-1751, 1903-1904, and 2514-2515.* The variation of CORS due to asphalt content is apparent between the lab and field mix types for each of the above materials in Tables 6 and 7. Table 7 indicates little variance in CORS with asphalt treatment of the above materials, probably due to the increase in lateral restraint, as is later explained in this report.

Comparison of the untreated, 4% and 5% treated laboratory mixes with their respective field mixes is difficult, however. Major inconsistencies of comparison of the field mixes and their closest laboratory mix asphalt content were noted during analyses. These inconsistencies were apparently related to gradation differences** and the effects of reheating the mixtures. A study by Hveem[10] indicates that asphalts harden and become more brittle (lowering of initial penetration) on cooling from an elevated temperature. Therefore on reheating and cooling an unknown additional amount of brittleness may have been introduced in the field-mixed samples.

---

*Respectively a limestone-dolomite, gravel, and limestone.

**The extracted gradations varied from recommended gradations. Project personnel were instructed by the ISHC to use only the recommended gradations.

There was no discernable trend for the variation of CORS with aggregate type. Some gravels had a very low CORS, material 1269 in particular, while some had relatively high CORS. Material 1750, a dolomitic limestone, had a low CORS while other dolomitic materials had high CORS. The traffic simulator study by Csanyi et al.[11], concluded that asphaltic mixes using softer aggregates tend to be displaced under traffic less than mixes with harder aggregates and that there is no direct relationship between stability and trafficability of a particular mix. It would appear then that some mixes containing soft aggregates could perform better under traffic than those containing hard aggregates and vice versa.

The flexible pavement research study by Nichols[8] concluded that deflections and performance seemed more closely allied with compaction than with pavement design characteristics. From this it would seem that deflections would decrease and performance increase with increasing density of the base course material. Figure 16 illustrates that, in general, CORS of the various materials increased with increasing density. A similar plot of density vs CORS of the field mixes was very erratic and was considered indicative of the effect of asphalt brittleness due to reheating and recooling.

Figure 17 illustrates a general trend for increasing CORS with increasing modulus of deformation[2] for the lab mixes only, at 10 psi lateral pressure. This plot is indicative that volumetric strain-axial strain at minimum volume is a measure of strength. A similar plot of modulus of deformation vs CORS of the field mixes was very erratic and was again considered indicative of the effect of asphalt brittleness.

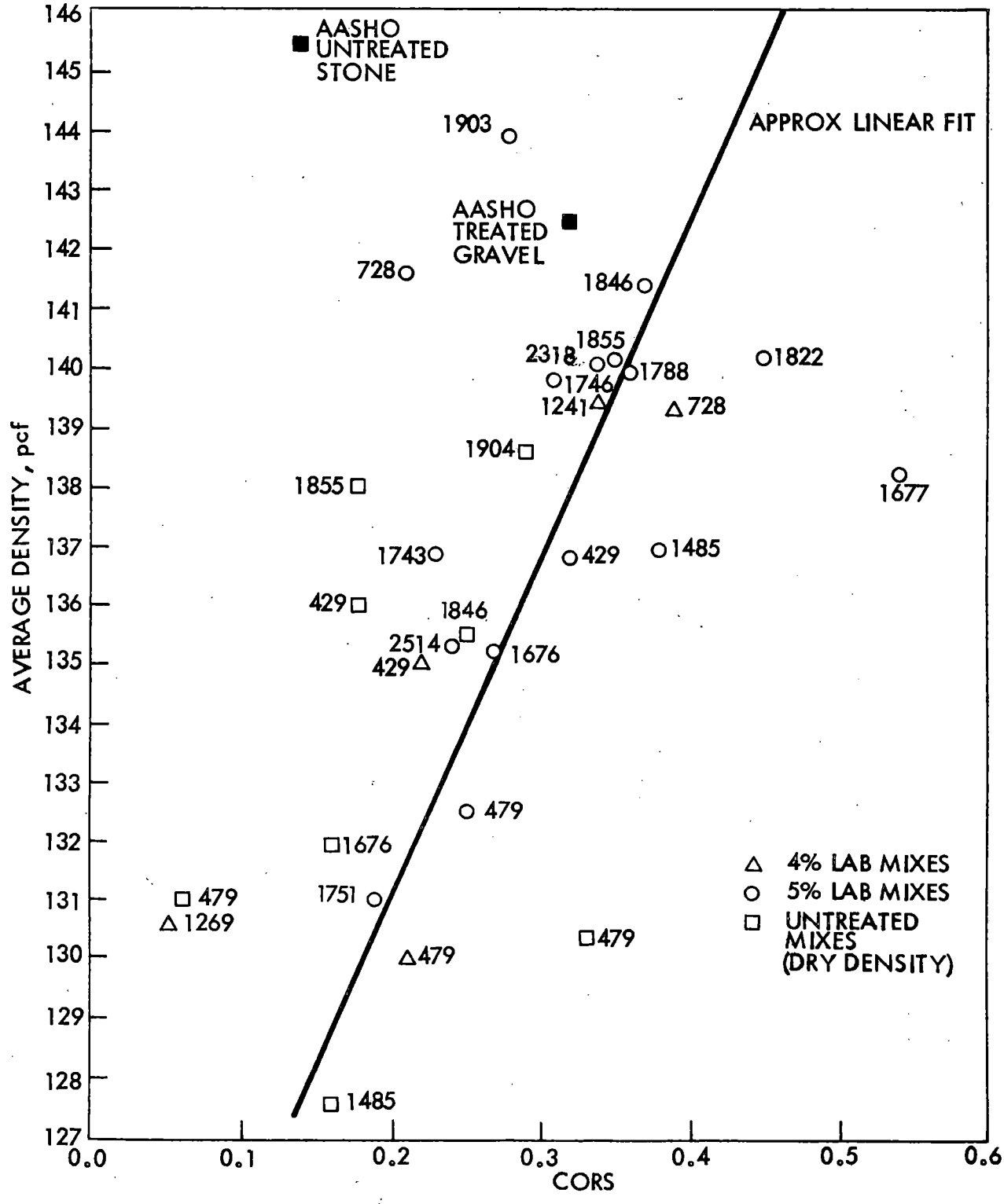

Fig. 16. Average density vs CORS determined on the basis of volumetric strain-axial strain at minimum volume, 10 psi lateral pressure.

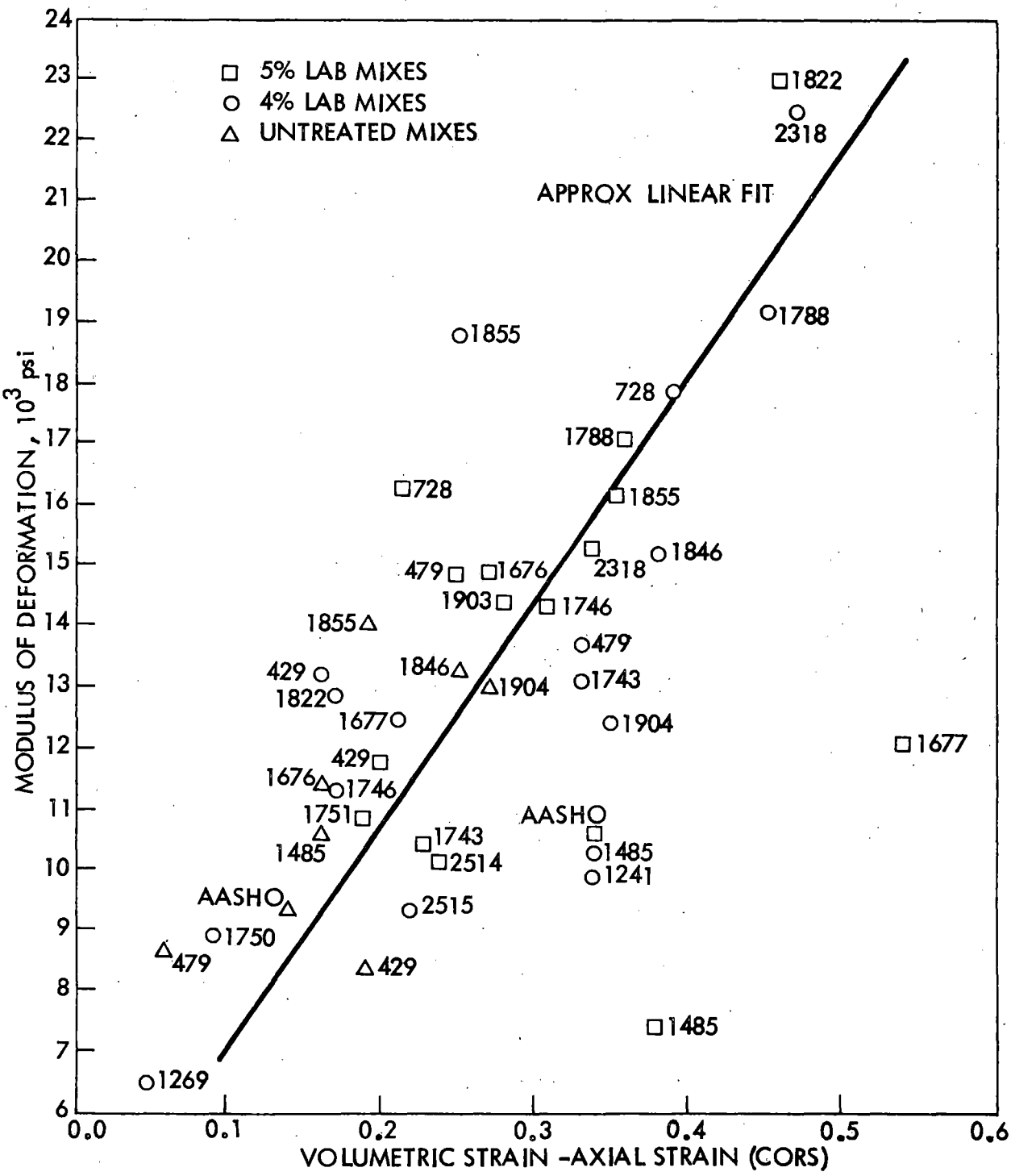

Fig. 17. Modulus of deformation at 10 psi lateral pressure vs volumetric strain-axial strain CORS at 10 psi minimum volume.

Comparison of the CORS for each individual material and mix type from 10 to 20 to 30 psi lateral pressures shows less variation in value than originally anticipated. At least a partial reason for this behavior is that the range of volumetric strain-axial strain at minimum volume between untreated and treated materials increased with increasing lateral pressure. A similar increase occurred between the two AASHO materials, thus tending to provide similar CORS for the various materials at each of the three lateral pressures.

It can be reasoned that as lateral restraint (pressure) is increased to a point of near total confinement, all materials will tend to behave similarly with their individual properties having much less effect than at low lateral pressures. Such reasoning substantiates the use of volumetric strain-axial strain as a means of flexible pavement materials evaluation. However, the variation of CORS with lateral pressure indicates that a knowledge of the lateral pressures that would exist in the field under design loads must be known for the CORS to be valid. Presently there is very little data available that indicate what lateral pressures are developed in flexible pavement structures. A very rough approximation utilizing a Boussinesq solution, assuming Poisson's ratio as 0.5, a 100 psi point load, a 6-in. depth, and offset distance of 1 ft, yielded about 13 psi. It must be recognized that none of the assumptions underlying the Boussinesq solution are met in flexible pavement structures and that Poisson's ratio is not 0.5 for soils. A decrease of Poisson's ratio, however, decreases calculated lateral stresses. Fish and Hoover[2] indicated that Poisson's ratio for the treated materials at minimum volume was about 0.40±. The untreated materials in this

study had a Poisson's ratio of about 0.30±. It is therefore likely that the lateral stress developed would be less than the very approximate figure of 13 psi calculated above. It would appear, from the previous discussion, that the most applicable values of CORS would thus be those obtained at 10 psi lateral pressure.

Variations in CORS within a particular material may occur due to individual test variations and the recording of test data at set increments of strain, and may lead to some minor inconsistencies in the CORS determined for a material. Readings in the minimum volume portion of the triaxial test were taken at intervals of 0.010 in. deflection. Assuming an 8-in. specimen height, 0.010 in. between readings is about 0.1% axial strain. Volume change readings were recordable to 0.01 in. of variation in water level in a 1-in. diameter tube. Assuming a sample volume of 100 cu in., a movement of 0.01 in. in the volume change tube is approximately 0.01% volumetric strain. Volumetric strain therefore changed more slowly than axial strain in this portion of the test, increasing the importance for precise determination of axial strain at which minimum volume occurs. It would be desirable in future studies to obtain continuous monitoring of volume change and axial deflection in order to firmly fix the point of minimum volume more accurately.

The concept presented in the preceding paragraph can be noted in the volumetric strain-axial strain data graphed in Figs. 18 through 27. It can be seen that many points on the plots appear to be grouped vertically. This results from the test data being taken at set intervals of axial deflection during the shear phase of the test. Continuous

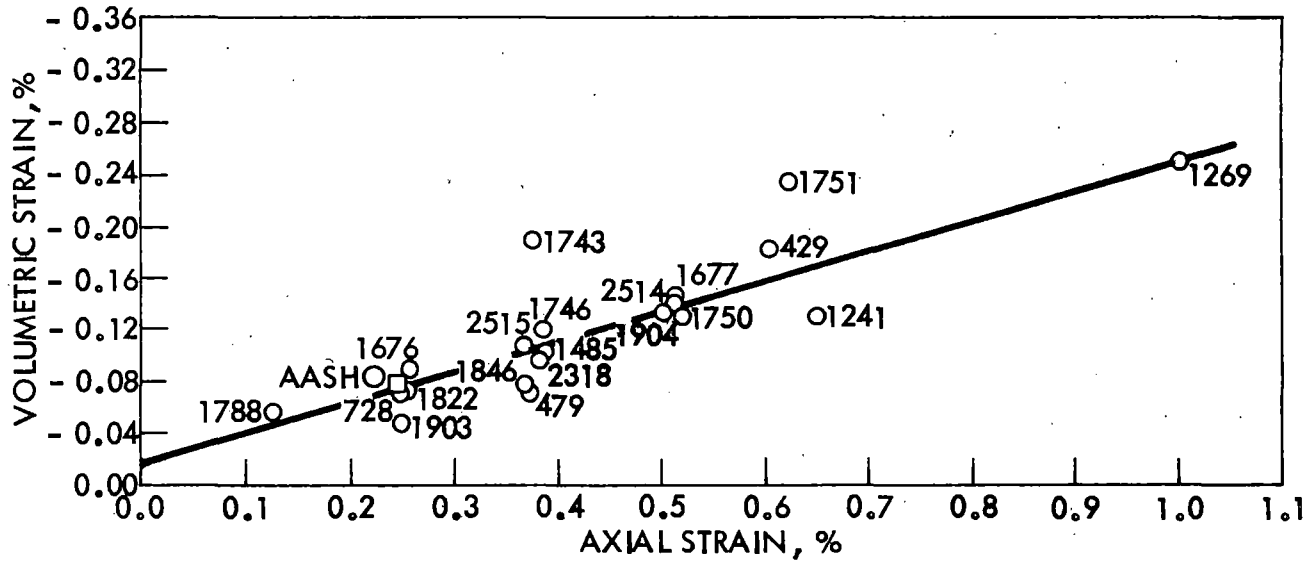

Fig. 18. Volumetric strain vs axial strain at minimum volume, 10 psi lateral pressure, field mixes.

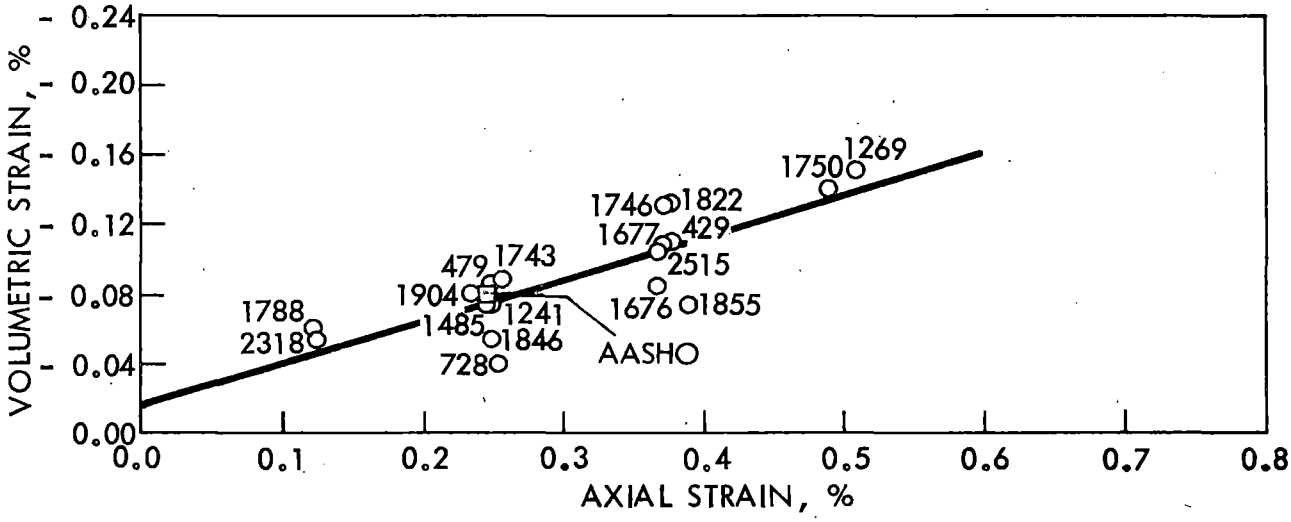

Fig. 19. Volumetric strain vs axial strain at minimum volume, 10 psi lateral pressure, 4% lab mixes.

and even more precise recording of test data would tend to separate the vertical nature of the plot and result in greater precision of pinpointing a CORS value in the laboratory using the techniques described in this report.

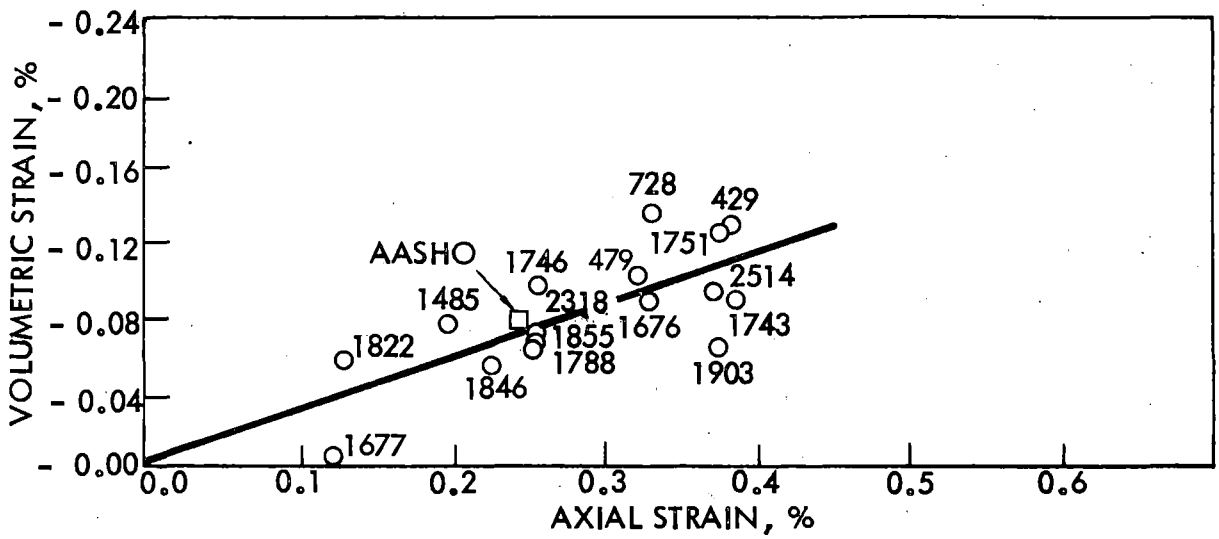

Fig. 20. Volumetric strain vs axial strain at minimum volume, 10 psi lateral pressure, 5% lab mixes.

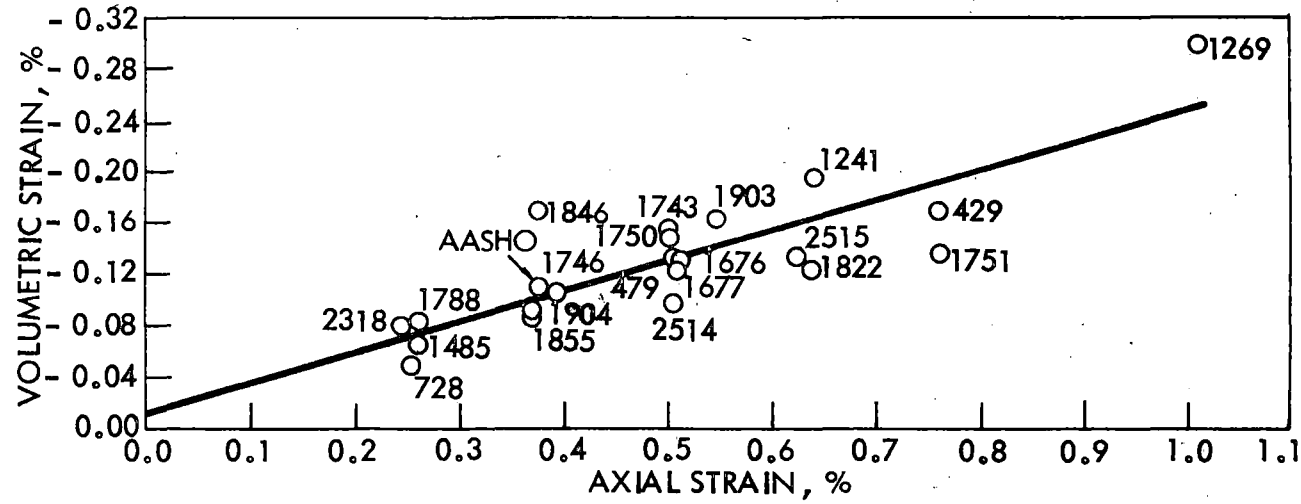

Fig. 21. Volumetric strain vs axial strain at minimum volume, 20 psi lateral pressure, field mixes.

It should be re-emphasized that the values of CORS obtained in this study are based on a very limited number of tests of the AASHO control materials. The quantity of material available was extremely limited. Four tests were run on each AASHO material at 10, 20, 30 and 40 psi

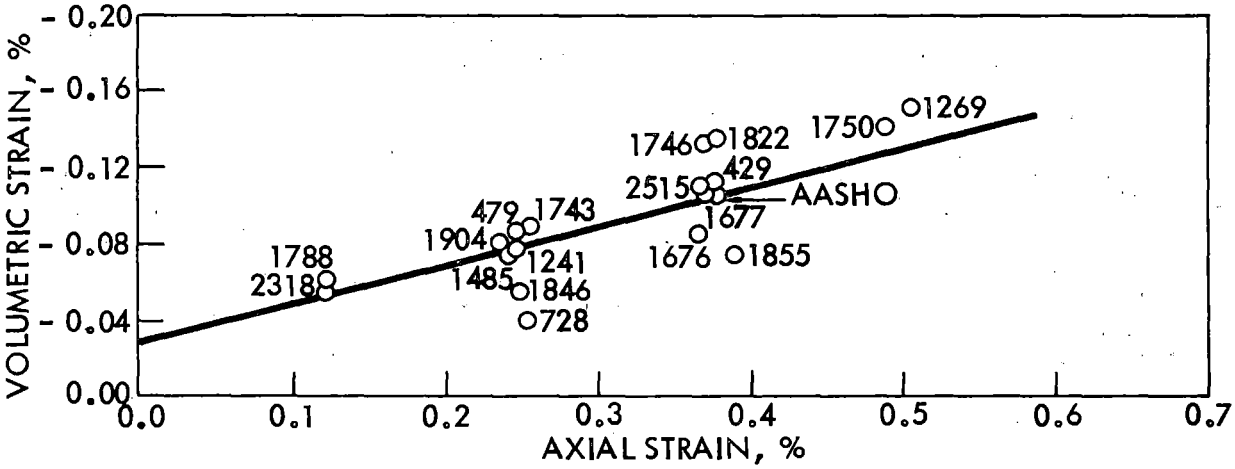

Fig. 22. Volumetric strain vs axial strain at minimum volume, 20 psi lateral pressure, 4% lab mixes.

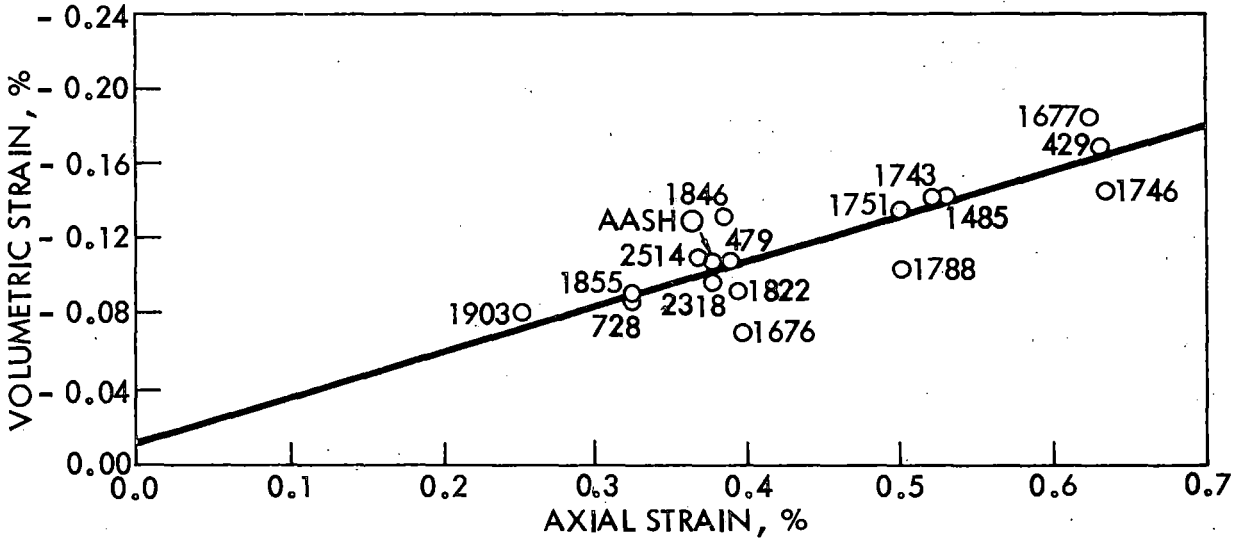

Fig. 23. Volumetric strain vs axial strain at minimum volume, 20 psi lateral pressure, 5% lab mixes.

lateral pressure. This resulted in the CORS at each lateral pressure being determined on the basis of two points (Figs. 13, 14 and 15), one for the AASHO untreated and one for the AASHO treated materials.

CORS Based on other Variables. As previously indicated under Section 2.5.1 of this report, the highest degree of correlation of

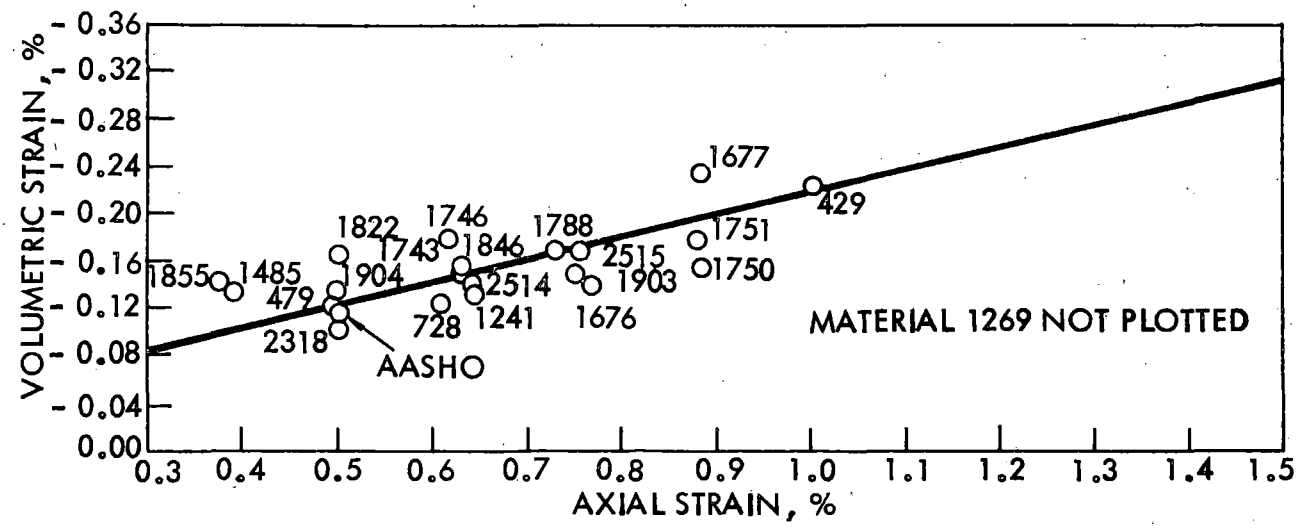

Fig. 24. Volumetric strain vs axial strain at minimum volume, 30 psi lateral pressure, field mixes.

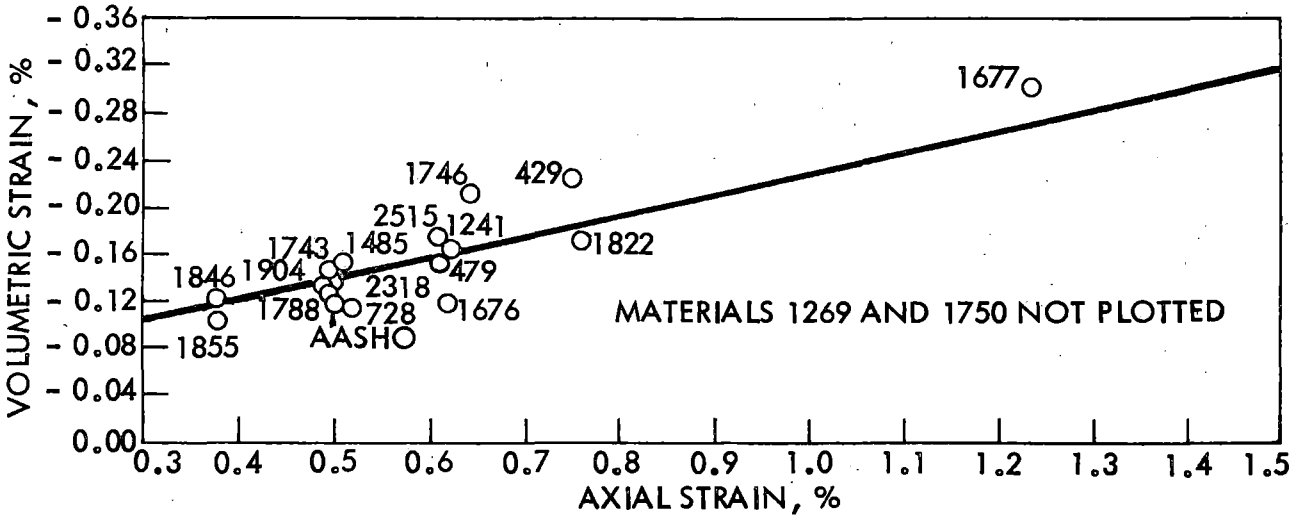

Fig. 25. Volumetric strain vs axial strain at minimum volume, 30 psi lateral pressure, 4% lab mixes.

data was obtained between volumetric strain and axial strain at minimum volume. For comparative purposes only, CORS were developed for other variables at minimum volume conditions using data showing lesser degrees of correlation than volumetric strain-axial strain. Development and use

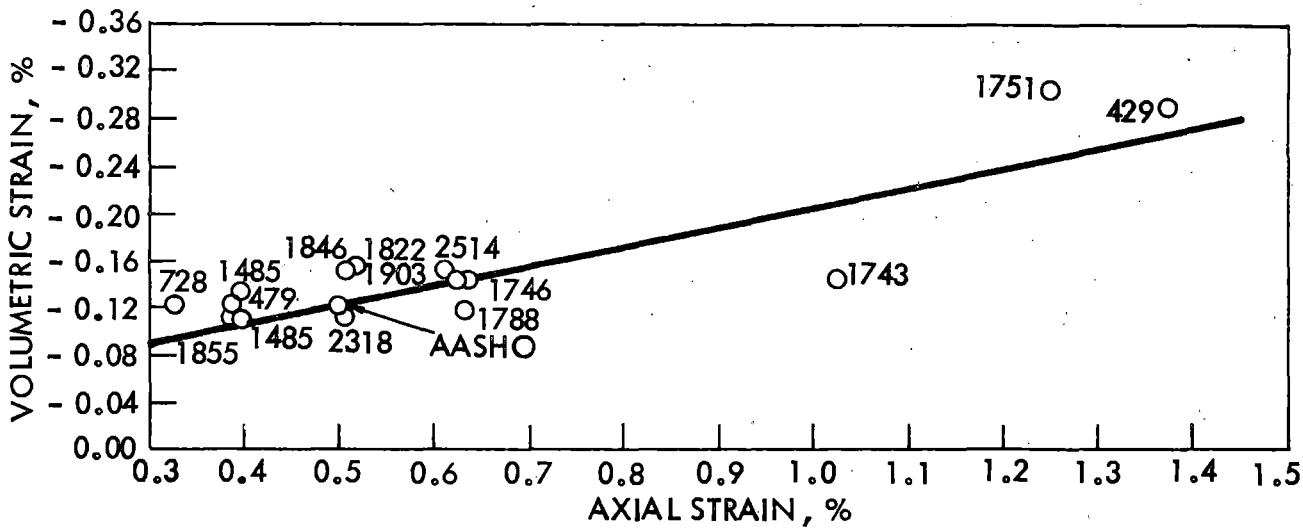

Fig. 26. Volumetric strain vs axial strain at minimum volume, 30 psi lateral pressure, 5% lab mixes.

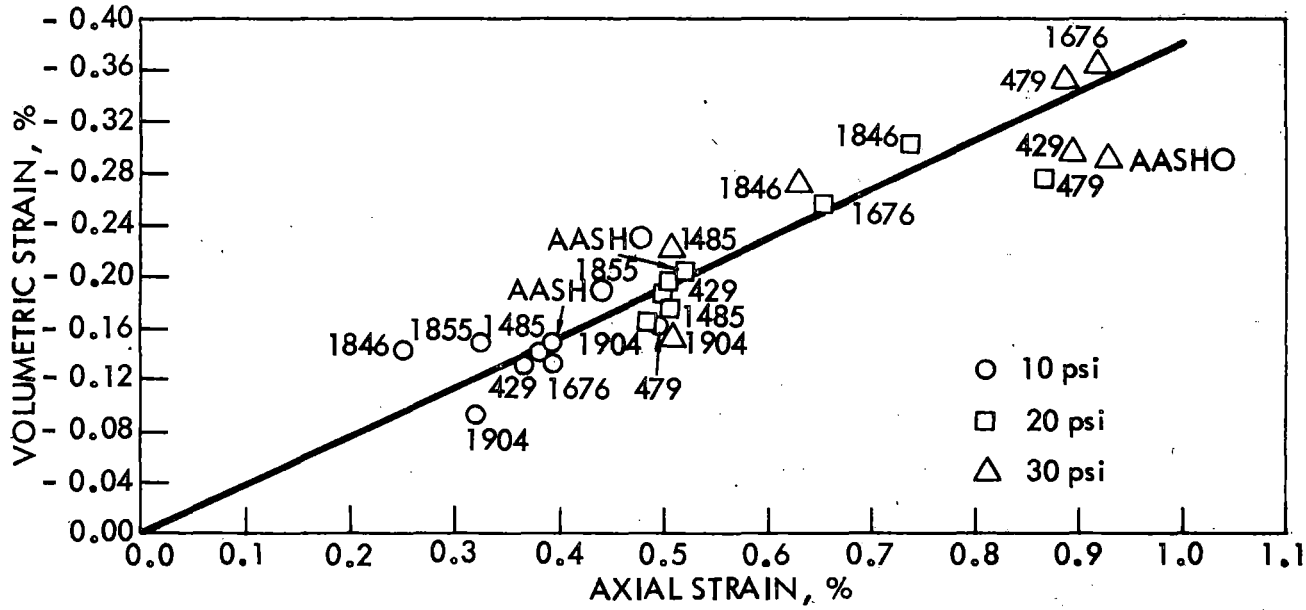

Fig. 27. Volumetric strain vs axial strain at minimum volume, 10, 20 and 30 psi lateral pressures, untreated, optimum moisture content.

procedures were somewhat different than those noted with Figs. 13, 14 and 15, since a single variable was plotted against the two AASHO-CORS and the CORS for each material and mix type were thus determined on the

basis of that single variable. Tables 9 and 10 present the CORS thus determined for the individual variables of (a) volumetric strain, (b) axial strain, (c) modulus of deformation, (d) effective stress ratio, and (e) average modulus of deformation, each at 10 psi lateral pressure and minimum volume. Table 10 also includes the single variable of effective stress ratio (ESR) at maximum effective stress ratio (MESR) failure criteria. The latter is discussed in the next section of this report.

Reasonably good comparisons of single variable CORS based on the volumetric strain ($\frac{\Delta V}{V}$) and axial strain (ε), at minimum volume, are noted with those presented in Table 6. Such comparisons indicate the potential of a simplified triaxial technique for determination of CORS using 10 psi lateral pressure and calculating only the precise axial strain at the precise, but continuously monitored, point of minimum volume.*

CORS determined using the modulus of deformation[2] at 10 psi lateral pressure varied widely within each mix type and material as well as among the various materials. The average modulus of deformation[2] CORS were not consistent with those determined using the modulus at 10 psi and still varied widely within a material for the different mix types although the variability among materials was considerably less.

CORS determined for 10 psi lateral pressure using the value of effective stress ratio (ESR) at minimum volume (MV) indicated relatively

---

*Development of a simplified triaxial test machine to provide a means of quick but reasonably precise determination of test data for development of CORS on granular base materials was originally a part of this project but was rejected by the cosponsors, Bureau of Public Roads.

Table 9. Coefficients of Relative Strength (CORS) Determined from Single Variables.

Material number	Material type	Basis of $\Delta V/V$ at M.V., σ_3 = 10 psi				Basis of ε (axial) at M.V., σ_3 = 10 psi				Basis of modulus of deformation, σ_3 = 10 psi			
		Field mix	4% A.C. lab	5% A.C. lab	Opt. M.C.	Field mix	4% A.C. lab	5% A.C. lab	Opt. M.C.	Field mix	4% A.C. lab	5% A.C. lab	Opt. M.C.
429	Limestone	0.05	0.25	0.29	0.19	0	0.16	0.33	0.18	0.07	0.73	0.52	0
479	Dolomite	0.36	0.31	0.27	0.11	0.17	0.35	0.24	0.01	1.52	0.80	1.00	0.04
728	Dolomite/chert	0.36	0.45	0.18	ND[b]	0.33	0.33	0.23	ND[b]	0.92	1.46	1.20	ND[b]
1241	Gravel	0.20	0.34	–[a]	ND	0	0.34	–[a]	ND	0.88	0.22	–[a]	ND
1269	Gravel	0	0.14	–[a]	ND	0	0	–[a]	ND	0	0	–[a]	ND
1485	Gravel/sandy	0.27	0.34	0.34	0.16	0.15	0.34	0.41	0.16	0	0.28	0	0.34
1676	Limestone	0.31	0.32	0.31	0.19	0.33	0.18	0.23	0.14	1.52	ND	0.99	0.46
1677	Limestone	0.15	0.25	0.54	ND	0	0.17	0.51	ND	1.13	0.62	0.56	ND
1743	Limestone	0.03	0.31	0.31	ND	0.17	0.33	0.15	ND	2.12	0.72	0.32	ND
1746	Limestone	0.22	0.19	0.29	ND	0.15	0.16	0.33	ND	3.03	0.44	0.92	ND
1750	Limestone/dolomite	0.20	0.17	–[a]	ND	0.10	0.01	–[a]	ND	1.38	0.08	–[a]	ND
1751	Limestone/dolomite	0	–[a]	0.21	ND	0	–[a]	0.16	ND	2.12	–[a]	0.38	ND
1788	Dolomite/chert	0.40	0.39	0.38	ND	0.50	0.51	0.33	ND	2.01	1.65	1.32	ND
1822	Dolomite	0.35	0.18	0.40	ND	0.33	0.16	0.50	ND	1.06	0.68	ND	ND
1846	Limestone	0.34	0.41	0.40	0.16	0.18	0.34	0.33	0.34	0.64	1.04	1.04	0.74
1855	Dolomite/chert	0.45	0.35	0.38	0.14	0.51	0.15	0.33	0.23	ND	1.59	1.20	0.86
1903	Gravel	0.43	–[a]	0.38	ND	0.34	–[a]	0.17	ND	0.42	–[a]	0.92	ND
1904	Gravel	0.18	0.33	–[a]	0.30	0	0.36	–[a]	0.24	1.26	0.60	–[a]	0.70
2318	Limestone	0.29	0.39	0.36	ND	0.15	0.51	0.34	ND	1.24	ND	1.06	ND
2514	Limestone	0.19	–[a]	0.30	ND	0	–[a]	0.17	ND	0	–[a]	0.28	ND
2515	Limestone	0.28	0.26	–[a]	ND	0.17	0.16	–[a]	ND	0.24	0.14	–[a]	ND

[a]This percentage lab mix not recommended for testing by ISHC.

[b]Not determined.

Note: CORS shown as zero were actually negative values.

Table 10. Coefficients of Relative Strength (CORS) Determined from Single Variables.

Material number	Material type	Basis of ESR at MESR, σ_3 = 10 psi				Basis of ESR at M.V., σ_3 = 10 psi				Basis of average modulus of deformation			
		Field mix	4% A.C. lab	5% A.C. lab	Opt. M.C.	Field mix	4% A.C. lab	5% A.C. lab	Opt. M.C.	Field mix	4% A.C. lab	5% A.C. lab	Opt. M.C.
429	Limestone	0.35	0.41	0.37	0.23	0.30	0.30	0.14	0.12	0.08	0	0	0
479	Dolomite	0.05	0.39	0.30	0.29	0.49	0.10	0.32	0.26	0.62	0.19	0.32	0
728	Dolomite/chert	0.18	0.31	0.19	ND[b]	0.12	0.23	0.34	ND[b]	0.39	0.52	0.57	ND[b]
1241	Gravel	0.01	0.44	–[a]	ND	0.57	0.11	–[a]	ND	0.36	0.02	–[a]	ND
1269	Gravel	0.38	0.49	–[a]	ND	0.47	0.15	–[a]	ND	0	0	–[a]	ND
1485	Gravel/sandy	0.48	0.53	0.53	0.42	0.02	0.01	0	0.17	0	0.01	0.09	0.21
1676	Limestone	0	0.18	0.19	0.25	0.09	0.57	0.35	0.30	0.49	0.95	0.49	0.10
1677	Limestone	0.05	0.39	ND	ND	0.65	0.32	0.09	ND	0.36	0	0	ND
1743	Limestone	0.04	0.41	0.41	ND	0.66	0.09	0.25	ND	0.46	0.24	0.11	ND
1746	Limestone	0	0.50	0.17	ND	0.78	0.24	0.20	ND	0.80	0.21	0.24	ND
1750	Limestone/dolomite	0.06	0.44	–[a]	ND	0.61	0.28	–[a]	ND	0.32	0	–[a]	ND
1751	Limestone/dolomite	0	–[a]	0.38	ND	0.80	–[a]	0.21	ND	0.38	–[a]	0	ND
1788	Dolomite/chert	0.24	0.35	0.25	ND	0.05	0	0.21	ND	0.57	0.58	0.54	ND
1822	Dolomite	0.34	0.32	0.18	ND	0.15	0.32	0.01	ND	0.40	0.22	ND	ND
1846	Limestone	0.35	0.40	0.33	0.28	0.25	0.15	0.16	0.11	0.20	0.29	0.24	0.21
1855	Dolomite/chert	0.29	0	0.15	0.10	0.02	0.30	0.24	0.24	0.83	0.66	0.63	0.41
1903	Gravel	0.18	–[a]	0.34	ND	0.04	–[a]	0.13	ND	0.20	–[a]	0.26	ND
1904	Gravel	0.04	0.32	–[a]	0.23	0.06	0.12	–[a]	0.25	0.44	0.26	–[a]	0.34
2318	Limestone	0.01	0.27	0.29	ND	0.39	0.12	0.16	ND	0.42	0.55	0.28	ND
2514	Limestone	0.34	–[a]	0.44	ND	0.25	–[a]	0.20	ND	0.15	–[a]	0.09	ND
2515	Limestone	0.33	0.35	–[a]	ND	0.21	0.21	–[a]	ND	0.14	0	–[a]	ND

[a]This percentage lab mix not recommended for testing by ISHC.

[b]Not determined.

Note: CORS shown as zero were actually zero values.

high variability within a material for different mix types as well as among materials. A number of the field mix CORS were high, which may be a reflection of the brittleness of the reheated and recooled mixes when analyzed on a strength basis. It was generally concluded that CORS developed on the basis of a strength parameter alone did not appear valid.

2.5.2. Maximum Effective Stress Ratio Criteria

Specimen conditions at maximum effective stress ratio may not be as indicative of actual field conditions as those at minimum volume. Ferguson and Hoover[3] concluded that stresses at the condition of minimum volume in a triaxial shear test, may be more closely related to actual field conditions than the stresses at maximum effective stress ratio. This conclusion appears especially valid in view of the relatively high value of Poisson's ratio (0.4±) for the bituminous-treated materials[2]. Loading past the point of minimum volume, results in a volume increase and consequently increased lateral strain. Under field conditions this increase of lateral strain would result in increased lateral pressure from adjacent material. In the triaxial test, lateral pressure remains constant, and therefore specimen conditions past the point of minimum volume might not be indicative of actual field response[4].

Coefficients of Relative Strength (CORS), Effective Stress Ratio-Cohesion Basis

A study of the correlation matrices developed for each mix type indicated that the only variables that had reasonably consistent correlations (between mix types) were effective stress ratio and cohesion.

Correlations were consistent among mix types for the 10 psi tests but dropped considerably within a mix type with increasing lateral pressure. Any CORS which were to be developed on the basis of the effective stress ratio-cohesion variables were thus entirely dependent on the increasing lateral pressure. As pointed out previously in this report, the most applicable value of CORS would be those obtained at about 10 psi lateral pressure. Consequently, the subsequent analysis deals only with the materials tested at 10 psi of lateral restraint.

Figures 28 through 31 present the plots of effective stress ratio vs cohesion at 10 psi lateral pressure, on the basis of maximum effective stress ratio criteria. A scattering of the data points is apparent and may be due in part to the manner in which axial load readings were taken at the various increments of axial deformation previously discussed. However, the scattering of data is much more significant in Figs. 28 — 31 than in Figs. 18 — 27 (volumetric strain-axial strain at minimum volume criteria) and are basically due to the following considerations:

- Cohesion is theoretically the same for a given material at all lateral pressures but is determined on the basis of three or more specimens at varying lateral pressures. Cohesion is thus determined as the ordinate intercept of the best fit of the failure envelope at its points of tangency, or near tangency on a Mohr-Coulomb diagram for example.
- The above consideration of point of tangency thus indicates a variation of maximum axial load between specimens of the same material. Any variation of maximum σ_1 is reflected in

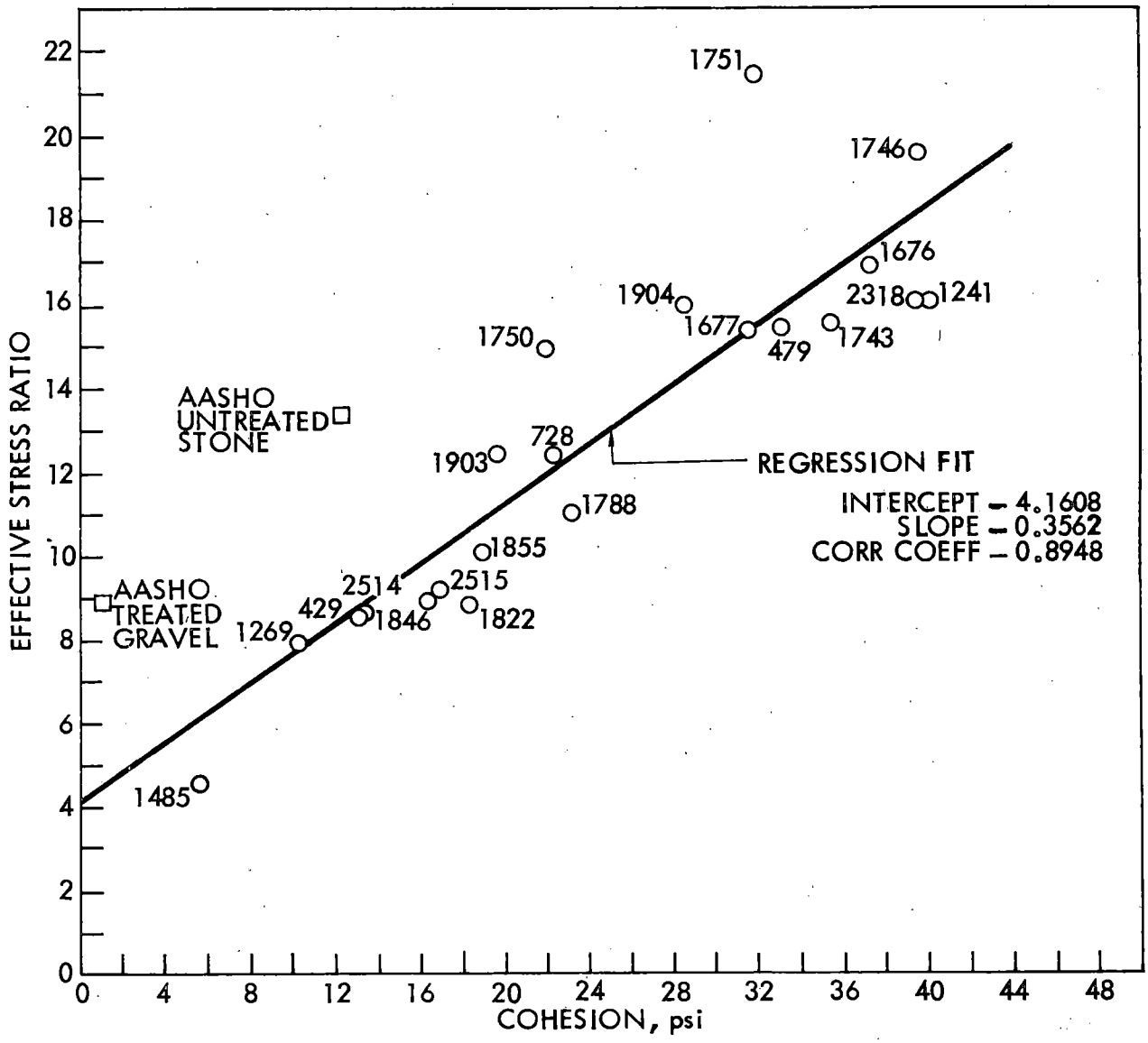

Fig. 28. Effective stress ratio vs cohesion at maximum effective stress ratio, 10 psi lateral pressure, field mixes.

determination of the effective stress ratio $\frac{\bar{\sigma}_1 - \bar{\sigma}_3}{\bar{\sigma}_3}$. The effective stress ratio (maximum) presented in Figs. 28 – 31 is, however, at only one lateral pressure, i.e., 10 psi. There appears to be little chance of using a maximum effective stress ratio which accounts for MESR at all lateral pressures since it

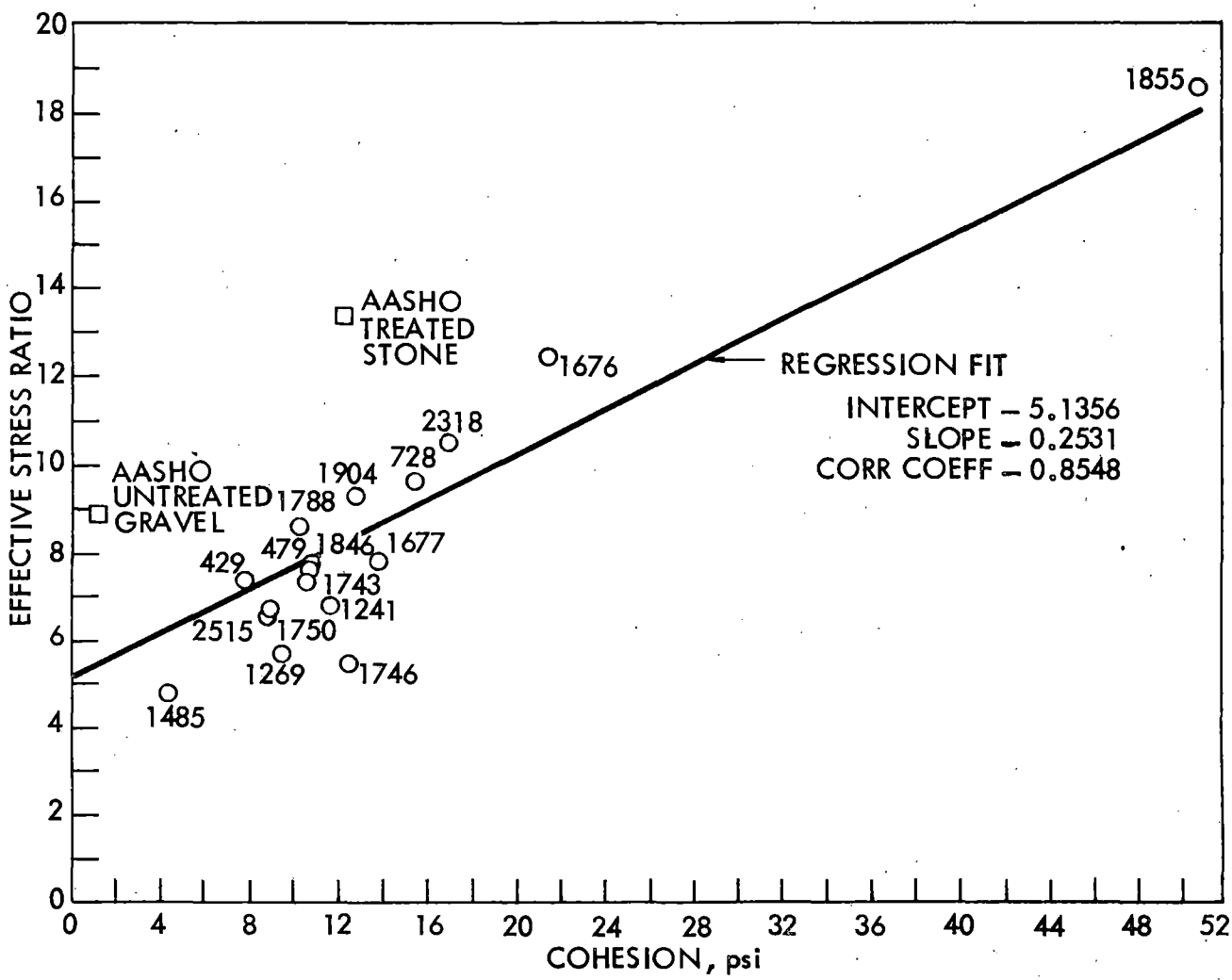

Fig. 29. Effective stress ratio vs cohesion at maximum effective stress ratio, 10 psi lateral pressure, 4% lab mixes.

is noted in Appendix A that MESR generally decreases significantly with increasing lateral pressure. It will be noted in Appendix A that effective stress ratio (ESR) for the minimum volume condition remains somewhat more constant at all lateral pressures.

- Pore pressures measured at maximum effective stress ratio range from negative to positive values indicating either slight

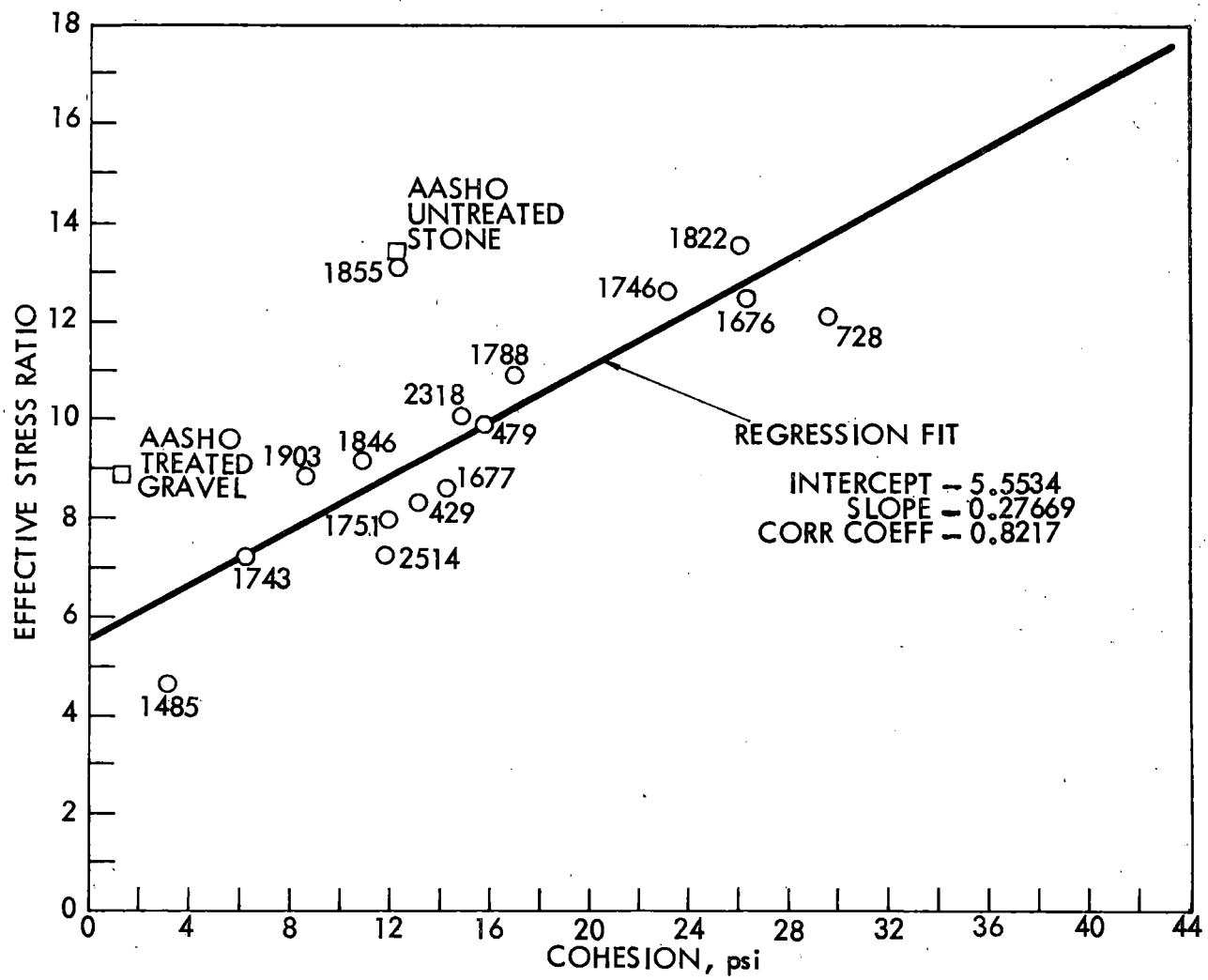

Fig. 30. Effective stress ratio vs cohesion at maximum effective stress ratio, 10 psi lateral pressure, 5% lab mixes.

volume increase or particle interlocking preventing volume increase, respectively. When σ_1 and σ_3 are corrected to $\bar{\sigma}_1$ and $\bar{\sigma}_3$, the effect of negative pore pressure reduces the maximum effective stress ratio from that at which the pore pressure may be slightly positive.

Thus, the above considerations combine to create a definite scattering of the effective stress ratio-cohesion data points in Figs. 28 – 31,

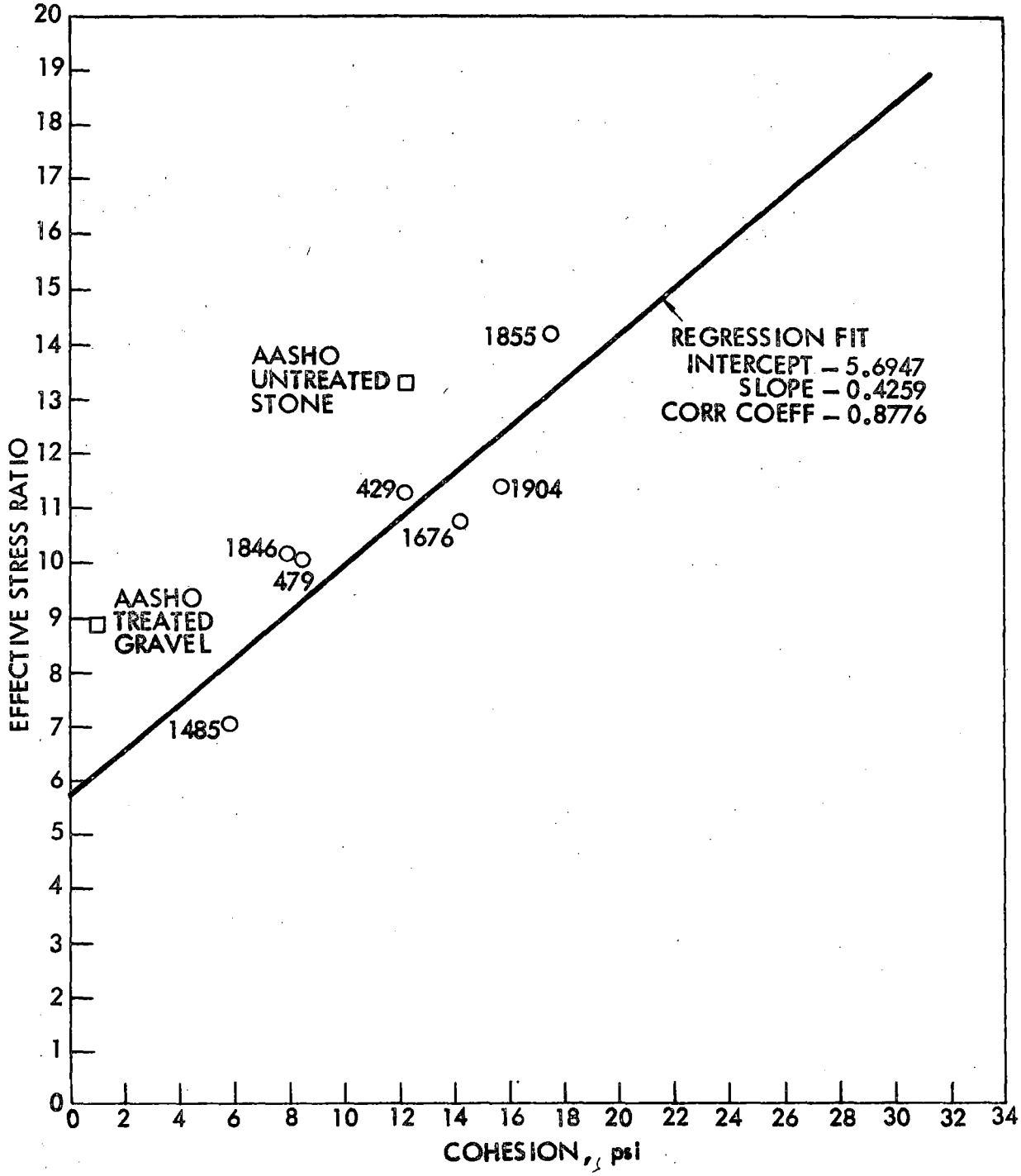

Fig. 31. Effective stress ratio vs cohesion at maximum effective stress ratio, 10 psi lateral pressure, untreated, optimum moisture content.

questioning the advisability of using a strength criteria for determination of CORS.

It was previously noted that the AASHO samples were not included in any of the correlation matrices since they were considered strictly as control samples. While the AASHO materials fit into the correlations at minimum volume, it is obvious in Figs. 28 — 31 that they do not fit into the maximum effective stress ratio criteria. Instead of falling on the ESR-C regression lines, the AASHO materials lay well above same. However, a straight line drawn between the control samples is nearly parallel to the regression fit of the Iowa materials. A study of the dry densities in Appendix A indicates that both the treated and untreated AASHO control mixes had higher densities than their respective laboratory and field mixes. This is probably due, in part, to the very tight gradation control on the AASHO materials previously discussed. It is believed that this density difference is the cause of the AASHO control points lying above the regression line for the Iowa materials. It was shown in Section 2.5 of this report that the CORS determined on the basis of volumetric strain-axial strain were partially a function of density, i.e., in general as density increased CORS increased. The AASHO materials volumetric strain-axial strain values of minimum volume, however, compared favorably with their respective laboratory and field mixes. This indicates that although volumetric strain-axial strain data is somewhat dependent on density, it is not nearly as sensitive to density changes as the strength criteria of ESR-C.

It can be re-emphasized, however, that the data presented are based on a very limited number of tests of the AASHO control materials and the plots of same in Figs. 28 – 31 represent only one AASHO untreated and one AASHO treated specimen, at one lateral pressure.

Figure 32 ranks each material according to its value of effective stress ratio-cohesion, at maximum effective stress ratio. The CORS

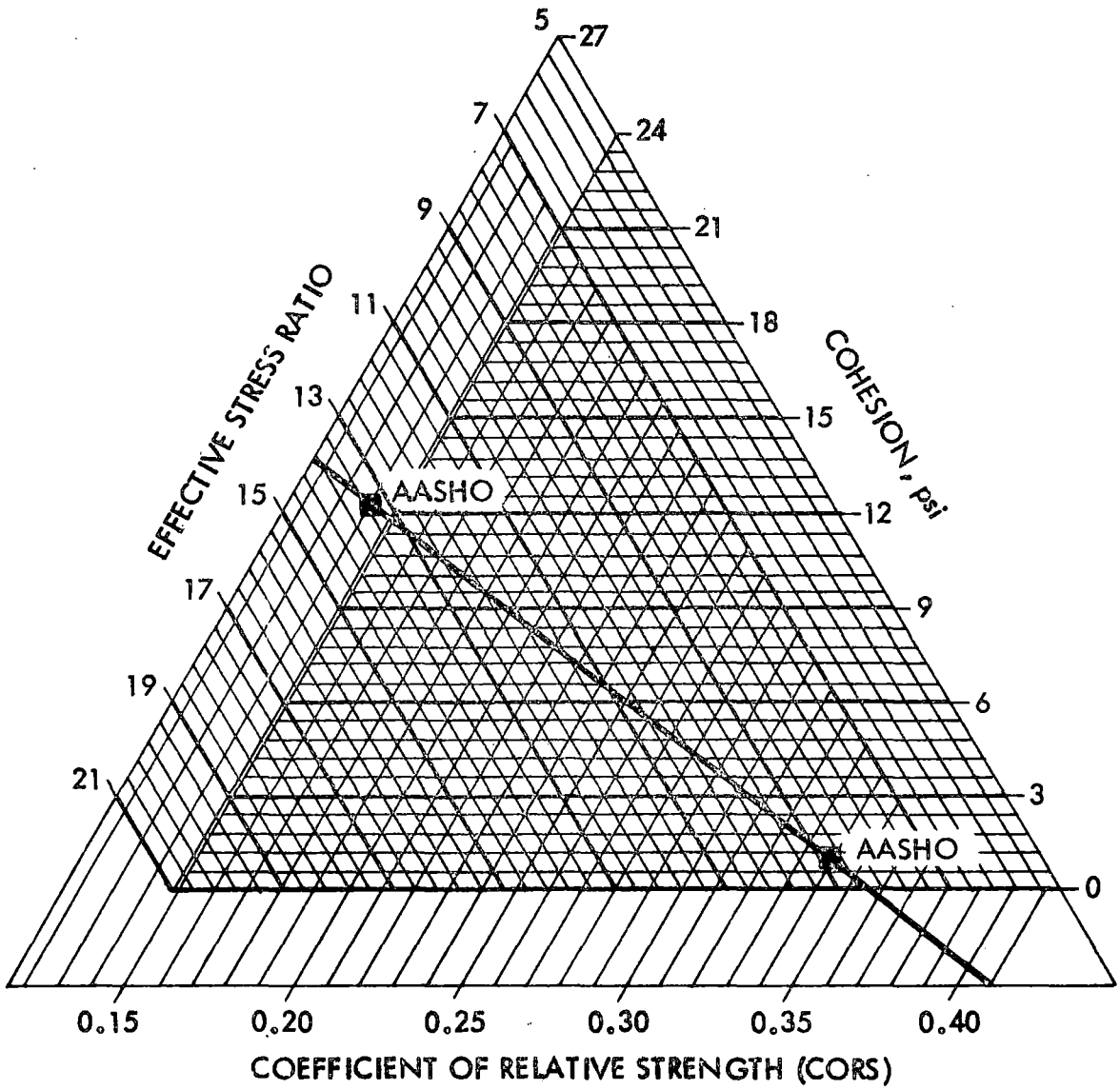

Fig. 32. Triangular chart for determining CORS at 10 psi lateral pressure, maximum effective stress ratio criteria.

thus determined are presented in Table 11. Field mixes are not included due to the high variability of the cohesion term. The extreme range of cohesion in the field mixes (Fig. 28) are probably the result of hardening of the asphalt and length of time prior to reheating for production of test specimens.

Note in Table 11 that in general there is only limited variation in CORS between materials and mix types. Materials 1485 and 1846 indicate no basic change of CORS from untreated to either 4 or 5% asphalt treated. Material 1676 indicates a higher value of CORS for the untreated than either treated mix, a rather unrealistic situation. CORS for material 1855 ranged from 0.07 to a negative value to 0.14 for the untreated 4% and 5% lab mixes respectively. The three pairs of lab mixes each using the same aggregate source, i.e., mixes 1750-1751, 1903-1904, and 2514-2515*, show little variation between asphalt content or aggregate source.

As a consequence of the above observations, CORS determined on the effective stress ratio-cohesion basis at MESR criteria do not appear valid for use in thickness design.

CORS Based on Effective Stress Ratio

The single variable of effective stress ratio (ESR) at maximum effective stress ratio criteria was plotted against the two AASHO-CORS for each material and mix type. CORS were thus determined on that single variable basis and are presented in Table 10. It will be noted that there is a wider variation in CORS between materials and mix types than with the combined ESR-C variables. However, the single

*Respectively, a limestone-dolomite, gravel, and limestone.

Table 11. CORS Determined on the Basis of Effective Stress Ratio-Cohesion Relationship at Maximum Effective Stress Ratio Criteria, 10 psi Lateral Pressure.

Material	4% Lab mix	5% Lab mix	Untreated
429	0.29	0.23	0.18
479	0.25	0.16	0.24
728	0.17	0	ND[b]
1241	0.26	–[a]	ND
1269	0.30	–[a]	ND
1485	0.37	0.39	0.32
1676	0.05	0	0.16
1677	0.22	0.20	ND[b]
1743	0.26	0.31	ND
1746	0.27	0.03	ND
1750	0.29	–[a]	ND
1751	–[a]	0.23	ND
1788	0.24	0.13	ND
1822	ND[b]	0	ND
1846	0.25	0.23	0.24
1855	0	0.14	0.07
1903	–[a]	0.25	ND[b]
1904	0.20	–[a]	0.14
2318	0.13	0.17	ND[b]

[a]This percentage lab mix not recommended for testing by ISHC.

[b]Not determined.

Note: CORS shown as zero were actually negative values.

Table 10. Continued.

Material	4% Lab mix	5% Lab mix	Untreated
2514	—[a]	0.25	ND
2515	0.29	—[a]	ND

variable ESR-CORS does not compare favorably with the combined ESR-C-CORS or with any of the CORS obtained from the minimum volume criteria. In fact, it is observed that some definite reversals occur in the single variable ESR-CORS when compared to the ESR-C-CORS.

2.6. CONCLUSIONS

Coefficients of relative strength determined in this laboratory study are based on a very limited number of control values established from the AASHO materials and should be viewed with this in mind. The validity of the CORS determined can only be fully ascertained after extensive analysis of the pavement field performance where each material and mix type have been used.

1. Volumetric strain-axial strain relationships appear to be appropriate evaluation parameters for determining coefficients of relative strength at minimum volume failure criteria.
2. Coefficients of relative strength determined on the basis of volumetric strain-axial strain tend to vary slightly with lateral pressure, all treated materials tending towards similar values of CORS as lateral pressure is increased.

CORS determined at 10 psi lateral pressure are probably more indicative of actual field conditions.

3. Coefficients of relative strength determined on the basis of effective stress ratio-cohesion, at maximum effective stress ratio criteria, do not appear valid for use in thickness design.

3. PHASE II: REPETITIVE LOAD RESPONSE

The purpose of this phase of the project was to delve into the relatively unknown area of repetitive, or cyclic, axial loading of granular materials in an effort to evaluate the more dynamic stability mechanism(s) of treated and untreated Iowa crushed stones.

The predominant study of this phase centered around the response of asphalt-treated granular base specimens to repetitive loadings, developing equations which provide a more rational basis for further studies of factors affecting deformation under cyclic stress conditions similar to that of a pavement subjected to transient loads. The second study of this phase centered around an unanticipated repetitive load response of untreated crushed stone base materials to slight variations of fines content (No. 200 sieve material) and suggests maximum desirable quantities of fines for various loads. The third and shortest study deals with the minimum volume load response of an asphalt-treated field-mixed material after 100,000 cycles of repetitive loading.

3.1. BEHAVIOR OF GRANULAR MATERIALS UNDER TRIAXIAL COMPRESSION WITH PULSATING DEVIATOR STRESS

J. J. Marley and R. L. Handy*

Reference is made to the major report by Marley and Handy[12] for a detailed analysis of this portion of the repetitive load response

*Respectively, Assistant Professor, Civil Engineering, University of Notre Dame, and Professor, Civil Engineering, Iowa State University.

study. Presented herein is but a summary of the conclusions and potential applications of this research.

A model for behavior of granular material subjected to repeated loads was proposed. This model is based on bonds formed at inter-particle contacts, resistance to rearrangement of particles, and internal structure of the material. Stresses applied to the material are transferred through the bonds, and deformation of the material occurs by breaking of bonds and rearrangement of particles. The total resistance to deformation constitutes an energy barrier to deformation of the material mass, termed the activation energy. This energy barrier may be surmounted by bonds having sufficient thermal and mechanical energy.

Based on this model of resistance to deformation, an equation was developed beginning with the Arrhenius equation of chemical kinetics. Separation of the contributions of various factors to the activation energy enabled determination of their individual effects. Equation (1) was shown to describe the observed behavior of both untreated and asphalt-treated granular materials over the range of variables considered.

$$\ln \dot{\epsilon} = \ln C - \frac{\Delta H^*}{kT_s} + \frac{\beta L}{2A} - \mu p - \alpha T_C \qquad (1)$$

where $\dot{\epsilon}$ = strain rate

C = a constant

ΔH^* = activation enthalpy

k = the Boltzman constant

T_s = the temperature at which shear occurs

β = a material parameter, $\frac{\beta'}{kT_s}$, where β' is the flow unit volume

L = the deviator stress applied to the specimen

A = the cross-sectional area of the specimen

μ = a parameter showing the effect of cell pressure on shear behavior of the specimen

p = the cell pressure

α = a parameter showing the effect of temperature on shear behavior of the specimen

T_c = the temperature of consolidation.

Using the equation developed from the energy barrier concept and an empirically determined relationship between total strain and number of applications of stress, an integrated equation was developed to relate number of applications of stress with other variables at fixed levels of deformation:

$$\ln N_\epsilon = \ln M + \frac{\Delta H^*}{kT_s} - \frac{\beta L}{2A} + \mu p + \alpha T_c \qquad (2)$$

where the coefficients C and M include the proportionality constants for the relationships between shear and axial deformation, frequency of load applications, and conversion of strain to percent strain. Equation (2) describes material behavior over the ranges of deviator stress considered, when other variables were held constant. However, Eq. (2) does not describe observed material behavior over the range of variables considered as well as Eq. (1) which was based only on energy barrier concepts.

Experimental tests, consisting of 64 repeated load triaxial compression tests on an untreated and asphalt-treated granular material provided the following observations:

1. Repeated load triaxial compression tests yield a linear relationship between the logarithm of strain rate and deviator stress. The proportionality coefficient may be used to evaluate volume of a flow unit. This volume was considerably smaller than that reported by others for finer grained materials.

2. Activation enthalpies obtained from coefficients of the relationship between logarithm of strain rate and reciprocal of absolute temperature of shear were about the same as the activation enthalpy of the pore fluid.

3. Repeated load tests yielded a linear relationship between the logarithm of stress applications at constant strain and deviator stress. The proportionality coefficient in the model equation was the same as the coefficient for deviator stress-logarithm of strain rate relationship. Experimentally determined values from each of the two methods are, in most cases, in close agreement.

4. Activation enthalpies determined from Eq. (1), based on strain rate, differ by about 50% from those determined from Eq. (2) based on total strain. Because the multiple linear regression correlation coefficients for Eq. (1) are higher than those of Eq. (2), activation enthalpies determined from Eq. (1) are considered better estimates.

5. Increased temperature of consolidation decreased the deformation rate, but the relationship is poorly defined since only two levels of consolidation temperature were used.

6. Increased confining pressure in the triaxial cell decreased the rate of deformation. This effect is interpreted as a decrease in

the size of flow units as the confining pressure is increased. Test methods used in this investigation did not permit determination of separate effects of normal stress and consolidation pressure.

This study of behavior of granular materials subjected to repeated loads yielded equations which reasonably describe deformation behavior of the materials. However, modification of Eq. (2) will probably be required if it is to describe material behavior as well as Eq. (1). Interdependency of some measured quantities (e.g. volume change, pore pressure and confining pressure) may dictate other modifications of the equations as their effects become more completely understood. Further investigation based on the equations proposed herein seem justified in order to confirm, and extend to a wider range of materials and other variables, the findings of this investigation. The model equation describes material behavior under stress conditions very similar to those imposed on pavement structures in terms of fundamental parameters which might be used as a rational basis for analysis of pavement deformations.

Equation (2) relates the number of applications of stress to produce a given deformation to those factors which affect the rate of deformation, viz., activation enthalpy, temperature, imposed stress, confining stress and flow unit size.

Application of this equation to design or analysis of prototype pavements will require empirical correlations between laboratory behavior and field performance. Because confining stress in a prototype pavement is variable depending on depth, vertical stress, and material properties, conditions of confining stress in prototype pavements

are difficult to simulate in laboratory tests, introducing the need for correlations between laboratory test and pavement performance.

Activation enthalpy can be determined in the laboratory and can be considered constant for the duration of the testing procedure. However, in the case of asphaltic concrete or asphalt-treated material, the chemical changes occurring in asphalt cement due to several years exposure to climatic elements may have considerable effect on activation enthalpy of the material. This effect should be determined or accounted for from experience to make the equations applicable to prototype pavements.

The dwell time of the imposed stress was held constant in this investigation. Since experience has shown that the greatest distress or deformation of flexible pavements occurs where traffic stress is static or slow moving, it is probable the time that stress remains on the pavement affects the rate and amount of deformation caused by a given number of applications. The effect on deformation due to variable dwell time could be determined by laboratory experimentation and probably field correlation. Other variables also should be considered, for example effects due to mixed traffic, such as wheel or axle load equivalency. These variables have been mentioned to illustrate some of the work necessary to extend findings from laboratory research described here to applications in prototype installations.

This discussion has assumed that a criterion of pavement performance can be based on limiting or specified deformations. This is tantamount to saying that a pavement "fails" when it reaches some amount of deformation, as opposed to rupture of the pavement mass. This

deformational criterion of pavement performance is essentially that used in the analysis of results from the AASHO Road Test (Highway Research Board Special Report 61E).

In that analysis, a pavement was considered to have "failed" when the present serviceability index (PSI) reached a given level. The equation for PSI indicates it is a function of measured pavement deformations represented by slope variance and rut depth, and localized rupture represented by cracking and patching. The major factor in serviceability loss was slope variance.

Since the equation used to analyze results of the AASHO road test and Eq. (2) are both based on deformation criteria, it may be instructive to compare Eq. (2) and the AASHO equation which was developed by using curve-fitting techniques.

The AASHO equation is

$$\frac{(C_o - p)}{(C_o - C_1)} = \left(\frac{W}{\rho}\right)B \qquad (3)$$

where p = the present serviceability index

C_o = the initial serviceability index

C_1 = the "failure" serviceability index

W = the weighted number of axle applications when the serviceability index is p

ρ = the weighted number of axle applications when $p = C_1$ or the number of axle applications to cause "failure"

B = an exponential multiplier which accounts for imposed stress, axial configuration (single or tandem) and pavement structure.

Taking logs of both sides of Eq. (3) gives

$$\log \left(\frac{C_o - p}{C_o - C_1}\right) = B(\log W - \log \rho). \tag{4}$$

For comparison, if the temperature is constant, the following equation may be written

$$\epsilon^3 = Z't \exp \frac{\beta L}{2A} \exp - \mu p \tag{5}$$

where Z includes effects of activation enthalpy and consolidation temperature. Making the same substitutions as in Eq. (2) to obtain an expression in terms of number of applications,

$$\epsilon^3 = Z'N \exp \frac{\beta L}{2A} \exp - \mu p. \tag{6}$$

Taking logs of both sides gives

$$3 \ln \epsilon = \ln Z' + \ln N + \frac{\beta L}{2A} - \mu p. \tag{7}$$

Comparison of Eqs. (4) and (7) indicates that on the left side of both equations is a logarithmic measure of deformation — serviceability loss in the case of Eq. (4) and percent strain in the case of Eq. (7). Both have a logarithmic intercept, ρ in Eq. (4) and Z' in Eq. (7). Both utilize a logarithmic measure of the number of load applications, W in Eq. (4) and N in Eq. (7).

The nature of the effect of stress intensity is different in the equations since this is included in the multiplier B in Eq. (4) and as a separate additive term in Eq. (7). Equation (7) also includes a term to account for confining pressure. It may appear that no such term is included in Eq. (4), but since confining pressure in a prototype pavement is a function of depth, vertical stress intensity, and material properties, an effect of lateral pressure is probably included

in Eq. (4). This is because the multiplier B includes effects of load intensity in addition to depth and relative strength coefficients for each layer of the pavement structure.

The relationships between AASHO equations and those developed in this study cannot be determined without a more complete knowledge of material behavior under repetitive loading conditions determined by further laboratory studies and correlation with performance of prototype pavements. However, it is significant that the quantities that control deformation based on theoretical considerations and experimentally verified in this study, are remarkably similar to those quantities which provided the best fit in the empirical curve-fitting techniques used in analyzing AASHO test road results.

3.2. EFFECT OF FINES CONTENT OF GRANULAR MATERIALS UNDER REPETITIVE LOAD TRIAXIAL TESTS

E. G. Ferguson and J. M. Hoover*

3.2.1. Introduction

Initially begun as a preparatory study of untreated materials to repetitive loading response for use with the preceding study, this portion of the project was expanded to enable a suggestion of maximum desirable quantities of fines for various cyclic loadings. The variables of primary interest were applied load, duration (time) of load

*Respectively, Instructor and Associate Professor, Civil Engineering, Iowa State University.

application and quantity of -#200 sieve material present in the test specimens.

3.2.2. Materials

Two crushed stones were used for this portion of the project. Each was previously studied in project HR-99, thus providing significant background information.

The materials are as follows:

1. A weathered, moderately hard limestone of the Pennsylvania System obtained from near Bedford, Taylor County, Iowa. Hereafter referred to as the Bedford sample. The system outcrops in nearly half of the state. Formations in this system are generally soft and contain relatively high amounts of clay.

2. A hard dolomite obtained from near Garner, Hancock County, Iowa. Hereafter referred to as the Garner sample. From the Devonian System, this material is very uniform and has shown remarkable similarity through several counties.

Reference is made to the HR-99 Final Report[1] for the detailed mineralogical, chemical and engineering properties of the Bedford and Garner samples.

3.2.3. Specimen Preparation

The specimens used for this investigation were compacted by vibratory compaction[1]. Previous work has shown that the moisture-density relationship for vibratory compaction differs somewhat from that determined through use of standard Proctor compaction. Vibratory compaction

achieves standard Proctor density but at a slightly lower moisture content. Therefore, the specimens were compacted at optimum moisture content as determined by vibratory compaction studies. The procedure for specimen preparation was as previously described in Section 2.2.2 of this report.

Following compaction, height of each specimen was measured while in the mold. They were then extruded, weighed, wrapped in two layers of Saran wrap and aluminum foil, and the ends sealed. The specimens were then cured in an atmosphere of about 75°F and near 100% relative humidity. Prior to testing each specimen was again weighed and the height and diameter measured.

3.2.4. Triaxial Compression Apparatus

The testing machine used in this study was fabricated by the ISU Engineering Shop to specifications established by the Soil Research Laboratory. The cell was a standard triaxial cell capable of handling 4-in. diameter by 8-in. high specimens.

Load was applied by a hydraulic cylinder, activated by an Enerpac Program control center. Timer, counter and several pressure switches manufactured by Enerpac provided control over the magnitude of the applied load and length of dwell time that the load was maintained. At the end of each dwell time (length of load application) the load rapidly decreased to zero and was immediately reapplied. No control of the rate of loading or unloading or the length of time at zero load was attempted but was set as dictated by the system used. In all cases the load dropped to zero and remained there for at least 0.1 sec or more.

Measurement of applied load was accomplished by use of a Dillon Series 200, 15,000-lb capacity load cell and Dillon Type B meter read-out.

Positive and negative pore pressures at the base of the specimen were measured with a 0 to - 100 psia pressure transducer manufactured by Consolidated Electrodynamics and read by a Daytronic Corporation Model 300D Amplifier-Indicator with Type 93 strain gage input module. The indicator was calibrated to read directly in pounds per square inch with an arbitrary zero reference taken at atmospheric pressure.

Volume change was measured with a unit developed by the Soil Research Laboratory having a direct reading precision of about 0.05 cu in. Vertical displacement was measured by an LVDT having a direct reading precision of 0.003 in.

A six-channel Brush oscillograph was used to monitor all output signals, allowing continuous recording of load, volume change, deflection and pore pressure.

3.2.5. Results

A total of 52 Garner specimens were used in this study. All were tested at a lateral pressure of 10 psi so that the effect of cyclic loading could be better studied at a lateral restraint condition more closely approximating that of a granular base course. The variables of loading during the drained tests were thus reduced to only the magnitude of load and length of time load was applied (dwell time).

Five axial loads were used ranging from 1150 to 1700 lb resulting in effective stress ratios* of from 9.16 to 14.4. This range of stress ratios was within the failure criterion of minimum volume and maximum effective stress ratio as determined by the standard test previously described. Three dwell times were used: 0.25, 0.50, and 1.00 sec.

Fifteen Bedford specimens were tested at a lateral pressure of 10 psi, dwell time of 0.50 sec, and applied axial load of 700 lb, the latter giving a maximum effective stress ratio of about 5.65. The 700-lb axial load was at about the point of minimum volume as determined by the conventional triaxial test.

In order to acquire information on the migration of moisture and fines during testing, each specimen following testing was divided into three equal segments, i.e., top, middle and bottom. Moisture content and particle size distribution of each segment was determined. These results allowed calculation of variation of moisture content and amount of No. 200 material. Though slight variation of both moisture and fines was noticeable between top, middle and bottom of each specimen, no discernible relationships were ascertained.

Twenty-one of the 52 Garner specimens were tested at an axial load of 1700 lb and a dwell time of 0.50 sec. As testing on this group progressed, it became evident that variation of fines content had a pronounced effect on failure rate of the specimen. By dry sieving only, the fines contents were altered in a less than rigorous manner. Following repetitive testing, the variation of fines, averaged for the three segments of each specimen, ranged from 2.11 to

---

*Effective stress ratios in this study are defined as $\frac{\bar{\sigma}_1}{\bar{\sigma}_3}$.

17.8% by total dry weight. The amount of fines present in each specimen prior to compaction was not determined. Consequently, the amount of degradation occurring during compaction and loading was not determinable. Though it is possible that the fines content observed following testing was somewhat greater than that of the original material, interpretation of degradation from Project HR-99[1] indicate a likely maximum increase of fines of about 1% by dry weight.

Previous studies have shown that excess fines are detrimental to the performance of a granular base course material[4]. Significance of fines content can best be illustrated by its affect on rate of axial strain during loading, shown in Fig. 33, which presents the axial strain of a number of specimens vs number of cycles. All tests

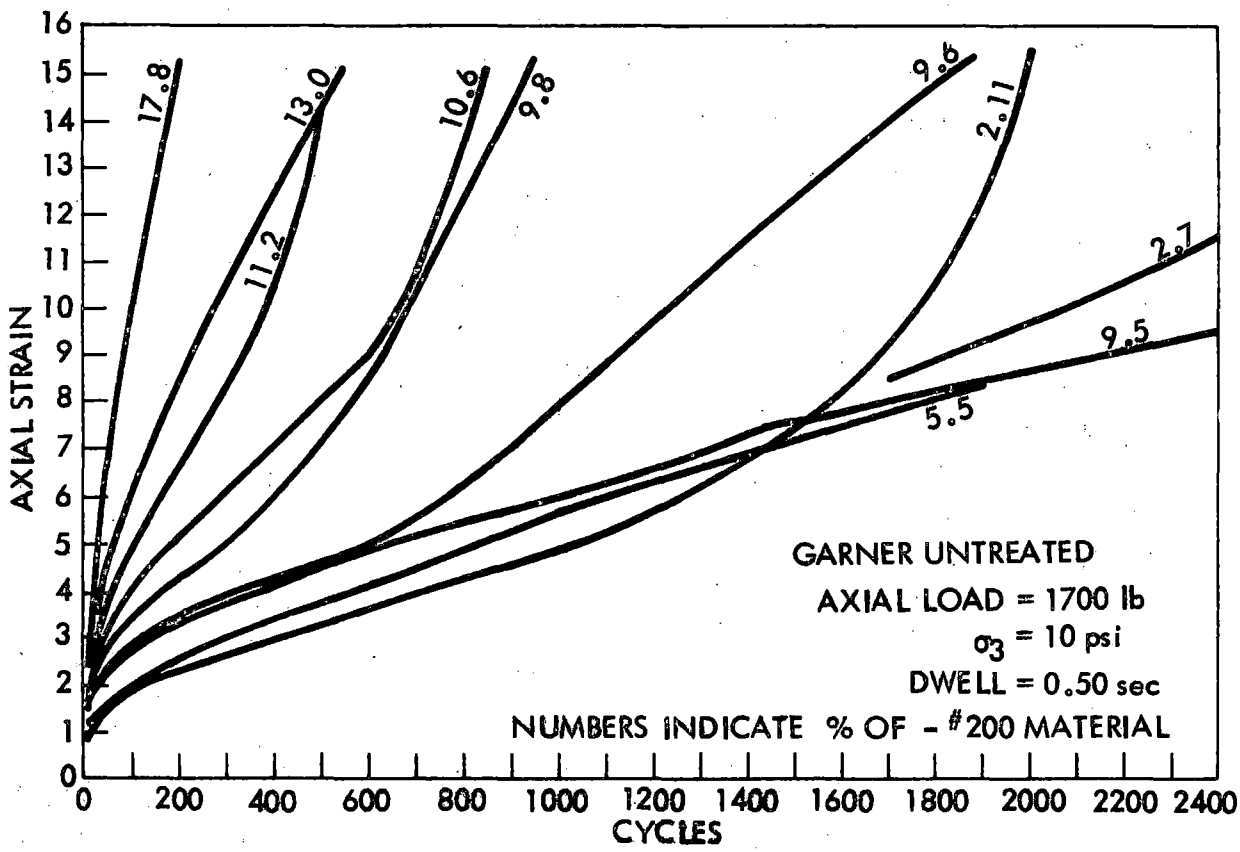

Fig. 33. Effect of fines content on strain rates, Garner stone.

shown have an axial load of 1700 lb applied in conjunction with a confining pressure of 10 psi, giving a maximum effective stress ratio of about 13.4. Dwell time was set at 0.50 sec, thereby reducing the variables to those of the material and not of the loading conditions. The wide variation of results indicate the rapid response of rate of strain increase with increased fine content.

Figure 34 shows similar results for the Bedford crushed stone, only with a much more pronounced effect. The axial load for the Bedford tests was 700 lb, considerably less than that used for the Garner series. A lateral pressure of 10 psi was used giving a maximum effective stress ratio of 5.65 as opposed to 13.4 for the Garner.

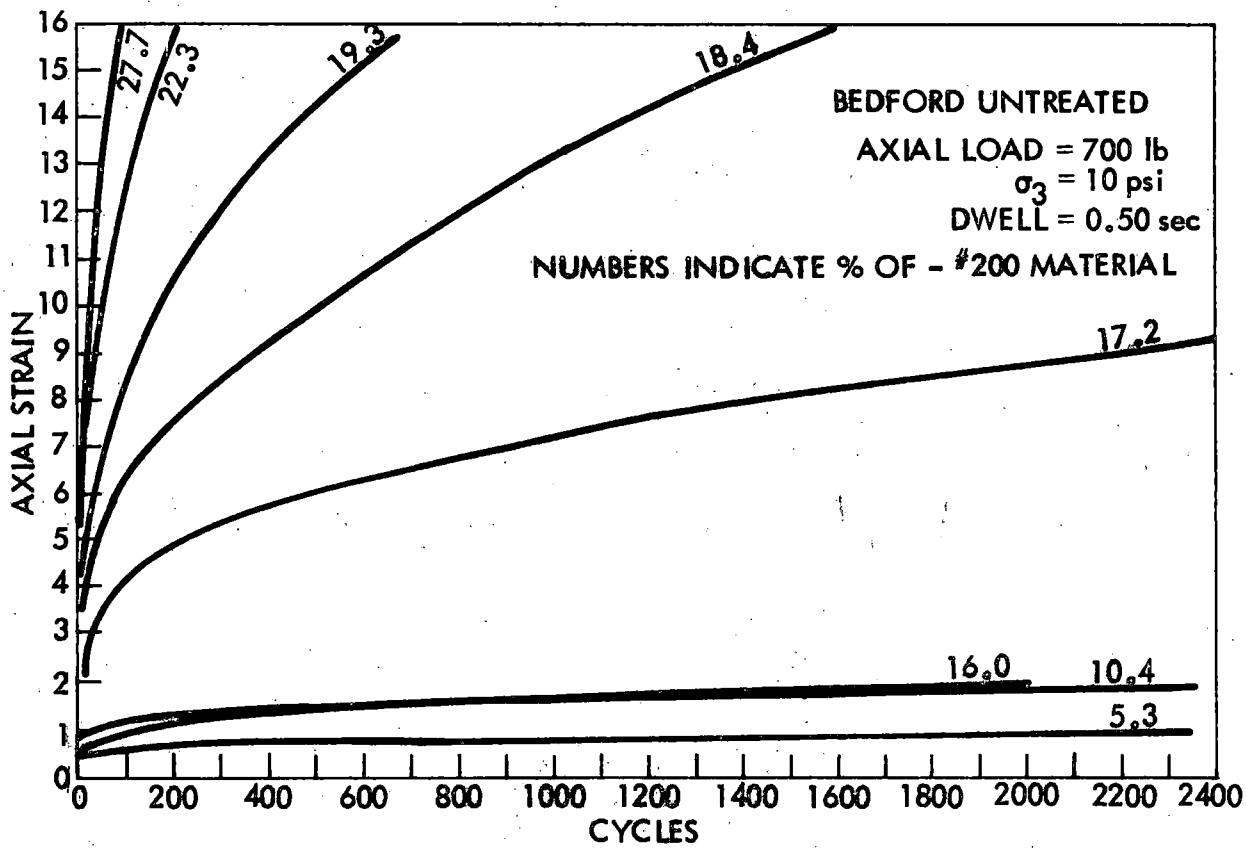

Fig. 34. Effect of fines content on strain rate, Bedford stone.

The three tests shown on Fig. 34 as having fines contents of 16% or less were not tested to failure. The test shown with 16.0% fines was terminated after 25,000 cycles and had undergone only 4.3% axial strain. The test with 10.4% fines developed 3.5% axial strain at 30,000 cycles termination and at 5.3% fines, 14,000 cycles of loading resulted in less than 1% axial strain. It is readily apparent that for this loading condition, a very slight increase of fines can change a relatively stable material to one that will fail after a relatively few heavy load applications.

The effect of fines content can better be presented by plotting axial strain produced after 100 cycles of loading vs fines content after testing, as shown in Figs. 35 and 36. For both materials there appears to be a maximum desirable fines content above which the amount of strain after 100 cycles of axial load increases rapidly with increased fines. Below this point, variation in fines content has little affect on the amount of strain developed. The maximum desirable fines content for the Garner crushed stone was around 9% while for the Bedford it was closer to 16% for the load conditions noted. Fines contents exceeding these amounts appear to decrease the stability of the specimens.

The results presented in Figs. 33 – 36 are for one loading condition and one dwell time. Thus the question arises as to whether these results are unique for these conditions and will vary with changes in stress or dwell time. For the Bedford series all tests were run with a dwell time of 0.50 sec, and axial load of 700 lb, thus providing little insight into this question. The Garner series however covered a wider range of test conditions and were used for analysis of this problem.

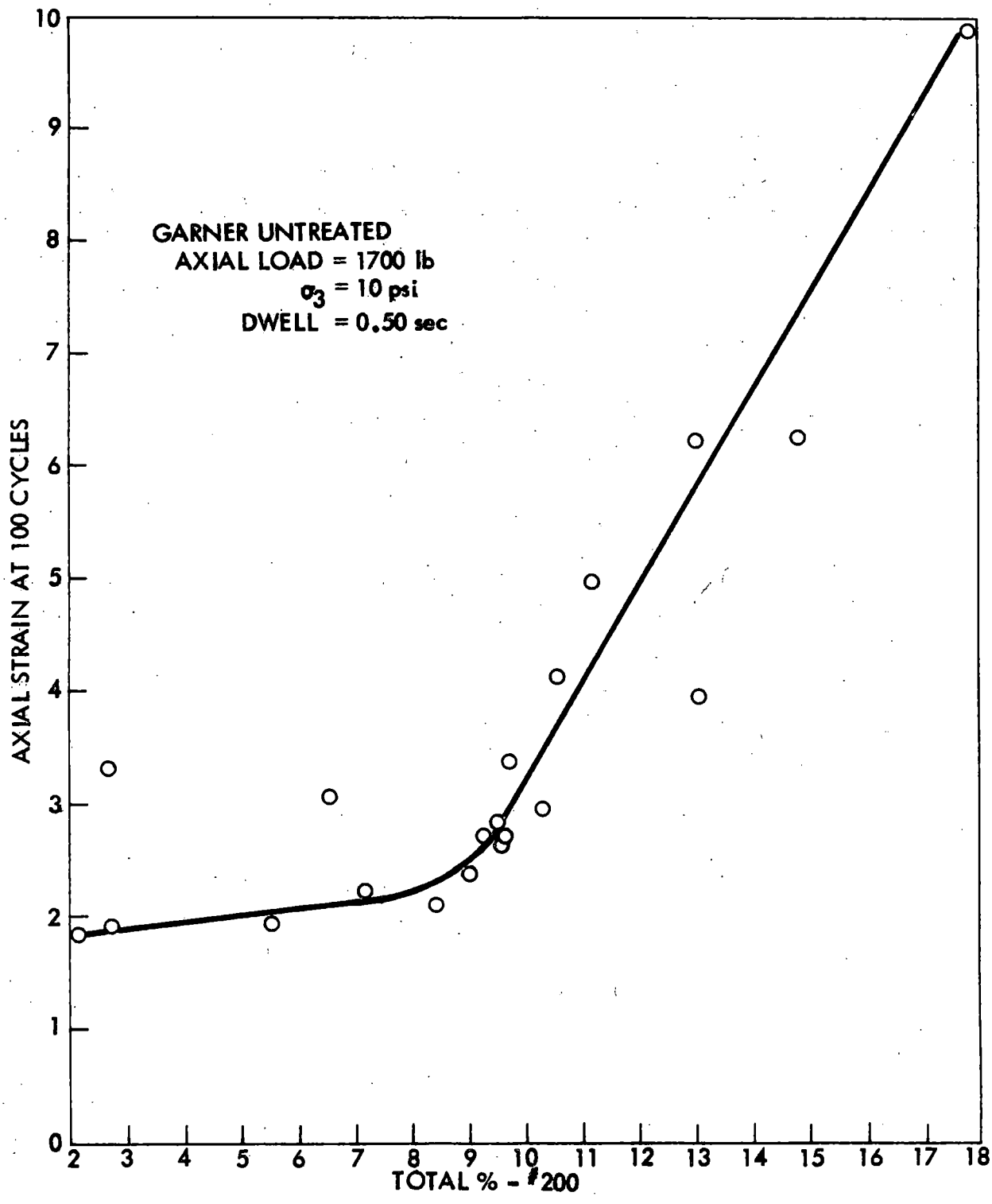

Fig. 35. Axial strain at 100 cycles vs fines content, Garner stone.

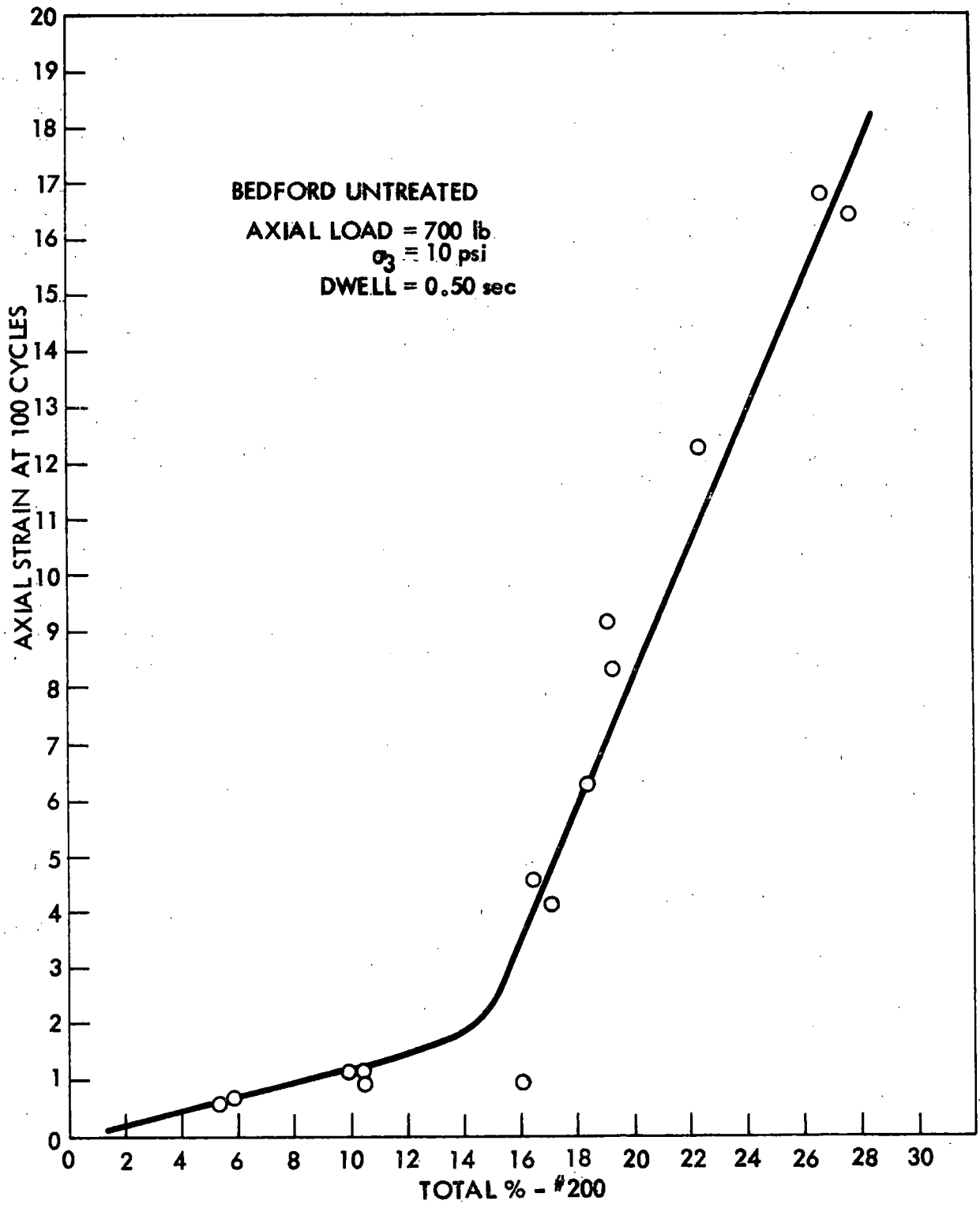

Fig. 36. Axial strain at 100 cycles vs fines content, Bedford stone.

Six Garner specimens were tested at the same stress conditions as shown in Fig. 35 but at dwell times of 0.25 and 1.00 sec and are shown in Fig. 37, in addition to the tests having dwell times of 0.50 sec. Unfortunately the range in fines content of these specimens was quite limited, but each tend to lie within the total range of the 0.50 sec tests. The four tests at dwell time of 0.25 sec appear to agree with the concept of a rapid increase in strain with a small increase in fines content as is shown by the tests having a 0.50 sec dwell time. Since no additional dwell tests having fines contents of less than 9% were performed, it is not certain whether the same trend will occur, though since there is close agreement at this point it appears that the maximum desirable fines content of 9% might also be valid for a dwell time of 0.25 sec. Only two tests were conducted having dwell time of 1.00 sec, with one test generally agreeing with the 0.50 sec tests.

Variations of dwell time, within the range used in Fig. 37, did not appear to have noticeable affect on the test results. It was observed from the recorder charts that essentially all deflection occurred at the instant of application of the load, with only a small additional amount occurring during the initial portion of the dwell period. As dwell time was increased no change from that noted above was detectable. Tests having dwell times of longer duration than those in this study may exhibit a form of progressive failure, or creep, within the period of load application, but it would appear that within the range of 0.25 – 1.00 sec, length of dwell time would produce no form of progressive failure.

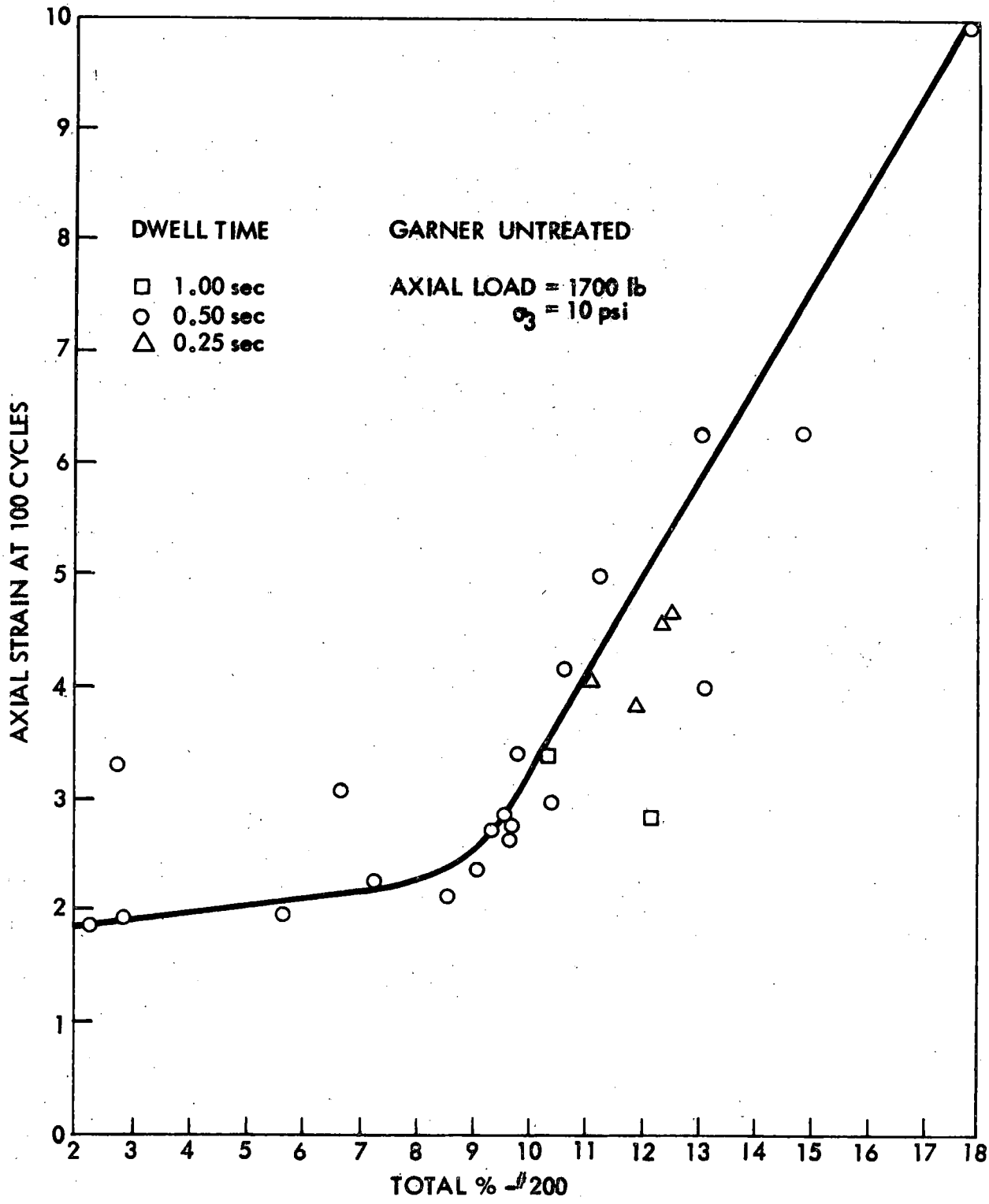

Fig. 37. Effect of dwell time on axial strain-fines content relationship, Garner stone.

The majority of the Garner specimens were tested with an axial load of 1700 lb. A limited number of tests were conducted at lower axial loads and are shown in Fig. 38 in addition to the axial strain-percent fines relationship established for the 1700-lb axial load condition presented in Fig. 35. The specimens tested with an axial load of 1550 lb had fine contents exceeding 9% and therefore showed no inflection point that would indicate a maximum desirable fines content. The tests generally tended to parallel those for the 1700-lb load but at a lower amount of axial strain. The four tests at an axial load of 1400 lb had a pattern similar to the 1700-lb series but appeared to have a higher optimum fines content of near 11%. The three specimens tested at 1150 lb axial load tend to indicate optimum fines of greater than 11%. Generally there appeared to be an increase in the desirable fines content as the applied load decreased.

By assuming that the relationship between axial strain and fines content consists of two straight line segments with the point of intersection being the maximum desirable fines content, from Fig. 38, it is possible to observe a potential effect of stress condition on quantity of fines. The number of Garner samples tested at the lower loads are quite limited but tend to follow the same pattern established in Fig. 35. Lines drawn through these points, parallel to the 1700-lb series, and having a decrease in strain proportionate to the decrease in load, provide at least a hint of the maximum desirable fines content for the load conditions. As was previously noted there appears to be an increase in maximum desirable fines content as the load is decreased.

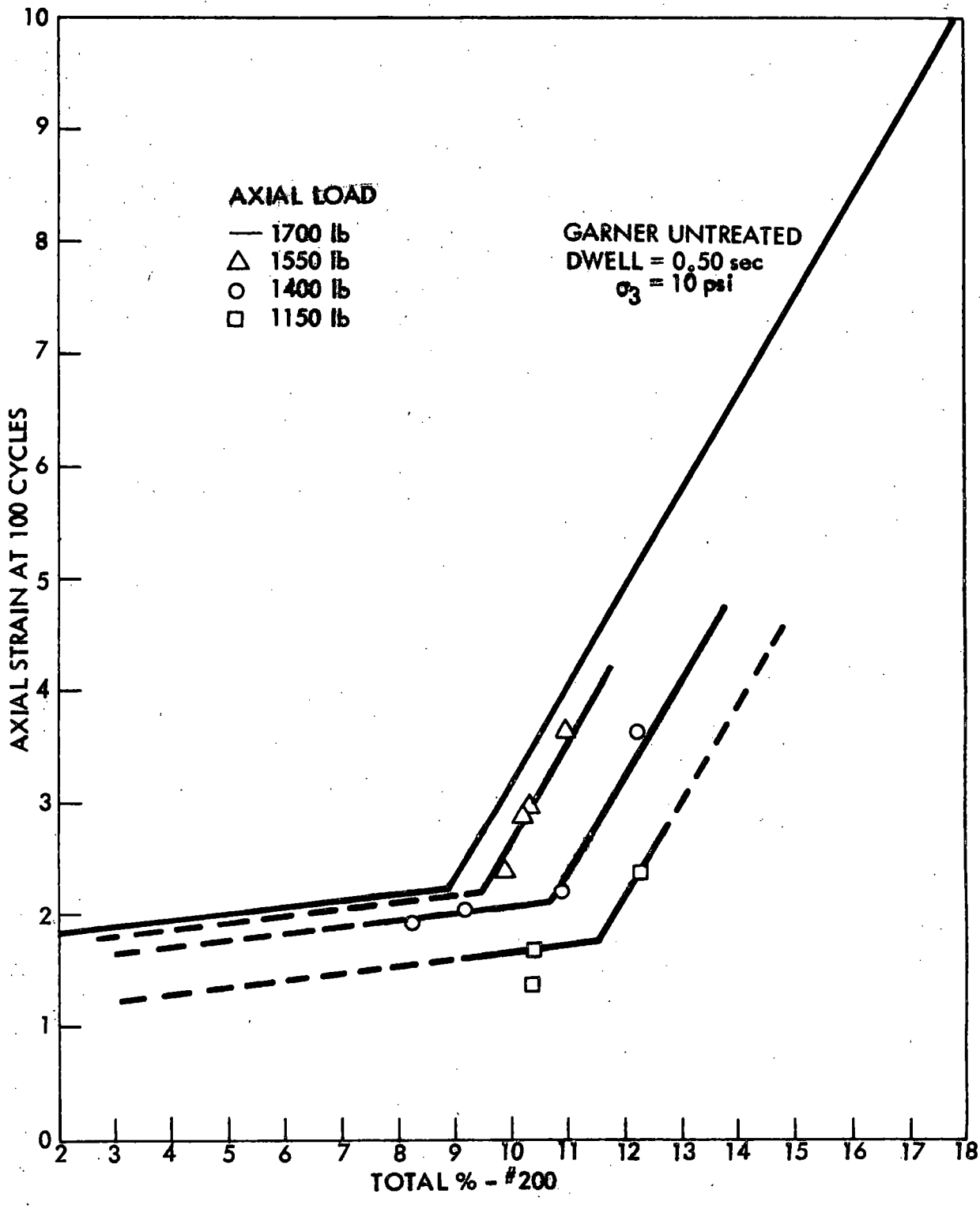

Fig. 38. Effect of axial load on axial strain-fines content relationship, Garner stone.

The fines contents thus noted from Fig. 38 and the average maximum stress ratio of the specimens in each series are shown in Fig. 39 for each of the four loads used for the Garner plus that for the 700-lb series of the Bedford material. The line drawn through the points represents the boundary between stable and unstable states of stress. Stress conditions lying below this line result in relatively low rates

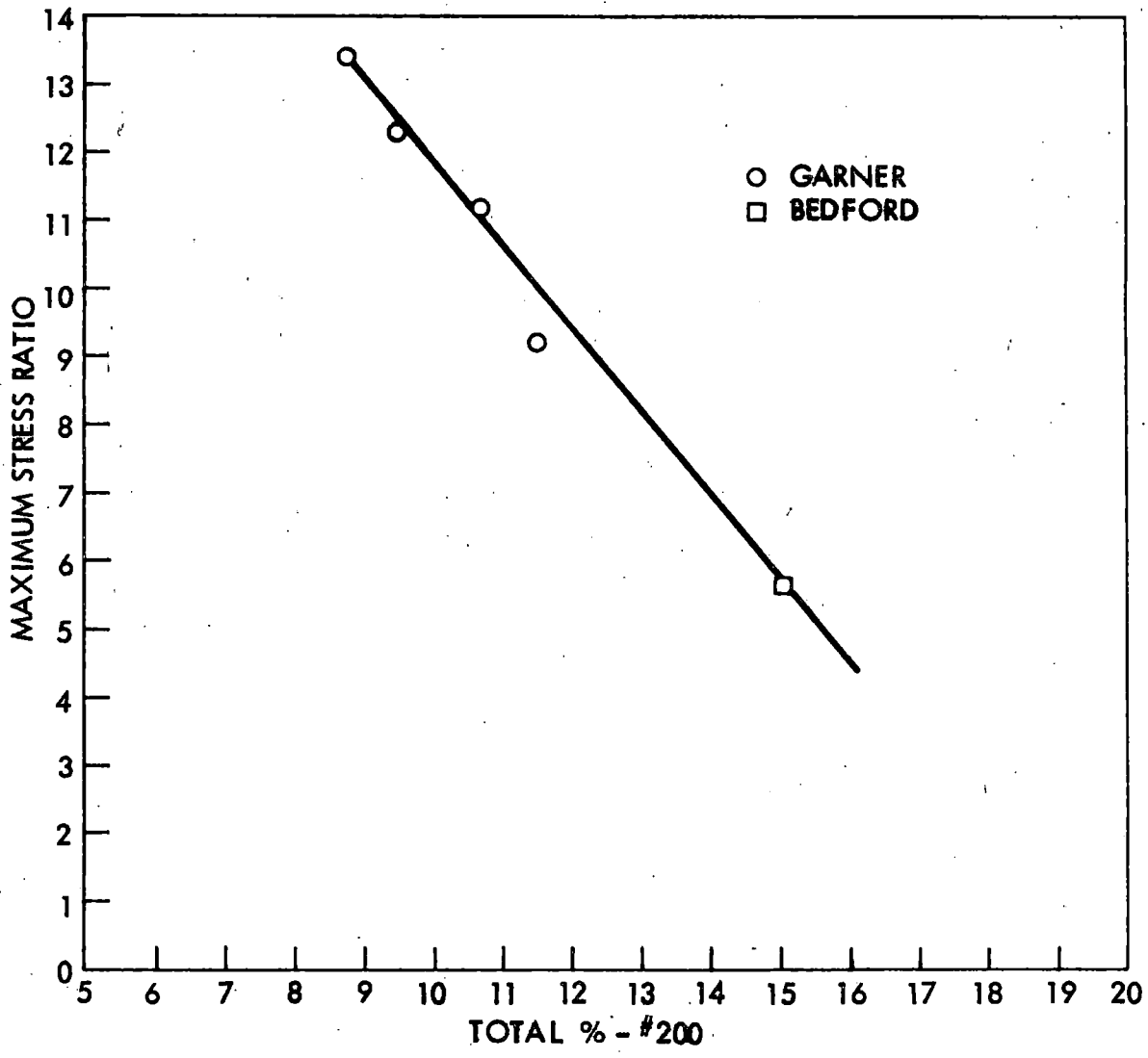

Fig. 39. Maximum stress ratio-maximum desirable fines content relationship.

of strain for repetitive loading conditions while above this line the rate of strain becomes much more rapid. Below the line, variations in fines content may have relatively little affect on the stability, whereas for stress conditions above the line, slight variations in fines may greatly alter the performance of the material under cyclic loading. The fact that the Bedford agrees with the four load conditions used for the Garner suggests the possibility that maximum fines content is dependent upon stress and may be independent of other physical properties of the materials.

3.2.6. Conclusions

Reaction to repetitive loading of the two granular base course materials appears to be highly dependent upon the amount of No. 200 sieve material present within the specimens upon completion of test. At the lower fines contents, an increase in the fines resulted in a slight increase in the amount of axial strain occurring after a set number of cycles of load had been applied. This increase appears to be linear, with the increase in fines content, up to a maximum desirable fines content, beyond which an increase in fines results in a much larger increase in axial strain that will develop after a fixed number of load cycles. In this area variations in fines content have a pronounced effect upon the resistance of the material to cyclic loading. Below this point, variation in fines content apparently have relatively little effect on stability. As was shown for the Bedford material, a specimen having a 16.0% fines content developed only 4.3% axial strain after 25,000 load applications while a

specimen with 17.2% fines developed the same amount of strain after only 120 load applications.

The maximum desirable fines content appears to be a function of stress conditions, decreasing linearly as the applied load is increased. Though only one point was determined, the Bedford stone (Fig. 39) appears to agree with the relationship established for the Garner indicating a possibility of independence from other physical properties of a base course material.

ISHC specifications (1964) require that the amount of No. 200 material does not exceed 16% for a rolled stone base. On the basis of the results presented in this study a material having 16%, or less, fines content will be within the stable region as long as the effective stress ratio does not exceed about 4.5. A 1% decrease in fines results in an increase in allowable effective stress ratio of 1.25. A reduction of fines content below that presently specified by the ISHC might be advisable, since field compaction normally results in material degradation.

Additional research at different stress conditions and for different materials will be required before any fully definitive conclusions can be made regarding effective stress ratio and maximum desirable fines content relationships. Similar research should be conducted on asphalt-treated materials having precisely controlled gradations.

3.3. MINIMUM VOLUME LOAD RESPONSE OF AN ASPHALT-TREATED GRANULAR MATERIAL

D. E. Fox and J. M. Hoover

It was observed from Project HR-99, as well as the project reported herein, that during a conventional consolidated-undrained triaxial shear test, the granular base specimen undergoes an initial volume decrease as axial load is applied. A point of minimum volume is reached after which the specimen increases in volume during the remainder of the test. Strain and load at minimum volume are less than at maximum effective stress ratio load. Both strain and load at minimum volume appear to produce a "proportional limit" indicating that failure of the specimen may have started. The question is then asked whether or not a specimen will withstand a large number of repeated load applications of the magnitude existing at the point of minimum volume failure criteria.

To examine this question, three saturated field-mixed asphalt-treated specimens* of material 1846 (Appendix A) were tested at lateral pressures of 10, 20, and 30 psi under repeated loads at a test temperature of 100°F. The axial loads applied to each specimen were the loads determined at the point of minimum volume during the CORS study in the conventional consolidated-undrained triaxial test apparatus. The minimum volume axial load at 10 psi lateral pressure produced a stress in the test specimen of about 70 psi, comparable to that

*Extra specimens molded, though unused, for the CORS study.

created in a flexible base course by a passing truck. The minimum volume loads at 20 and 30 psi lateral pressures were equivalently higher. Each specimen was consolidated for 36 min under the lateral pressure. Load application dwell time was maintained at 0.50 sec for each specimen, with 100,000 applications of load the arbitrary cutoff point. Strain, volume change and pore pressure were continuously recorded during testing.

Within the first few applications of repetitive axial load, each specimen underwent a volumetric strain decrease, and axial strain and pore pressure increase. Each of these parameters continued their respective increase or decrease up to 30,000 – 50,000 cycles, after which there was only negligible change in each. At 100,000 cycles, the above parameters were still somewhat less than the corresponding CORS tested specimens.

The post-repetitive test condition of each specimen was analyzed by retesting under the conventional consolidated-undrained triaxial test using the identical test conditions of the CORS study. Examination of the data showed each specimen exhibited a slight volume decrease, axial-strain increase, and increasing pore pressure to the point of minimum volume, coupled with increasing effective stress ratio. Three factors were indicated:

1. None of the specimens had "failed."

2. During removal from the repetitive apparatus, resaturation process, and placement in the conventional apparatus, each specimen may have partially rebounded elastically.

3. Because of the continued volume decrease during cyclic loading, each specimen had apparently increased in density.

Further analysis of the cyclic/conventional test data indicated each specimen had higher strength characteristics and effective stress ratios, than the corresponding conventionally tested CORS specimens. This factor, coupled with the density increase, may have contributed to the lack of full elastic rebound following the repetitive loading tests of each specimen.

In addition, the cyclic/conventional test data indicated that axial strain to reproduce minimum volume was less than the corresponding conventionally tested CORS specimens. This indicates a hardening effect of the treated specimens during cyclic loading. However, by adding the axial strain produced during the cyclic loading only, the combined or total axial strain of the cyclic/conventional tested specimens was nearly identical to the corresponding conventionally tested CORS specimens.

Volumetric strain and pore pressure, after cyclic/conventional tests, followed the same pattern as axial strain. By adding the values of each, obtained during cyclic loading only, the combined values of total volumetric strain and total pore pressure were nearly identical to the conventionally tested CORS specimens.

It therefore appeared likely that the slow, progressive movements (possibly creep conditions) associated with the original conventional triaxial tests, were not fully mobilized in the repetitive tests, though minimum volume loads were utilized. This indicates two factors: either (a) the response of the recording equipment was too slow, or (b) somewhat larger loads can be applied to a treated granular base material before minimum volume failure criteria is reached. It is felt

that the latter is more likely. If so, minimum volume failure criteria from a conventional triaxial test could produce a factor of safety against failure of a base course from transient traffic loads.

It is reasoned that the results of this series of tests indicate a further potential feasibility of the use of minimum volume failure criteria for analysis of the coefficient of relative strength in thickness design of a granular base material.

ACKNOWLEDGMENTS

Sincere appreciation is extended to the following organizations and personnel: the Iowa Highway Research Board, Iowa State Highway Commission and US Bureau of Public Roads for their individual recognition of the importance and value of research; Messers. S. E. Roberts, Research Engineer, and Bernard Ortgies, Bituminous Engineer, Iowa State Highway Commission, for their assistance and counseling.

In addition to those authors noted with the various sections of this report, a special thanks to the following personnel of the Engineering Research Institute, Soil Research Laboratory for their untiring and valuable contributions to the research involved in this project: Dr. Turgut Demirel, Professor of Civil Engineering, for his efforts relating to the study by Marley and Handy (Ref. 12); to Messers. Dick Johnson, Tim Peterson, Anthony Fung, Mike Lindebak, Don Davidson, Brad Moses, Ed Basart, Dick Leland, Linda Bientema, Janice Kreamer and John Schomburg who assisted as laboratory technicians at various periods throughout the project; and to Mrs. Edna Wiser, secretary, Soil Research Laboratory, who pulled her hair so often while typing and retyping reports that a wig was needed to cover what was left.

SELECTED REFERENCES

1. J. M. Hoover, "Factors Influencing Stability of Granular Base Course Mixes," Final Report, Iowa Highway Research Board Project HR-99. Engineering Research Institute, Iowa State University, Contribution No. 67-10 of the Soil Research Laboratory (1967).

2. Russell O. Fish, J. M. Hoover, "Deformation Moduli of Asphalt Treated Granular Materials," Special Report, Iowa Highway Research Board Project HR-131. Engineering Research Institute, Iowa State University, Contribution No. 69-4 of the Soil Research Laboratory (1969).

3. E. G. Ferguson, J. M. Hoover, "Effect of Portland Cement Treatment of Crushed Stone Base Materials as Observed from Triaxial Shear Tests," Highway Research Record 255, pp. 1-15 (1968).

4. T. W. Best, J. M. Hoover, "Stability of Granular Base Course Mixes Compacted to Modified Density," Special Report, Iowa Highway Research Board Project HR-99. Engineering Research Institute, Iowa State University, Contribution No. 66-15 of the Soil Research Laboratory (1966).

5. H. H. Harmon, "Modern Factor Analysis," 2nd ed. revised, University of Chicago Press (1967).

6. N. C. Matalas, B. J. Reiher, "Some Comments on the Use of Factorial Analysis," Water Resources Research, 3: 1, 213-223 (1967).

7. L. H. Csanyi, H. P. Fung, "Traffic Simulator for Checking Mix Behavior," Highway Research Record 51, pp. 57-67 (1964).

8. F. R. Nichols, "Flexible Pavement Research in Virginia," Highway Research Board Bulletin 269, pp. 35-50 (1960).

9. P. Arena, S. G. Shah, V. Adam, "Compaction Type Tests for Asphaltic Concrete Pavement," Highway Division Newsletter, American Society of Civil Engineers, p. 5 (Feb 1967).

10. F. H. Hveem, "Effects of Time and Temperature on Hardening of Asphalts," Highway Research Board, Special Report 54 (1960).

11. L. H. Csanyi, R. E. Cox, C. R. Teagle, "Effect of Fillers on Asphaltic Concrete Mixes," Highway Research Record 51, pp. 68-88 (1964).

12. J. J. Marley, R. L. Handy, "Behavior of Granular Materials under Triaxial Compression with Pulsating Deviator Stress," Special Report, Iowa Highway Research Board Project HR-131. Engineering Research Institute, Iowa State University, Contribution No. 69-5 of the Soil Research Laboratory (1969).

APPENDIX A

Table A-1. Triaxial test results for asphalt cement treated specimens at minimum volume (MV) and maximum effective stress ratio (MESR) conditions.

Material	Asphalt content, %	Cohesion, psi		∅, degrees		Lateral pressure, psi	Test density, pcf	Effective stress ratio		Pore pressure, psi			Axial strain, %		Volumetric strain, %		Modulus of deformation, M, psi	Average modulus, M, psi	Poisson's ratio	
		MV	MESR	MV	MESR			MV	MESR	Max	MV	MESR	MV	MESR	MV	MESR			Eq. 13[a]	Eq. 21[a]
429 Limestone	4.27	3.57	13.16	43.56	42.38	10.0	134.4	5.21	8.55	0.3	0.3	- 0.3	0.602	1.687	- 0.182	0.083	8,900		0.399	
						20.0	135.5	7.04	10.27	0.4	0.4	0.0	0.759	1.517	- 0.169	- 0.016	21,200		0.409	
						30.0	135.4	4.37	5.35	0.4	0.4	0.0	1.006	2.640	- 0.224	0.0	12,000		0.439	
						40.0	134.0	4.69	5.27	0.8	0.8	0.2	1.692	3.625	- 0.464	- 0.315	9,800		0.425	
						60.0	134.7	4.69	4.95	0.7	0.6	0.4	1.758	3.390	- 0.397	- 0.316				
																		12,980		0.347
	4.27	2.10	7.82	39.86	39.58	10.0	136.7	5.19	7.38	0.3	0.3	- 0.8	0.377	1.257	- 0.111	0.270	13,200		0.408	
	4.34					20.0	134.4	3.50	4.44	0.9	0.9	- 0.4	0.876	3.002	- 0.240	0.016	6,600		0.437	
	4.31					30.0	135.5	4.01	5.23	0.5	0.5	- 0.5	0.749	2.371	- 0.224	0.064	12,800		0.431	
	4.31					40.0	133.5	3.79	4.01	1.0	1.0	0.4	1.844	4.916	- 0.391	- 0.188	6,000		0.456	
																		9,650		0.379
	5.02	- 0.06	13.06	42.69	37.06	10.0	137.4	3.70	7.48	0.3	0.3	- 1.2	0.253	1.518	- 0.095	0.355				
	5.02					10.0 dup	137.6	5.09	8.30	0.3	0.3	- 0.8	0.384	1.279	- 0.129	0.162	11,800		0.403	
	4.98					20.0	136.0	3.89	5.39	0.5	0.5	- 1.0	0.632	2.529	- 0.169	0.250	9,400		0.441	
	4.98					30.0	136.1	4.27	4.79	1.5	1.4	- 0.6	1.371	3.489	- 0.293	0.095	7,300		0.449	
																		9,480		0.382
479 Dolomite	4.27	9.39	33.06	40.41	38.11	10.0	129.3	6.85	15.40	0.1	0.1	- 0.2	0.374	1.122	- 0.070	0.281	18,800		0.434	
						20.0	130.1	6.17	11.61	0.1	0.1	- 0.1	0.504	1.387	- 0.131	0.262	25,900		0.427	
						30.0	129.3	4.73	7.44	0.1	0.1	- 0.1	0.499	1.373	- 0.119	0.150	28,500		0.434	
						40.0	131.3	4.09	6.39	0.1	0.1	0.0	0.508	1.651	- 0.121	0.282	32,000		0.432	
						60.0	130.4	4.33	5.45	0.2	0.2	0.0	1.006	2.011	- 0.193	0.064				
																		26,300		0.421
	4.15	- 1.15	10.77	42.05	40.28	10.0	130.4	3.38	7.69	0.2	0.2	- 0.9	0.246	1.232	- 0.087	0.342	13,700		0.405	
	4.26					20.0	130.8	3.87	6.19	0.4	0.4	- 0.4	0.372	1.488	- 0.103	0.254	16,200		0.438	
	4.26					30.0	130.0	3.94	5.13	0.3	0.3	- 0.3	0.613	1.839	- 0.151	0.071	18,000		0.434	
	4.40					40.0	130.3	3.88	4.80	0.5	0.5	- 0.1	0.863	3.082	- 0.257	- 0.056	14,400		0.432	
																		15,580		0.382
	5.00	1.39	15.73	40.13	40.38	10.0	132.4	5.33	9.90	0.3	0.3	- 1.0	0.323	1.163	- 0.102	0.253	14,950		0.406	
	5.00					20.0	132.1	3.92	7.03	0.3	0.3	- 0.7	0.388	1.681	- 0.107	0.287	18,600		0.427	
	5.00					30.0	132.1	3.14	5.80	0.3	0.3	- 0.6	0.384	1.793	- 0.122	0.163	21,300		0.429	
	5.00					40.0	133.2	4.04	5.42	0.8	0.8	- 0.1	0.777	2.072	- 0.257	- 0.108	19,100		0.411	
																		18,460		0.352
728 Dolomite (cherty)	4.47	- 2.27	22.35	41.25	39.53	10.0	135.2	3.58	12.40	0.1	0.1	- 0.6	0.249	1.118	- 0.071	0.362	14,400		0.422	
						20.0	135.0	2.86	8.38	0.2	0.2	- 0.3	0.251	1.255	- 0.048	0.305	22,300		0.454	
						30.0	135.5	3.61	6.45	0.2	0.2	- 0.6	0.609	2.069	- 0.123	0.384	19,800		0.438	
						40.0	135.4	4.02	5.94	0.3	0.3	- 0.6	0.517	1.937	- 0.166	0.191	24,800		0.427	
						60.0	136.0	3.71	5.09	0.3	0.3	0.0	0.884	2.400	- 0.288	0.098				
																		20,320		0.403
	4.46	- 1.63	15.33	40.92	42.68	10.0	139.2	4.55	9.63	0.1	0.1	- 1.9	0.254	1.270	- 0.040	0.703	17,900		0.452	
	4.49					20.0	139.6	2.36	7.67	0.3	0.3	- 1.8	0.259	1.556	- 0.099	0.575	18,200		0.415	
	4.49					30.0	139.7	4.19	6.77	0.4	0.4	- 1.2	0.518	1.682	- 0.116	0.406	25,200		0.431	
	4.51					40.0	138.7	3.31	5.68	0.4	0.3	- 0.7	0.385	1.923	- 0.124	0.288	31,000		0.423	
																		23,100		0.410
	5.00	10.22	29.58	31.98	38.52	10.0	141.7	5.50	12.10	0.6	0.6	- 0.7	0.327	1.047	- 0.136	0.297	16,300		0.361	
	4.98					20.0	141.6	5.37	10.31	0.3	0.3	- 1.3	0.325	1.431	- 0.089	0.646	29,700		0.420	
	5.00					30.0	142.1	3.14	6.98	0.4	0.4	- 1.4	0.326	1.824	- 0.122	0.546	23,000		0.429	
	4.98					40.0	140.9	2.99	6.05	0.6	0.5	- 1.1	0.391	1.826	- 0.167	0.209	28,700		0.399	
																		24,400		0.377

[a]See selected reference 2.

Table A-1. Continued.

Material	Asphalt content, %	Cohesion, psi MV	Cohesion, psi MESR	φ, degrees MV	φ, degrees MESR	Lateral pressure, psi	Test density pcf	Effective stress ratio MV	Effective stress ratio MESR	Pore pressure, psi Max	Pore pressure, psi MV	Pore pressure, psi MESR	Axial strain, % MV	Axial strain, % MESR	Volumetric strain, % MV	Volumetric strain, % MESR	Modulus of deformation, M, psi	Average modulus, M, psi	Poisson's ratio Eq. 13[a]	Poisson's ratio Eq. 21[a]
1241 Gravel	4.3	11.85	40.71	36.17	31.53	10.0	139.5	7.55	16.09	0.2	0.2	- 0.5	0.647	1.554	- 0.130	0.220	14,200		0.411	
						20.0	138.7	6.62	9.23	0.4	0.4	- 0.2	0.641	1.538	- 0.196	0.008	18,400		0.405 0.416	
						30.0	139.9	4.21	7.38	0.4	0.1	- 0.8	0.645	2.064	- 0.131	0.246	24,400		0.426	
						40.0	140.7 139.5	3.40	5.53	0.1	0.1	- 0.2	1.034	2.326	- 0.187	0.228	20,800		0.424	
						40.0 dup	140.8	2.44	5.88	0.5	0.4	- 0.5	0.389	1.815	- 0.067	0.267				
						60.0	137.4	3.78	4.62	0.5	0.5	0.0	1.143	2.922	- 0.195	0.098				
																		19,450		0.396
	4.24	0.70	11.62	35.53	34.89	10.0	138.7	3.47	6.76	0.3	0.3	- 1.6	0.249	1.244	- 0.078	0.298	9,900		0.439	
	4.21					20.0	139.8	2.60	4.70	0.3	0.3	- 1.3	0.377	2.136	- 0.127	0.420	11,300		0.435 0.448	
	4.24 4.24					30.0	139.1 139.4	2.92	3.95	0.7	0.6	- 1.1	0.624	2.620	- 0.165	0.362	10,100		0.453	
	4.29					40.0	139.9	2.86	3.85	0.4	0.4	- 0.9	0.502	2.257	- 0.096	0.385	15,500		0.468	
																		11,700		0.473
				No 5% mix		10.0														
						20.0														
						30.0														
						40.0														
1269 Gravel	3.90	6.50	10.30	36.68	35.73	10.0	130.1	6.69	7.99	0.5	0.5	0.1	1.036	1.943	- 0.250	- 0.042	7,010		0.468	
						20.0	129.7	4.42	4.90	0.4	0.4	0.0	1.015	2.665	- 0.299	- 0.097	7,610		0.422 0.446	
						30.0	130.8	3.43	3.60	0.6	0.6	0.6	2.294	3.059	- 0.486	- 0.478	2,920		0.463	
						40.0	129.3 130.3	3.44	3.81	1.1	1.1	0.7	3.005	4.884	- 0.731	- 0.626	4,590		0.434	
						40.0 dup	131.8	3.60	3.76	0.8	0.8	0.5	2.317	3.862	- 0.480	- 0.422				
						60.0	130.0	3.53	3.58	1.2	1.1	1.1	5.415	5.667	- 0.862	- 0.862				
																		5,530		0.348
	3.98	1.46	9.42	38.35	33.50	10.0	131.4	3.77	5.69	0.6	0.6	- 0.5	0.507	2.154	- 0.151	0.231	6,510		0.423	
	3.95					20.0	131.2 6	3.74	4.27	0.3	0.3	0.2	1.515	3.788	- 0.344	- 0.216	3,310		0.458	
	3.95 3.92					30.0	130.7 130.6	3.42	3.76	1.6	1.5	1.3	2.395	4.413	- 0.498	- 0.458	2,830		0.462 0.453	
	3.76					40.0	129.8	3.34	3.34	2.1	2.1	2.1	5.627	5.627	- 0.820	- 0.820				
	3.98					40.0 dup	130.1	3.21	3.30	2.3	2.2	1.9	4.464	7.652	- 0.920	- 0.855	1,500		0.471	
																		3,530		0.384
				No 5% mix		10.0														
						20.0														
						30.0														
						40.0														
1485 Gravel (sand)	3.93	- 3.48	4.53	36.02	40.57	10.0	133.5	2.71	5.63	0.1	0.1	- 0.5	0.387	1.808	- 0.104	0.553	6,000		0.445	
						20.0	134.3	2.25	5.04	0.2	0.2	- 0.1	0.260	1.691	- 0.065	0.562	12,000		0.450 0.446	
						20.0 dup	134.0 133.9	1.75	4.49	0.1	0.1	- 0.4	0.254	2.159	- 0.079	0.938				
						30.0	134.3	2.15	4.70	0.3	0.3	- 0.9	0.391	2.344	- 0.133	0.624	15,000		0.435	
						40.0	133.4	2.51	4.03	0.2	0.2	- 0.2	0.661	2.643	- 0.167	0.551	12,000		0.454	
						60.0	133.6	2.68	4.05	0.4	0.4	- 0.5	0.772	2.444	- 0.182	0.207				
																		11,250		0.422
	3.89	- 0.16	4.20	33.54	37.90	10.0	132.2	2.53	4.80	0.2	0.2	- 1.2	0.245	1.471	- 0.077	0.497	10,300		0.427	
	3.89					20.0	132.0 132.3	2.38	3.92	0.3	0.3	- 1.9	0.366	2.195	- 0.092	0.641	11,300		0.451 0.443	
	3.91 3.91					30.0	131.8	2.42	3.71	0.5	0.4	- 1.3	0.489	2.324	- 0.148	0.397	11,200		0.448	
	3.96					40.0	133.1	2.48	3.63	0.6	0.5	- 0.8	0.616	2.773	- 0.173	0.467	13,000		0.448	
																		11,450		0.409
	4.99	1.84	3.05	32.01	41.17	10.0	136.5	2.44	4.63	0.2	0.2	- 1.3	0.196	1.436	- 0.078	0.592	7,418		0.446	
	4.99					20.0	137.1 136.9	3.18	4.91	0.6	0.6	- 0.9	0.529	1.720	- 0.141	0.332	9,953		0.441 0.440	
	5.02 5.00					30.0	136.1	2.34	4.21	0.4	0.3	- 1.3	0.394	2.103	- 0.133	0.475	15,687		0.434	
	5.02					40.0	137.8	2.37	4.13	0.4	0.4	- 1.0	0.397	1.984	- 0.126	0.413	20,084		0.440	
																		13,285		0.397

[a] See selected reference 2.

Table A-1. Continued.

Material	Asphalt content, %	Cohesion, psi		ϕ, degrees		Lateral pressure, psi	Test density, pcf	Effective stress ratio		Pore pressure, psi			Axial strain, %		Volumetric strain, %		Modulus of deformation, M, psi	Average modulus, M, psi	Poisson's ratio	
		MV	MESR	MV	MESR			MV	MESR	Max	MV	MESR	MV	MESR	MV	MESR			Eq. 13[a]	Eq. 21[a]
1676 Limestone	3.87	4.22	37.26	39.92	34.83	10.0	132.3	3.29	16.90	0.2	0.2	- 0.4	0.257	1.029	- 0.089	0.341	18,600		0.366	
						20.0	132.15	5.60	9.69	0.2	0.2	- 0.2	0.513	1.155	- 0.129	0.185	23,700		0.410 0.411	
						30.0	132.3 132.5	4.16	6.90	0.4	0.3	- 0.4	0.767	1.918	- 0.139	0.229	21,800		0.429	
						40.0	133.0	4.43	6.54	0.3	0.3	- 0.1	0.902	1.804	- 0.141	0.083	25,800		0.438	
						60.0	132.7	4.57	4.99	1.0	1.0	0.3	1.660	2.426	- 0.507	- 0.407				
																		22,480		0.406
	3.95	5.60	21.40	40.38	36.58	10.0	129.1	7.55	12.39	0.2	0.2	- 0.4	0.367	0.857	- 0.085	0.132	41,800		0.328	
	3.94 3.95					20.0	129.2	4.13	6.58	0.2	0.2	- 0.4	0.367	1.347	- 0.101	0.232	52,800		0.311 0.378	
	3.94					30.0	130.2 129.7	4.41	5.48	0.4	0.4	- 0.2	0.617	1.481	- 0.117	0.078	18,600		0.450	
	3.96					40.0	130.4	4.40	5.24	0.4	0.4	- 0.1	0.986	2.219	- 0.245	- 0.079	18,600		0.422	
																		32,970		0.282
	5.06	6.71	26.26	35.71	38.26	10.0	135.2	5.59	12.47	0.2	0.1	- 1.2	0.330	1.188	- 0.088	0.267	14,876		0.423	
	5.06 5.03					20.0	135.8 135.2	4.32	8.78	0.4	0.2	- 0.8	0.397	1.457	- 0.069	0.319	23,971		0.443 0.431	
	5.00					30.0	135.4	3.37	6.88	0.2	0.2	- 1.0	0.395	1.713	- 0.110	0.262	25,270		0.427	
	5.00					40.0	134.4	3.57	5.77	0.5	0.5	- 0.8	0.525	2.101	- 0.143	0.244	25,684		0.429	
																		22,450		0.390
1677 Limestone	4.00	9.93	31.58	40.01	36.30	10.0	141.3	8.29	15.38	0.3	0.3	- 0.2	0.510	1.276	- 0.145	0.194	15,800		0.396	
						20.0	141.4	5.01	9.49	0.3	0.3	- 0.3	0.508	1.396	- 0.121	0.137	21,800		0.417 0.416	
						30.0	139.1	5.33	6.56	0.3	0.3	- 0.2	0.884	2.020	- 0.234	0.016	17,800		0.416	
						40.0	138.0 140.2	5.10	6.04	0.3	0.3	0.0	0.997	2.118	- 0.184	0.032	22,200		0.437	
						60.0	141.4	4.09	5.03	0.9	0.9	0.2	1.151	2.814	- 0.295	- 0.082				
																		19,400		0.406
	4.03	4.51	13.66	40.12	37.41	10.0	136.4	5.30	7.79	0.1	0.1	- 0.5	0.372	0.993	- 0.109	0.086	12,500		0.418	
	4.03 4.03					20.0	135.2 136.1	4.87	6.51	0.3	0.3	- 0.4	0.611	1.711	- 0.170	0.070	12,800		0.430 0.427	
	4.04					30.0	136.4	4.24	4.79	0.6	0.6	0.2	1.232	2.464	- 0.300	- 0.229	10,500		0.427	
	4.04					40.0	136.3	4.10	4.41	1.6	1.5	0.5	1.728	3.702	- 0.450	- 0.316	8,200		0.433	
																		11,000		0.346
	4.96	- 0.73	14.26	43.02	38.74	10.0	136.4	3.26	8.57	0.3	0.3	- 0.4	0.123	1.349	- 0.008	0.531	12,100		0.493	
	4.96 4.97					20.0	138.8 138.2	4.74	6.66	0.6	0.5	- 0.7	0.625	2.126	- 0.184	0.176	11,100		0.433 0.450	
	4.98					40.0	139.4	4.07	4.74	1.5	1.3	0.2	1.383	3.143	- 0.435	- 0.274	9,600		0.424	
																		8,200		0.376
1743 Limestone	4.27	12.88	35.47	36.76	31.83	10.0	132.2	8.40	15.55	0.6	0.6	- 0.3	0.374	0.998	- 0.190	0.071	22,200		0.304	
						20.0	131.7 132.8	5.53	8.25	0.9	0.9	- 0.1	0.492	1.108	- 0.148	0.016	21,200		0.404 0.387	
						30.0	133.9	4.58	5.98	0.7	0.7	0.1	0.632	1.391	- 0.153	- 0.016	20,100		0.431	
						40.0	133.0	4.79	6.01	0.5	0.5	- 0.1	0.751	1.627	- 0.231	- 0.048	23,600		0.412	
						60.0	133.2	3.65	4.16	1.2	1.3	0.6	1.121	2.366	- 0.302	- 0.183				
																		21,780		0.390
	4.08	0.23	10.58	39.12	39.28	10.0	134.4	3.26	7.32	0.2	0.2	- 0.9	0.255	1.021	- 0.088	0.384	13,100		0.406	
	4.08 4.06					20.0	134.7 134.1	3.76	5.75	0.4	0.4	- 1.1	0.382	1.273	- 0.105	0.257	16,500		0.435 0.424	
	4.04					30.0	133.6	3.35	4.91	0.3	0.3	- 0.8	0.508	2.288	- 0.153	0.339	17,200		0.431	
	4.04					40.0	133.6	3.44	4.52	0.6	0.6	- 0.4	0.631	2.399	- 0.185	0.169	20,300		0.427	
																		16,780		0.401
	5.01	2.23	6.20	40.41	44.84	10.0	136.5	4.74	7.26	0.3	0.3	- 0.7	0.387	1.162	- 0.089	0.292	10,500		0.438	
	5.01 4.98					20.0	138.6 136.9	4.12	6.61	0.5	0.5	- 1.2	0.522	1.567	- 0.141	0.232	16,300		0.418 0.435	
	4.94 4.94					30.0	136.8	4.03	5.57	0.4	0.4	- 0.8	1.031	2.448	- 0.148	0.363	14,500		0.449	
						40.0	135.5	Membrane failure										13,770		0.414

[a] See selected reference 2.

Table A-1. Continued.

Material	Asphalt content, %	Cohesion, psi		ϕ, degrees		Lateral pressure, psi	Test density, pcf	Effective stress ratio		Pore pressure, psi			Axial strain, %		Volumetric strain, %		Modulus of deformation, M, psi	Average modulus, M, psi	Poisson's ratio	
		MV	MESR	MV	MESR			MV	MESR	Max	MV	MESR	MV	MESR	MV	MESR			Eq. 13[a]	Eq. 21[a]
1746 Limestone	4.07	8.18	39.54	44.24	37.75	10.0	133.9	9.66	19.64	0.0	0.0	- 0.4	0.385	1.025	- 0.120	0.256	28,100		0.367	
						20.0	134.9	5.73	11.54	0.0	0.0	- 0.2	0.390	1.040	- 0.107	0.049	29,800		0.409	
						30.0	130.3 134.2	5.87	7.58	0.1	0.1	0.0	0.618	1.360	- 0.181	- 0.055	27,400		0.406 0.400	
						40.0	135.1	5.84	7.49	0.4	0.4	- 0.1	0.778	1.686	- 0.174	0.033	32,800		0.419	
						60.0	136.9	5.21	5.80	0.8	0.7	- 0.2	1.179	2.358	- 0.228	- 0.068				
																		29,530		0.399
	3.87	- 1.09	12.42	44.38	41.45	10.0	134.2	4.64	9.43	0.5	0.5	- 0.5	0.370	1.232	- 0.132	0.186	11,300		0.398	
	3.87					20.0	134.1 134.6	4.24	6.47	0.5	0.4	- 0.4	0.625	1.749	- 0.134	0.150	16,000		0.425 0.415	
	4.18					30.0	135.3	4.22	5.66	0.5	0.5	- 0.4	0.642	2.310	- 0.212	0.073	20,000		0.401	
	4.18					40.0	135.0	4.66	5.35	0.8	0.6	- 0.1	0.996	2.490	- 0.224	- 0.016	16,500		0.439	
																		15,950		0.416
	5.04	2.52	23.08	40.34	38.95	10.0	140.0	4.27	12.62	0.3	0.3	- 1.0	0.256	1.410	- 0.097	0.411	14,300		0.402	
	5.35					20.0	139.0 139.6	4.62	7.86	0.4	0.4	- 0.7	0.635	2.161	- 0.145	0.378	15,530		0.425	
	5.35					30.0	138.4	4.15	6.32	0.4	0.4	- 0.8	0.635	2.160	- 0.146	0.162	19,070		0.435 0.423	
	5.04					40.0	141.0	3.81	6.08	2.3	1.7	2.1	0.773	2.898	- 0.198	0.259	18,070		0.432	
																		16,740		0.408
1750 Limestone dolomite	4.33	3.78	22.01	41.90	39.81	10.0	136.5	7.95	14.99	0.3	0.3	- 0.7	0.515	1.289	- 0.130	0.243	17,500		0.393	
						20.0	132.6 134.6	4.53	6.97	0.3	0.3	- 0.5	0.494	1.729	- 0.141	0.157	11,700		0.445	
						30.0	133.2	3.90	6.23	0.6	0.6	- 0.2	0.882	2.268	- 0.153	0.088	18,400		0.431 0.416	
						40.0	135.9	4.43	6.25	0.3	0.3	- 0.2	0.768	1.920	- 0.230	0.049	26,600		0.397	
						60.0	134.9	4.42	5.05	1.0	1.0	0.2	1.395	2.536	- 0.349	- 0.211				
																		18,550		0.382
	3.90	1.86	8.79	41.05	37.85	10.0	126.2	5.03	6.59	0.2	0.1	- 0.2	0.488	1.220	- 0.140	0.062	8,940		0.422	
	3.90					20.0	127.8 127.9	3.99	5.10	0.6	0.6	- 0.2	0.724	3.015	- 0.124	0.256	10,950		0.450 0.456	
	4.00					30.0	129.1	4.09	4.33	1.2	1.2	0.8	2.184	3.854	- 0.404	- 0.330	4,010		0.500	
	4.00					40.0	128.4	4.08	4.14	1.3	1.2	1.0	3.867	5.156	- 0.702	- 0.660	3,780		0.452	
																		6,920		0.343
1751 Limestone dolomite (1750)	5.5	11.58	31.96	40.76	40.37	10.0	136.9	13.95	21.49	0.5	0.5	- 0.2	0.617	1.357	- 0.235	0.008	22,200		0.339	
						20.0	139.2	5.81	8.58	0.7	0.6	- 0.3	0.763	1.780	- 0.137	0.217	16,900		0.4333	
						30.0	141.6 138.6	4.27	8.18	0.6	0.4	- 0.5	0.880	2.388	- 0.178	0.371	19,400		0.420 0.403	
						40.0	140.6	4.78	7.23	1.8	1.4	1.2	1.138	2.529	- 0.227	0.114	21,300		0.420	
						40.0 dup	136.7	4.27	7.27	0.6	0.5	- 0.2	0.762	2.414	- 0.165	0.182				
						60.0	136.6	4.78	5.92	0.6	0.6	- 0.1	1.373	2.622	- 0.326	- 0.147				
																		19,950		0.371
	4.90	- 1.86	11.97	44.43	38.63	10.0	130.6	4.32	7.96	0.2	0.2	- 0.5	0.376	1.503	- 0.126	0.275	10,900		0.405	
	4.90					20.0	130.3 131.0	4.00	5.98	0.2	0.1	- 0.2	0.500	1.999	- 0.136	0.296	13,800		0.4331	
	4.99					30.0	132.5	4.16	4.86	0.8	0.8	0.0	1.249	3.436	- 0.309	- 0.059	8,300		0.439 0.431	
	4.99					40.0	130.7	4.57	4.63	1.3	1.1	1.0	3.051	3.662	- 0.607	- 0.591	5,200		0.447	
																		9,550		0.326
1772 Gravel	Emulsion	0.59	1.55	37.28	37.03	10.0	127.0	3.51	4.07	0.3	0.3	0.0	0.491	1.717	- 0.116	0.000				
						20.0	125.6 127.7	3.10	3.11	1.9	1.9	1.7	3.644	4.858	- 0.564	- 0.564				
						30.0	127.9	3.12	3.19	2.5	2.5	2.4	3.194	4.471	- 0.548	- 0.532				
						40.0	130.3	3.17	3.25	2.0	2.0	1.8	3.035	4.288	- 0.630	- 0.617				

[a]See selected reference 2.

Table A-1. Continued.

Material	Asphalt content, %	Cohesion, psi MV	Cohesion, psi MESR	Φ, degrees MV	Φ, degrees MESR	Lateral pressure, psi	Test density, pcf	Effective stress ratio MV	Effective stress ratio MESR	Pore pressure, psi Max	Pore pressure, psi MV	Pore pressure, psi MESR	Axial strain, % MV	Axial strain, % MESR	Volumetric strain, % MV	Volumetric strain, % MESR	Modulus of deformation, M, psi	Average modulus, M, psi	Poisson's ratio Eq. 13[a]	Poisson's ratio Eq. 21[a]
1788 Dolomite with chert	4.20	- 4.12	23.13	44.33	40.30	10.0	140.9	2.92	11.07	0.2	0.2	- 2.2	0.127	1.013	- 0.056	0.669	21,500		0.396	
						20.0	139.9 140.2	3.07	8.27	0.4	0.4	- 1.5	0.257	1.283	- 0.081	0.445	23,700		0.419 0.400	
						30.0	139.7	4.00	7.20	0.8	0.8	- 1.3	0.729	1.823	- 0.170	0.262	20,200		0.416	
						40.0	140.9	4.65	6.53	0.6	0.5	- 1.3	0.632	1.644	- 0.250	0.161	31,600		0.370	
						60.0	135.5	4.10	5.01	0.9	0.9	- 0.7	0.889	2.285	- 0.195	0.081		24,250		0.188
	4.04	- 6.85	10.37	46.36	43.77	10.0	136.6	2.37	8.61	0.1	0.1	- 1.4	0.122	0.856	- 0.061	0.375	19,200		0.390	
	4.04					20.0	136.7 137.1	3.13	6.72	0.2	0.1	- 1.4	0.247	1.481	- 0.094	0.507	20,000		0.423 0.410	
	4.05					30.0	138.1	4.05	6.33	0.5	0.4	- 0.6	0.494	1.481	- 0.125	0.241	31,700		0.405	
	4.05					40.0	137.2	4.44	5.56	0.4	0.4	- 0.5	0.742	1.856	- 0.165	0.142	27,300		0.424	
																		24,550		0.394
	5.03	4.23	16.93	37.65	41.72	10.0	140.2	4.32	10.89	0.2	0.2	- 0.8	0.252	1.008	- 0.063	0.411	17,100		0.425	
	5.03					20.0	139.4 139.7	4.51	7.38	0.4	0.4	- 1.8	0.501	1.627	- 0.103	0.481	20,100		0.430 0.425	
	5.01					30.0	139.9	3.74	6.62	0.5	0.5	- 1.0	0.629	1.635	- 0.119	0.421	25,400		0.424	
	5.01					40.0	139.3	3.46	5.70	0.6	0.5	- 1.7	0.501	2.129	- 0.128	0.440	31,500		0.421	
																		23,530		0.379
1846 Limestone	3.80	2.47	13.37	39.01	39.68	10.0	137.6	4.69	8.65	0.1	0.1	- 1.1	0.367	1.224	- 0.077	0.400	12,600		0.436	
						10.0 rep	138.0	3.87	8.96	0.1	0.1	- 0.7	0.249	0.872	- 0.071	0.251				
						20.0	140.0	3.59	5.80	0.2	0.1	- 2.2	0.375	2.373	- 0.166	0.719	17,100		0.392	
						20.0 rep	138.6 138.4	4.03	7.78	0.1	0.1	- 0.5	0.250	0.625	- 0.063	0.118			0.419	
						30.0	138.2	3.60	5.55	0.4	0.4	- 1.0	0.632	2.528	- 0.154	0.479	16,000		0.437	
						30.0 rep	138.8	4.95	7.53	0.4	0.4	- 0.5	0.383	0.638	- 0.118	- 0.008				
	-					40.0	137.5	4.09	5.09	0.8	0.8	- 0.2	0.740	2.836	- 0.278	0.072	17,300		0.414	
						60.0	138.5	3.43	4.40	0.5	0.5	- 0.4	0.994	3.231	- 0.263	0.032				
																		15,750		0.363
	4.05	1.04	10.73	37.60	41.40	10.0	138.0	3.76	7.64	0.1	0.1	- 2.2	0.248	1.613	- 0.054	0.691	15,200		0.439	
	4.05 4.05					20.0	137.8 138.2	3.54	6.26	0.3	0.3	- 1.1	0.499	1.745	- 0.094	0.383	14,900		0.391 0.426	
	4.06					30.0	137.9	2.91	5.49	0.3	0.3	- 1.0	0.376	2.128	- 0.120	0.367	16,600		0.443	
	4.06					40.0	139.2	3.36	5.02	0.4	0.4	- 1.0	0.502	2.258	- 0.144	0.327	23,400		0.433	
																		17,530		0.403
	5.00	2.38	10.94	36.31	43.90	10.0	141.6	3.88	9.12	0.2	0.2	- 0.9	0.255	1.276	- 0.056	0.451	15,200		0.437	
	5.00 4.98					20.0	142.2 141.4	3.25	7.13	0.6	0.6	- 1.0	0.385	1.670	- 0.131	0.409	14,600		0.421 0.427	
	4.96					30.0	140.8	3.43	6.11	0.5	0.5	- 1.1	0.510	2.169	- 0.155	0.480	17,800		0.427	
	4.96					40.0	141.0	3.05	5.79	0.8	0.7	- 1.0	0.513	2.566	- 0.189	0.444	19,500		0.423	
																		16,780		0.388
1855 Dolomite cherty	4.13	- 1.79	18.96	45.43	42.45	10.0	134.2	2.69	10.14	0.1	0.1	- 1.2	0.124	0.993	- 0.039	0.484				
						20.0	133.4	5.75	9.51	0.1	0.1	- 0.4	0.369	0.984	- 0.086	0.156	30,800		0.424	
						30.0	134.7 134.6	4.35	7.29	0.2	0.2	- 0.3	0.375	1.249	- 0.142	0.087	30,300		0.402 0.413	
						40.0	135.9	4.88	6.19	0.4	0.4	- 0.1	0.623	1.620	- 0.185	0.000	29,400		0.413	
						60.0	134.9	4.68	5.44	0.4	0.4	0.0	0.756	1.764	- 0.248	- 0.128				
																		30,200		0.358
	4.24	1.65	50.93	43.63	30.43	10.0	140.8	5.22	18.50	0.1	0.1	- 0.9	0.389	1.295	- 0.074	0.082	18,800		0.415	
	4.24 4.29					20.0	142.9 139.8	5.18	11.02	0.3	0.3	- 0.2	0.393	1.441	- 0.091	0.497	26,500		0.425 0.426	
	4.24					30.0	137.5	4.36	7.68	0.2	0.2	- 0.2	0.377	1.382	- 0.105	0.177	33,300		0.420	
	4.44					40.0	138.0	4.74	6.59	0.2	0.2	0.0	0.631	1.766	- 0.122	0.130	27,500		0.446	
																		26,500		0.439
	5.03	- 1.35	12.35	44.15	49.70	10.0	137.8	4.65	13.11	0.2	0.2	- 0.7	0.255	1.020	- 0.065	0.290	16,200		0.430	
	5.00 5.01					20.0	141.7	4.29	10.56	0.3	0.3	- 1.3	0.325	1.302	- 0.087	0.387	23,900		0.428	
	5.03					30.0	137.8 140.2	3.83	7.59	0.2	0.2	- 0.1	0.382	1.911	- 0.114	0.383	27,500		0.423 0.424	
	5.00					40.0	143.3	4.65	8.26	0.4	0.4	- 0.5	0.529	1.720	- 0.144	0.246	35,400		0.416	
																		25,750		0.392

[a]See selected reference 2.

Table A-1. Continued.

Material	Asphalt content, %	Cohesion, psi MV	Cohesion, psi MESR	ϕ, degrees MV	ϕ, degrees MESR	Lateral pressure, psi	Test density, pcf	Effective stress ratio MV	Effective stress ratio MESR	Pore pressure, psi Max	Pore pressure, psi MV	Pore pressure, psi MESR	Axial strain, % MV	Axial strain, % MESR	Volumetric strain, % MV	Volumetric strain, % MESR	Modulus of deformation, M. psi	Average modulus, M. psi	Poisson's ratio Eq. 13[a]	Poisson's ratio Eq. 21[a]
1903 Gravel	5.33	- 2.24	19.61	42.82	43.90	10.0	147.4	2.81	12.41	1.1	0.5	0.3	0.250	1.622	- 0.047	0.644	11,200		0.452	
						20.0	148.1 147.6	3.91	9.35	0.2	0.1	- 0.1	0.507	1.900	- 0.160	0.433	14,800		0.414 0.431	
						30.0	147.6	4.45	8.90	0.4	0.3	- 0.5	0.751	2.252	- 0.151	0.318	21,300		0.427	
						40.0	147.8	3.53	6.53	0.7	0.5	0.0	0.753	2.636	- 0.214	0.427	16,000		0.434	
						60.0	146.9	4.10	5.76	0.9	0.8	0.2	1.494	3.486	- 0.853	- 0.274				
																		15,830		0.394
	5.06	- 4.79	8.70	42.97	45.56	10.0	143.1	3.66	8.83	0.4	0.4	- 1.1	0.374	0.698	- 0.063	0.644	14,400		0.429	
	5.06					20.0	144.9 143.9	2.23	6.75	0.7	0.5	- 3.2	0.251	1.885	- 0.080	0.590	17,600		0.431 0.430	
	5.07					30.0	144.6	3.45	6.52	0.9	0.8	- 0.3	0.618	2.224	- 0.142	0.354	18,300		0.431	
	5.07					40.0	143.0	3.83	6.01	0.7	0.6	- 0.3	0.737	2.455	- 0.211	0.164	18,300		0.430	
																		17,150		0.385
1904 Gravel (1903)	3.80	4.37	28.52	40.84	39.48	10.0	142.8	7.79	15.98	0.6	0.6	- 0.9	0.500	1.500	- 0.134	0.307	16,700		0.390	
						20.0	144.0 143.3	4.55	9.52	0.2	0.2	- 1.3	0.371	1.485	- 0.086	0.476	22,400		0.436 0.414	
						30.0	142.8	3.62	6.40	0.5	0.5	- 1.4	0.500	1.999	- 0.134	0.443	20,600		0.429	
						40.0	143.6	4.40	6.47	0.5	0.5	- 1.1	0.746	2.112	- 0.222	0.348	25,800		0.403	
						60.0	143.1	4.17	5.58	0.6	0.6	- 0.3	0.995	2.486	- 0.238	0.103				
																		21,380		0.390
	4.09	2.61	12.67	36.14	41.60	10.0	138.0	3.54	9.26	0.2	0.2	- 0.8	0.234	1.403	- 0.081	0.444	12,400		0.422	
	4.09					20.0	139.3 138.9	3.55	6.61	0.3	0.0	- 1.5	0.386	2.186	- 0.098	0.561	16,100		0.440 0.429	
	4.09 4.09					30.0	138.3	3.64	5.76	0.6	- 0.1	0.6	0.489	2.323	- 0.133	0.376	17,100		0.443	
	4.09					40.0	140.1	2.83	5.37	0.7	0.7	- 1.0	0.505	3.470	- 0.169	0.469	23,500		0.414	
																		17,275		0.406
2318 Limestone	4.7	2.46	39.45	37.96	31.75	10.0	140.4	6.00	16.12	0.2	0.2	- 1.1	0.381	1.142	- 0.096	0.385	16,600		0.410	
						20.0	140.4 139.2	2.77	8.25	0.5	0.5	- 2.0	0.247	1.361	- 0.078	0.515	19,700		0.432 0.433	
						30.0	139.2	3.18	6.53	0.1	0.1	- 0.4	0.501	1.754	- 0.103	0.555	21,200		0.441	
						40.0	139.1	3.61	5.80	0.6	0.6	- 1.5	0.640	2.047	- 0.130	0.464	25,900		0.449	
						60.0	137.1	0.41	0.50	5.0	5.0	3.0	1.134	1.765	- 0.219	- 0.081				
																		20,850		0.412
	3.86	- 1.77	16.98	41.20	41.32	10.0	137.7	3.57	10.49	0.1	0.1	- 1.5	0.124	0.869	- 0.055	0.368				
	3.86					20.0	137.4 137.6	2.91	7.53	0.4	0.4	- 1.2	0.249	1.367	- 0.079	0.456	23,400		0.420	
	3.94					30.0	137.6	4.21	6.39	0.3	0.1	- 1.6	0.494	1.607	- 0.133	0.368	23,500		0.428 0.427	
	3.94					40.0	137.7	3.35	5.83	0.4	0.4	- 1.2	0.620	1.859	- 0.134	0.300	24,900		0.434	
																		23,900		0.384
	4.76	- 1.16	14.81	40.99	42.97	10.0	139.4	3.89	10.07	0.2	0.2	- 1.6	0.254	1.270	- 0.072	0.522	15,300		0.419	
	4.81					20.0	139.6 139.8	3.06	7.34	0.4	0.4	- 2.1	0.378	1.892	- 0.096	0.632	13,800		0.444	
	4.76					30.0	140.2	3.79	6.58	0.4	0.3	- 1.8	0.507	1.900	- 0.112	0.521	19,300		0.447 0.442	
	4.81					40.0	139.9 139.9	3.67	5.86	0.0	- 0.5	- 1.0	0.632	1.895	- 0.104	0.394	22,200		0.457	
																		17,650		0.458

[a]See selected reference 2.

Table A-1. Continued.

Material	Asphalt content, %	Cohesion, psi		ϕ, degrees		Lateral pressure, psi	Test density, pcf	Effective stress ratio		Pore pressure, psi			Axial strain, %		Volumetric strain, %		Modulus of deformation, M, psi	Average modulus, M, psi	Poisson's ratio	
		MV	MESR	MV	MESR			MV	MESR	Max	MV	MESR	MV	MESR	MV	MESR			Eq. 13[a]	Eq. 21[a]
1822 Dolomite	4.07	1.41	18.32	41.68	39.15	10.0	130.7	3.86	8.86	0.2	0.2	- 0.4	0.255	1.020	- 0.073	0.259	15,400		0.417	
						20.0	133.3	4.74	7.74	0.3	0.3	- 0.6	0.637	1.593	- 0.121	0.303	17,400		0.431	
						30.0	133.9	4.43	6.84	0.3	0.3	- 0.5	0.502	1.507	- 0.160	0.144	26,000		0.406	0.419
						40.0	134.5	3.91	5.51	0.4	0.4	- 0.2	0.885	2.022	- 0.186	0.008	23,200		0.422	
						60.0	132.9	4.07	4.31	0.4	0.4	0.3	1.518	3.036	- 0.293	- 0.277				
																		20,500		0.387
	3.96	- 5.87	- 1.25	47.17	49.18	10.0	134.4	5.33	9.41	0.4	0.4	- 0.7	0.376	1.129	- 0.134	0.205	12,900		0.392	
	3.96					20.0	136.0	2.27	3.83	0.4	0.4	- 0.4	0.611	1.833	- 0.128	0.080	7,600		0.453	
	3.91					30.0	135.7	4.78	6.17	0.4	0.3	- 0.1	0.758	1.643	- 0.170	0.016	20,300		0.426	0.424
	3.91					40.0	136.6	4.66	5.95	0.3	0.3	0.1	0.640	1.535	- 0.180	- 0.025	24,900		0.427	
																		16,420		0.437
	4.78	- 1.62	26.03	43.15	40.75	10.0	139.9	2.61	13.53	0.0	0.0	- 1.2	0.129	1.033	- 0.057	0.372				
	4.78					20.0	140.1	4.95	10.22	0.1	0.1	- 0.8	0.393	1.310	- 0.091	0.266	25,600		0.427	
	4.96					30.0	140.0	4.04	7.06	0.5	0.5	- 0.7	0.517	1.939	- 0.157	0.248	21,600		0.419	0.426
	4.96					40.0	140.3	3.91	6.50	0.5	0.5	- 0.5	0.521	1.824	- 0.142	0.117	26,300		0.432	
																		24,500		0.409
2514 Limestone	5.07	2.52	16.37	38.79	38.28	10.0	140.7	4.72	8.93	0.4	0.4	- 1.6	0.511	1.914	- 0.145	0.644	8,300		0.419	
						20.0	138.9	4.02	6.76	0.3	0.3	- 1.3	0.506	1.770	- 0.097	0.419	16,100		0.444	
						30.0	138.8	3.57	5.59	0.7	0.7	- 1.1	0.638	2.298	- 0.138	0.341	19,600		0.430	0.431
						40.0	138.5	3.51	4.57	1.2	1.2	- 0.5	1.006	3.394	- 0.232	0.184	14,400		0.434	
						60.0	139.1	3.60	4.46	1.7	1.7	0.6	1.642	4.043	- 0.387	- 0.107				
																		14,600		0.394
	4.90	0.82	11.92	38.97	40.14	10.0	135.2	4.29	7.25	0.4	0.4	- 1.2	0.371	1.606	- 0.093	0.443	10,200		0.434	
	4.90					20.0	135.5	3.17	7.31	0.4	0.4	- 0.4	0.368	1.226	- 0.108	0.092	13,500		0.440	
	4.91					30.0	135.3	3.55	5.20	0.6	0.6	- 1.1	0.613	2.757	- 0.156	0.378	12,100		0.451	0.440
	4.91					40.0	135.3	3.51	4.63	0.8	0.7	- 0.6	0.858	2.759	- 0.194	0.128	17,300		0.434	
																		13,280		0.416
2515 Limestone (2514)	4.27	2.17	16.90	37.26	39.32	10.0	136.0	4.10	9.21	0.1	0.1	- 0.9	0.373	1.614	- 0.117	0.539	10,000		0.417	
						20.0	136.9	3.93	6.90	0.3	0.3	- 1.0	0.624	2.122	- 0.134	0.379	13,700		0.433	
						30.0	137.0	3.97	6.17	0.6	0.6	- 0.8	0.754	2.388	- 0.167	0.359	16,400		0.434	0.427
						40.0	138.0	3.46	5.36	0.3	0.2	0.0	1.008	3.276	- 0.225	0.411	17,300		0.425	
						60.0	138.5	3.50	4.50	0.8	0.8	- 0.1	1.155	3.209	- 0.280	- 0.025				
																		14,350		0.386
	3.95	- 0.21	8.84	40.22	39.29	10.0	133.1	4.37	6.61	0.3	0.3	- 1.2	0.367	1.713	- 0.108	0.425	9,300		0.430	
	3.95					20.0	131.0	3.42	5.26	0.4	0.4	- 1.0	0.484	3.628	- 0.138	0.529	9,500		0.448	
	3.98					30.0	133.2	3.21	4.90	2.3	0.7	0.8	0.613	3.065	- 0.173	0.220	11,500		0.446	0.444
	3.98					40.0	131.7	3.81	4.30	1.0	1.0	0.2	1.579	4.252	- 0.312	- 0.125	8,000		0.454	
																		9,570		0.402
AASHO 203 Gravel	4.99	0.86	1.07	42.03	49.93	10.0	140.8	4.17	8.88	0.3	0.3	- 0.5	0.247	1.236	- 0.078	0.492	10,650		0.365	
	5.00					20.0	142.1	3.86	6.53	0.2	0.2	- 1.2	0.376	1.379	- 0.109	0.414	16,350		0.342	
	5.00					30.0	142.4	3.52	5.55	0.4	0.4	- 1.3	0.500	1.750	- 0.119	0.365	17,150		0.363	0.351
	5.01					40.0	144.3	4.12	7.09	0.6	0.4	0.3	0.507	1.393	- 0.129	0.290	32,000		0.333	
																		19,040		0.644

[a]See selected reference 2.

Table A-2. Triaxial test results for optimum moisture-treated specimens at minimum volume (MV) and maximum effective stress ratio (MESR) conditions.

Material	Moisture content, %	Cohesion, psi		φ, degrees		Lateral pressure, psi	Dry density, pcf	Effective stress ratio		Pore pressure, psi			Axial strain, %		Volumetric strain, %		Modulus of deformation, psi	Average modulus, psi	Poisson's ratio	
		Min vol	MESR	Min vol	MESR			Min vol	MESR	Max	Min vol	MESR	Min vol	MESR	Min vol	MESR			Eq. 13[a]	Eq. 13[a]
429	7.37	- 4.51	12.20	45.18	45.56	10.0	136.48	3.56	11.23	2.0	0.8	0.6	0.364	2.425	- 0.131	1.054	8,393		0.409	
	7.52					20.0	136.46	3.10	8.13	1.9	1.0	1.5	0.515	2.577	- 0.197	0.683	10,676		0.409	
	7.21					30.0	137.26	4.07	7.39	1.8	1.0	1.4	0.896	3.201	- 0.295	0.730	12,997		0.406	
	7.45					40.0	135.71	4.42	6.41	2.3	1.2	2.1	1.311	3.277	- 0.484	0.221	12,802		0.392	
	7.39						136.47												0.404	
																		11,217		0.333
479	9.45	0.38	8.40	42.52	47.29	10.0	132.78	4.81	10.0	0.3	0.3	- 1.0	0.491	1.842	- 0.162	0.663	8,675		0.407	
	9.81					20.0	130.51	3.90	7.01	1.2	0.9	0.3	0.870	3.729	- 0.275	0.984	7,578		0.421	
	9.27					30.0	130.92	4.29	7.66	1.2	0.9	0.8	0.886	3.166	- 0.353	0.763	13,478		0.388	
	9.05					40.0	130.58	4.23	6.34	1.1	1.0	0.1	1.138	3.161	- 0.441	0.321	14,409		0.387	
	9.40						131.20												0.401	
																		11,035		0.336
1485	6.97	1.15	5.87	38.93	44.16	10.0	126.99	3.98	7.03	0.2	0.2	- 0.3	0.378	1.258	- 0.142	0.507	10,596		0.390	
	7.26					20.0	127.69	3.74	6.03	0.1	0.1	- 0.8	0.502	1.882	- 0.183	0.732	14,439		0.401	
	6.83					30.0	128.05	3.33	5.68	0.3	0.3	- 0.2	0.508	1.777	- 0.243	0.388	19,622		0.373	
	7.65					40.0	127.85	3.58	5.18	0.3	0.3	- 0.2	0.741	2.161	- 0.301	0.321	19,405		0.388	
	7.18						127.65												0.388	
																		16,015		0.315
1676	7.90	3.00	14.20	41.69	45.62	10.0	132.85	5.14	10.75	0.4	0.3	- 0.9	0.393	1.638	- 0.132	0.737	11,422		0.405	
	7.95					20.0	131.64	4.68	8.99	0.7	0.3	- 0.2	0.656	1.967	- 0.256	0.429	13,028		0.390	
	7.83					30.0	132.18	4.64	7.46	0.5	0.5	0.2	0.920	2.301	- 0.366	0.262	14,049		0.386	
	8.24					40.0	131.78	4.19	6.62	1.3	1.2	1.0	1.043	2.608	- 0.421	0.107	15,493		0.383	
	7.98						132.11												0.391	
																		13,498		0.307
1846	6.91	- 1.83	7.92	44.33	48.64	10.0	135.45	3.49	10.14	0.5	0.5	- 0.5	0.249	1.866	- 0.142	0.789	13,291		0.347	
	6.70					20.0	135.23	4.88	8.13	0.9	0.8	- 0.8	0.746	2.486	- 0.302	0.778	12,495		0.375	
	6.89					30.0	135.07	3.85	7.20	1.1	0.4	0.0	0.632	2.527	- 0.274	0.597	17,822		0.379	
	6.67					40.0	136.22	4.51	7.15	1.0	0.8	- 0.1	0.869	2.593	- 0.368	0.437	21,008		0.369	
	6.79						135.49												0.368	
																		16,154		0.318
1855	6.08	- 3.16	17.52	46.55	47.86	10.0	139.21	4.64	14.19	0.8	0.7	- 0.6	0.324	1.684	- 0.151	1.023	14,041		0.350	
	7.02					20.0	137.18	4.82	10.65	0.5	0.5	- 0.3	0.510	1.914	- 0.194	0.802	18,221		0.384	
	6.16					30.0	137.53	3.81	8.50	0.2	0.2	- 0.5	0.507	1.646	- 0.161	0.524	23,460		0.407	
	7.04					40.0	137.87	5.20	8.02	0.6	0.6	- 0.3	0.778	2.269	- 0.316	0.237	26,787		0.369	
	6.58						137.95												0.377	
																		20,627		0.331
1904	5.31	0.67	15.67	42.02	44.80	10.0	139.53	4.67	11.35	0.2	0.2	- 0.9	0.318	1.656	- 0.092	0.987	12,977		0.420	
	5.57					20.0	138.70	4.30	8.70	0.7	0.4	- 0.2	0.489	1.833	- 0.162	0.664	16,719		0.405	
	5.47					30.0	138.49	3.80	7.31	0.4	0.3	- 0.8	0.507	2.219	- 0.185	0.766	21,320		0.403	
	5.35					40.0	137.75	4.26	6.53	0.3	0.3	- 0.7	0.644	2.255	- 0.213	0.479	25,390		0.406	
	5.43						138.62												0.409	
																		19,101		0.360
AASHO	6.00	- 5.74	12.20	49.01	50.17	10.0	144.2	3.72	13.32	0.6	0.4	- 0.1	0.393	2.486	- 0.150	0.935	9,350		0.232	
295	6.00					20.0	147.6	3.79	9.61	0.7	0.6	- 0.1	0.525	2.623	- 0.203	0.797	13,300		0.251	
crushed	6.00					30.0	145.6	5.63	9.65	1.3	1.0	0.7	0.928	2.981	- 0.290	0.704	17,850		0.307	
stone	6.00					40.0	144.5	5.18	7.97	1.1	0.9	0.7	1.176	3.266	- 0.512	0.128	17,500		0.226	
							145.5												0.234	
																		14,490		0.336

[a]See selected reference 2.

APPENDIX B

Table B-1. Correlation matrix, bituminous-treated field mixes, minimum volume conditions, 10 psi lateral pressure.

	Percent asphalt	Sand equivalent	Minus No. 200 sieve	Specific gravity	ϕ	Cohesion	Average modulus of deformation	Poisson's ratio[a]	Effective stress ratio	Pore pressure	Axial strain	Volumetric strain	Modulus of deformation	Poisson's ratio[b]	Density
Percent asphalt	1.000														
Sand equivalent	- 0.094	1.000													
Minus No. 200 sieve	0.159	- 0.267	1.000												
Specific gravity	0.248	- 0.161	0.392	1.000											
ϕ	0.092	- 0.232	0.530	0.685	1.000										
Cohesion	0.030	- 0.463	0.224	- 0.129	- 0.356	1.000									
Average modulus of deformation	- 0.044	- 0.172	0.661	0.539	0.512	0.152	1.000								
Poisson's ratio[a]	0.097	0.192	- 0.048	- 0.142	- 0.418	0.289	- 0.091	1.000							
Effective stress ratio	0.244	- 0.500	0.303	- 0.011	- 0.139	0.828	0.146	0.159	1.000						
Pore pressure	0.339	- 0.028	- 0.097	0.015	- 0.232	0.300	- 0.372	- 0.019	0.353	1.000					
Axial strain	0.005	- 0.202	- 0.116	- 0.598	- 0.497	0.540	- 0.583	0.138	0.534	0.441	1.000				
Volumetric strain	- 0.123	0.375	0.082	0.396	0.408	- 0.632	0.444	- 0.054	- 0.690	- 0.602	- 0.855	1.000			
Modulus of deformation	- 0.021	- 0.312	0.724	0.487	0.519	0.244	0.911	- 0.206	0.318	- 0.210	- 0.435	0.205	1.000		
Poisson's ratio[b]	- 0.102	0.496	- 0.292	- 0.341	- 0.091	- 0.535	- 0.485	0.052	- 0.566	- 0.262	0.116	0.328	- 0.614	1.000	
Density	0.428	0.280	- 0.037	0.245	0.126	- 0.211	- 0.041	- 0.126	- 0.032	0.311	- 0.121	0.190	- 0.119	0.083	1.000

[a]Equation (21), selected reference 2.

[b]Equation (13), selected reference 2.